

NPS-57C071111A

Naval Postgraduate School



THE APPLICATION OF HOLOGRAPHIC INTERFEROMETRY TO THE
DETERMINATION OF THE FLOW FIELD AROUND
A RIGHT CIRCULAR CONE AT ANGLE OF ATTACK

by

D. J. Collins

and

R. C. Jagota

December
December 1971

Approved for public release; distribution unlimited

FEDDOCS
D 208.14/2:NPS-57C071111A

153

NAVAL POSTGRADUATE SCHOOL
Monterey, California 93940

Rear Admiral A. S. Goodfellow
Superintendent

M. U. Clauser
Provost

ABSTRACT

The successful application of holography to the study of three dimensional flow fields due to phase objects has been reported in the literature. The present report extends this technique to the study of density fields around opaque bodies as would normally be encountered in wind tunnel experiments. The density field around a 10 degree half-angle cone at zero and ten degree angle of attack has been investigated by means of the finite fringe holographic interferometry. The three dimensional density field obtained from the reduction of the interferograms was found to agree with that obtained from an analytical solution of the governing equations.

This report was supported by: Airtask No. A310310A/551A/1 R010-03-01

TABLE OF CONTENTS

Introduction	1
Appendix I	I-1

INTRODUCTION

This is a report on holographic investigations directed towards the determination of complex three-dimensional density fields. The report consists of essentially Appendix I which includes the thesis of R. C. Jagota on the determination of density fields about a cone at angle of attack in a wind tunnel.

A paper based on this thesis, "Finite Fringe Holographic Interferometry Applied to a Right Circular Cone at Angle of Attack, by R. C. Jagota and D. J. Collins, has been accepted for publication by the Journal of Applied Mechanics.

Further work on the determination of the density in corner flows was begun towards the end of the contract year. This work is directed at determining the flow in a wing fuselage junction at transonic speeds.

A preliminary program using a flat plate-fin in the Naval Postgraduate School wind tunnel has been started at Monterey. This preliminary program is designed to solve some of the holographic problems associated with the transonic test that are to be conducted at NSRDC. Further reports on this work will be forthcoming in December.

APPENDIX I

United States Naval Postgraduate School



THE SIS

THE APPLICATION OF HOLOGRAPHIC INTERFEROMETRY
TO THE DETERMINATION OF THE FLOW FIELD AROUND
A RIGHT CIRCULAR CONE AT ANGLE OF ATTACK

by

Ravi Chandar Jagota

December 1970

This document has been approved for public release and sale; its distribution is unlimited.

The Application of Holographic Interferometry
to the Determination of the Flow Field Around
a Right Circular Cone at Angle of Attack

by

Ravi Chandar Jagota
Lieutenant Commander, Indian Navy

Submitted in partial fulfillment of the
requirements for the degree of

AERONAUTICAL ENGINEER

from the
NAVAL POSTGRADUATE SCHOOL
December 1970

ABSTRACT

The successful application of holography to the study of three dimensional flow fields due to phase objects has been reported in the literature. The present report extends this technique to the study of density fields around opaque bodies as would normally be encountered in wind tunnel experiments. The density field around a 10 degree half-angle cone at zero and ten degree angle of attack has been investigated in the Naval Postgraduate School supersonic wind tunnel. In these experiments, the finite fringe method for the production of interferograms has, for the first time, been applied to holographic interferometry. The density field obtained from the reduction of the interferograms was found to agree with that obtained from an analytical solution of the governing equations as reported by D. J. Jones in Reference 1. The computer program used for the reduction of the interferograms has been evaluated for the effect of the presence of the cone and the shock wave and has been found to yield stable and accurate results.

TABLE OF CONTENTS

I.	INTRODUCTION -----	5
II.	EXPERIMENTAL APPARATUS -----	9
	A. THE WIND TUNNEL -----	9
	B. THE EXPERIMENTAL SETUP FOR PRESSURE MEASUREMENT -----	10
	C. THE HOLOGRAPHIC ARRANGEMENT -----	10
	D. THE WIND TUNNEL MODEL -----	12
III.	THEORETICAL CONSIDERATIONS -----	14
	A. EVALUATION OF THE DENSITY FROM HOLOGRAPHIC INTERFEROGRAMS -----	14
	1. The Basic Equation of Interferometry ----	14
	2. The Integral Inversion -----	16
	3. The Numerical Procedure -----	19
	B. THE FLOW AROUND A RIGHT CIRCULAR CONE -----	21
	1. Axisymmetric Case -----	21
	2. Flow Around Cones with Small Yaw -----	25
IV.	DESCRIPTION OF THE EXPERIMENT -----	27
	A. NUMERICAL SIMULATION OF THE EXPERIMENT -----	27
	B. EXPERIMENTAL PROCEDURE -----	28
	1. Laboratory Techniques -----	28
	2. Photographic Techniques -----	30
	3. Data Reduction -----	31
V.	EXPERIMENTAL RESULTS AND DISCUSSION -----	34
	A. DENSITY FIELD OBTAINED EXPERIMENTALLY -----	34

1. Computer Simulation Results -----	34
2. Experimental Results -----	35
B. ERROR ANALYSIS -----	37
VI. SUMMARY -----	39
A. CONCLUSIONS -----	39
B. ACKNOWLEDGEMENTS -----	39
APPENDIX A: REDUCTION OF AN INTERFEROGRAM TO OBTAIN FRINGE SHIFTS -----	83
APPENDIX B: DESCRIPTION OF COMPUTER PROGRAM "HOLOFER" -----	86
APPENDIX C: COMPUTER PROGRAMS USED FOR INTERPOLATION -----	137
A. COMPUTER PROGRAM 1 -----	137
B. COMPUTER PROGRAM 2 -----	141
BIBLIOGRAPHY -----	146
INITIAL DISTRIBUTION LIST -----	148
FORM DD 1473 -----	149

I. INTRODUCTION

For over three decades, the Mach-Zehnder interferometer has been widely used and has come to be accepted as a standard tool for the measurement of the flow field around bodies. Until the advent of the laser, its use required extreme stability from vibrations and precision optical components. Even with a laser as a light source, the resulting interferograms are purely two-dimensional in nature in that they provide fringe information for only one direction of view through the wind tunnel. Furthermore, due to the limit imposed by existing camera shutter speeds, the interferogram obtained does not truly represent the instantaneous flow field around the body but rather is an average over the interval of shutter opening.

The advent of holography together with the development of the high power Q-switched laser has introduced a new dimension in the field of flow measurement. Apart from removing the need for precision optical quality components in the case of double exposed holograms, the use of holography has, for the first time, enabled a three-dimensional view of the flow field to be obtained from a single hologram. The high power of the laser and the Q-switch mechanism have together enabled film exposure times in the region of 20 nano-seconds to be attained thus, in effect, "freezing" the flow during the hologram production process.

Techniques for the application of holography to interferometry have been reported in Reference 1 (Heflinger et al, 1966) and in Reference 2 (Brooks et al, 1966). Holographic interferometry has been used to determine the three-dimensional asymmetric field produced by free-jet flow (Reference 3). In this report, a series of holograms placed in a 90 degree sector around the jet were obtained simultaneously from a single exposure. Interferograms were then obtained from the holograms at suitable angular orientations within a 90 degree field of view. This provided sufficient information to determine the entire flow field since the jet was planar symmetric. Reduction of the fringe data to density information was accomplished by expressing the density in a series of orthogonal polynomials and inverting the fringe-density integral equation by a computer program using a scheme reported in References 4 and 5.

In the present report, the applicability of holography interferometry has been extended to those three-dimensional density fields produced by opaque bodies as would be encountered in wind tunnel experiments. The experiments were conducted in the Naval Postgraduate School supersonic blowdown wind tunnel at a Mach number of 2.8 using a ten degree half-angle cone at zero and ten degrees angle of attack. In this case, the multiple hologram technique was not employed. Since the flow fields investigated were steady, the procedure adopted was to obtain holograms to cover various sectors of the flow field by rotating the cone within

the wind tunnel, this being a method that would be fully applicable to any conventional wind tunnel setup.

Whereas in an infinite fringe field, the fringe information is obtained in a discontinuous manner, that is, at the points of maxima and minima, the interferogram from a finite fringe field can be evaluated at any desired point quite readily. This is of particular significance in the case of density fields where the variations in density are small. In the present case, the total variation in fringe number was generally in the region of only one to two fringes. The finite fringe method was also selected since it is less sensitive to vibrations than is the infinite fringe field, a problem encountered in Reference 3. The finite fringe field was produced by a translation of the diffusing screen in the scene beam a distance of between .025" and .030" between the two exposures of the hologram. A vertical fringe field, obtained by horizontal translation of the diffuser, was chosen in spite of the greater effort required to reduce the interferograms at a particular section owing to the greater uniformity and clarity of the fringes thus obtained as compared to horizontal fringes. Fringe data obtained from the interferograms was reduced to density using the same computer program as used in Reference 3. The density field obtained experimentally was compared with the analytical solution reported in Reference 6, interpolating the results therein for the actual mach number of the experiments. Good correlation was achieved, thus demonstrating

the utility of holographic interferometry for normal wind tunnel experimentation.

II. EXPERIMENTAL APPARATUS

A. THE WIND TUNNEL

This investigation was conducted in the Naval Postgraduate School blow-down supersonic wind tunnel. The wind tunnel is a blowdown-to-atmosphere facility which has a test section 4 inches by 4 inches in cross-section and 6 inches in length. Interchangeable nozzles are available for producing nominal test section mach numbers of 4.0, 2.8, and 1.7. The nominal run time is 5 minutes at a mach number of 2.8 with a maximum stagnation pressure of about 105 pounds per square inch. For this series of experiments, the side walls of the wind tunnel were replaced by plexiglas walls two inches thick having a refractive index of 1.49 so that a complete view of the flow in the test section could be obtained.

B. THE EXPERIMENTAL SETUP FOR PRESSURE MEASUREMENT

Figure 1 is a schematic representation of the equipment arrangement used for pressure measurement. The static pressures on 16 out of a total of 30 orifices on the surface of the cone were measured by a Scanivalve (Model 48J4-1065 with a 0-10 psia. transducer) which was calibrated in inches of mercury vacuum. The measurements were recorded on a Honeywell 2106 twelve channel Viscicorder. The scanivalve was capable of scanning 15 ports per second. Photographs of the experimental setup are provided in Figures 2 and 3. The plexiglas side walls of the wind tunnel with the Scanivalve

mounted on top of the test section are shown in Figure 2. The power supply, control box and Viscicorder can be seen in Figure 3.

C. THE HOLOGRAPHIC ARRANGEMENT

A schematic of the holographic arrangement employed is shown in Figure 4 and photographs thereof are in Figures 5(a) and 5(b). The equipment was mounted on a table that rested on a portion of the floor that was vibrationally isolated from the rest of the building. The monochromatic light source used was a Korad K-1 pulsed ruby laser operating at a wavelength of 6943 Angstroms together with a Pockels cell Q-switching device. The resulting effective exposure time was about 20 nanoseconds and, with a cavity length of the laser of 37 cms., a coherence length of about 2 cms. was obtained. A side band geometry was employed to obtain the holograms of the flow field around the cone. A diffuse glass in the path of the scene beam was used to produce light field holograms, which because of the diffusion of the direction of the rays in the scene beam, produced an effective field of view in a hologram of approximately 16 degrees. A continuous wave helium-neon laser was used for alignment of the Q-switched laser and the optics. A Lauda constant temperature circulator Model N controlled by an electronic relay type R-10 was used in conjunction with a Culligan de-ionizer to maintain the laser head and output etalon at a constant temperature of 28.4 degrees Centigrade.

In Figure 4, details of the side band geometry employed can be seen. The reference beam was led on top of the wind tunnel by means of the two mirrors M and the size of the beam could be adjusted by means of lenses U. The positions of the diffuser plate and the two grids, one on each of the wind tunnel side walls, are also shown therein. In Figure 5(a), the Korad K-1 laser and the smaller alignment laser are shown together with the arrangement of the optical equipment. The diffuser plate mounted on the precision X-Y slide can also be seen. The holographic table and test section was completely enclosed in a wooden box to enable the experiments to be conducted in the daytime. This is shown in Figure 5(b). Also shown therein are the Korad K-1 laser power supply and shutter control assemblies, the Culligan de-ionizer and the Lauda constant temperature circulator.

In order to be able to view the cone at angle of attack always in a direction perpendicular to its axis when it was rotated in the wind tunnel, it was necessary to construct separate grids for each rotational angle at which the holograms were taken. The front grid used for the 82.5 degree rotational position of the cone is shown in position in Figure 6. The grid lines can be seen to be parallel and perpendicular to the cone axis for this particular angular position. The orientation of the grids was designed to be at the correct angle for the particular rotational position of the cone. Since, on rotation, the axis of the cone was not in a vertical plane, it was necessary to offset the two

grids with respect to each other in such a manner that on lining up the grids, the correct viewing position perpendicular to the cone axis was automatically obtained. The method of obtaining the orientations and the relative offset of the grids is shown in Figures 7(a) and 7(b). Since the cone spindle was bent at a distance of 0.7 inches from the base of the cone, the various rotational positions of the cone tip are indicated in the end view in Figure 7(a). The corresponding positions of the cone axis in the side and bottom views are also shown therein. The orientation of the grid lines for each rotational position of the cone as shown in Figure 7(b) were obtained from the positions of the cone axis in the side view for each particular case. In order to be normal to the cone axis, lines perpendicular to the orientation of the cone axis in the bottom view were transcribed, each of these representing a line of sight. Since the distance between the grids was $7 \frac{7}{8}$ inches, the necessary amount by which the two grids were required to be offset for each rotational position of the cone tip were obtained as shown in Figure 7(b).

D. THE WIND TUNNEL MODEL

The cone model used is shown in Figure 8. The 10 degree semi-apex angle cone model was fabricated out of stainless steel and had pressure ports at three cross-sections, the angular position of the ports being so arranged as to lie on a ray from the apex of the cone. Since a fixed mount was

employed, provision was made to attach the cone to spindles bent to various angles to achieve the desired angle of attack. Stainless steel tubing of .036 inches internal diameter was used from the static pressure orifices on the surface of the cone up to the base of the model, the diameter of this being adequate to provide sufficient time response of the Scanivalve. Any fifteen out of the thirty ports could be connected at a time to the Scanivalve through the hollow cone spindle and mount, this restriction being imposed by the internal diameter of the spindle.

Rotation of the model about the horizontal axis of the spindle necessitated drilling 4 holes on each side of the wind tunnel side walls through which the model spindle could be unlocked from the mount and rotated. The plexiglas side walls of the test section and the holes therein can be seen in Figure 6. The collar on the model spindle containing radial holes (also visible in the figure) was used to rotate the cone by means of a spike arrangement inserted through one of the holes in the tunnel side walls. The angle of rotation was established by lining up graduations on the spindle sleeve with a graduation on the mount. The model and spindle used for the axisymmetric case can be seen in Figure 9. The pressure ports at the three stations and one of the pressure tubes from the cone passing through the hollow spindle are visible in the photograph. After the spindle was screwed into the cone, it was locked in position by means of the setscrew shown.

III. THEORETICAL CONSIDERATIONS

A. EVALUATION OF THE DENSITY FROM HOLOGRAPHIC INTERFEROGRAMS

1. The Basic Equation of Interferometry

The interferometry principle is based on the fact that two originally coherent rays of light will reinforce or annul each other at a screen on which both rays are projected depending on their relative phase there. The phase difference is directly a function of the difference in the lengths of the optical paths traversed by the two rays. If the optical path is changed by an amount $N\lambda$, where λ is the wavelength of the light and N is an integer, then the order of interference changes by an amount N , that is, a shift of N fringes occurs. The change in optical path can be related to the density through the index of refraction and the Gladstone-Dale constant. If the speed of light in a medium is represented by $\frac{c_0}{n}$ where c_0 is the speed of light in vacuum and n is the index of refraction, the additional time required to traverse the test section due to a change in the index of refraction from n_1 to n_2 can be calculated to be equal to $\Delta t = \frac{L}{c_0}(n_2 - n_1)$ and thus the change in optical path obtained is $c_0 \Delta t$, that is, $L(n_2 - n_1)$. The fringe shift, g , which is equal to $\frac{\Delta L}{\lambda}$ is thus given by $L(n_2 - n_1)$.

For a given substance and for a given wavelength of light, the index of refraction is a function of density. In the case of gases, since the speed of light varies only slightly

from that in vacuum, it can be represented very accurately by the first two terms of the Taylor series:

$$n = 1 + \beta \frac{\rho}{\rho_s} \quad (1)$$

where

ρ_s = reference density at 0°C, 760 mm. Hg.

β = dimensionless constant related to the Gladstone-Dale constant by:

$$K = \frac{\beta}{\rho_s}$$

The value of β for air at $\lambda = 5893$ Angstroms is 0.000292, the variation with wavelength being small. The fringe shift relation for a fixed difference in index of refraction between the two beams becomes:

$$g = \beta \frac{L}{\lambda} \left(\frac{\rho_2 - \rho_\infty}{\rho_s} \right) \quad (2)$$

If the density is variable in the test section, the net change in optical path is the integrated effect along the ray which gives the relationship:

$$g = \frac{\beta}{\lambda \rho_s} \int_0^L (\rho - \rho_\infty) ds = Q \int_0^L f(x, y, z_c) ds \quad (3)$$

where

$$f(x, y, z_c) = \frac{\rho(x, y, z_c)}{\rho_\infty} - 1 \quad (4)$$

$$Q = \frac{\beta \rho_\infty}{\lambda \rho_s} \quad (5)$$

ds = incremental distance along a ray

z_c = a plane of constant z .

Equation (3) is the basic equation which has to be inverted to obtain the unknown density from the known fringe shift values obtained from an interferogram.

2. The Integral Inversion

The integral inversion method used was first reported by C. D. Maldonado et al in 1965 (1965; Olsen, 1968) and subsequently used by R. D. Matulka (Reference 3) to calculate the density variation in an asymmetric free jet from the fringe numbers obtained from holographic interferograms. The procedure involves the representation of the function $f(x,y,z_c)$ by a complete set of orthogonal functions, with the unknown coefficients being evaluated by use of the orthogonality relationship between the set of functions. The set of functions employed have a region of orthogonality that covers the entire plane and have the property that they are "invariant in form" to a rotation of the co-ordinate system. The co-ordinate system used for the inversion is shown in Figure 10 where X and Y represent fixed laboratory co-ordinates and X' and Y' the co-ordinates in which the fringe number function is defined. These co-ordinates, therefore, rotate with respect to the fixed co-ordinates X and Y as the angle of view through the test section is varied.

In operator form, equation (3) can be represented as:

$$g(\xi, \eta', z_c) = T f(x, y, z_c) \quad (6)$$

and the object of the procedure is to evaluate f , that is, to obtain:

$$f(x, y, z_c) = T^{-1} g(\xi, y', z_c) \quad (7)$$

where T^{-1} represents the inverse of T .

This inversion is achieved by utilizing a pair of orthogonal polynomials $U_{m+2k}^{\pm m}(\alpha x, \alpha y)$ and $H_{m+2k}(\alpha y')$ which are related by the transform relationship:

$$T \left\{ U_{2k}(\alpha x, \alpha y) e^{-\alpha^2 x'^2} \right\} = \frac{e^{\pm i m \xi}}{[k!(m+k)!]^{1/2}} \frac{1}{2^{m+2k}} H_{m+2k}(\alpha y') \quad (8)$$

where:

$$H_{m+2k}(\alpha y') = e^{\alpha^2 y'^2} [d^{2k} d(\alpha x)^{2k}] [e^{-\alpha^2 y'^2} H_m(\alpha y')] \quad (9)$$

and H_m are the Hermite polynomials.

The function $f(x, y, z_c)$ is first expanded in a series of the polynomials U_{m+2k} as:

$$f(x, y, z_c) = \sum_{m=0}^{\infty} \sum_{k=0}^{\infty} \epsilon_m C_{m+2k}^{\pm m}(\alpha) U_{m+2k}^{\pm m}(\alpha x, \alpha y) e^{-(\alpha^2 x'^2 + \alpha^2 y'^2)} \quad (10)$$

where $\epsilon_m = \frac{1}{2}$ for $m = 0$ and 1 for $m = 1, 2, 3, \dots$, α is an arbitrary scale factor, and $C_{m+2k}^{\pm m}$ are the unknown expansion coefficients. In order to evaluate these coefficients, an expression for the function $g(\xi, y', z_c)$ is obtained in terms of the polynomials by transforming $f(x, y, z_c)$ in accordance with equation (6). Using the transform relation given by equation (8), the following expression is obtained:

$$g(\xi, y', z_c) = \sum_{m=0}^{\infty} \sum_{k=0}^{\infty} \epsilon_m [k! (m+k)! 2^{2(m+2k)}]^{-1/2} C_{m+2k}^{\pm m}(\alpha) e^{\pm i m \xi} H_{m+2k}(\alpha y') e^{-\alpha^2 y'^2} \quad (11)$$

The expansion coefficients can then be evaluated by applying the following orthogonality relationship to Equation (11):

$$\int_{-\pi}^{\pi} e^{\pm i m \xi} e^{\mp i m \xi} d\xi \int_{-\infty}^{\infty} H_{m+2k}(\alpha y') H_{n+2l}(\alpha y') e^{-\alpha^2 y'^2} dy' = \frac{2\pi^{3/2}}{\alpha} \left[(m+2k)! (n+2l)! 2^{m+2k} 2^{n+2l} \epsilon_{mn} \int_{-\infty}^{\infty} \delta_{m+2k, n+2l} \right] e^{\mp i m \xi} H_{n+2l}(\alpha y') \quad (12)$$

that is, by taking the scalar product of equation (11) with $e^{\mp i m \xi} H_{n+2l}(\alpha y')$ and using equation (12), the coefficients of the series in equation (10) are obtained as:

$$C_{m+2k}^{\pm m}(\alpha) = \frac{\alpha}{2\pi^{3/2}} \left[\frac{\{k! (m+k)!\}^{1/2}}{(m+2k)!} \int_{-\pi}^{\pi} g(y', \xi, z_c) H_{m+2k}(\alpha y') e^{\mp i m \xi} dy' d\xi \right] \quad (13)$$

Substitution of equation (13) into equation (10) results

in the density variation being given by:

$$f(x, y, z_c) = \left(\frac{\alpha}{\pi}\right)^2 \sum_{m=0}^{\infty} \sum_{k=0}^{\infty} \epsilon_m \frac{\{k! (m+k)!\}^{1/2}}{(m+2k)!} e^{-(\alpha^2 x^2 + \alpha^2 y^2)} \text{Re} \left[\int_{-\pi}^{\pi} \int_{-\infty}^{\infty} g(y', \xi, z_c) e^{-i m \xi} H_{m+2k}(\alpha y') dy' d\xi \right] U_{m+2k}^m(\alpha x, \alpha y) \quad (14)$$

The functions U_{m+2k}^m employed are complex polynomials

defined as:

$$U_{m+2k}^{\pm m}(\alpha x, \alpha y) = (-i)^k \left(\frac{\alpha}{\pi}\right)^{1/2} \left(\frac{k!}{(m+2k)!}\right)^{1/2} \left[\alpha^2 (x'^2 + y'^2) \right]^{m/2} e^{\pm i m \phi} L_k^m \left[\alpha^2 (x'^2 + y'^2) \right] \quad (15)$$

where $\phi = \tan^{-1} \frac{y}{x}$ and L_k^m are the Associated Laguerre polynomials:

$$L_k^m(\alpha^2 x^2 + \alpha^2 y^2) = \sum_{s=0}^m \frac{(m+k)!}{(k-s)!(m+s)!s!} \left[(-1)^s (\alpha^2 x^2 + \alpha^2 y^2) \right]^s \quad (16)$$

Substitution of equation (15) into equation (14) yields:

$$f(x, y, z_c) = \left(\frac{\alpha}{\pi} \right)^2 \sum_{m=0}^{\infty} \sum_{k=0}^{\infty} \frac{(-1)^k k!}{(m+2k)!} (\alpha^2 x^2 + \alpha^2 y^2)^{m/2} L_k^m(\alpha^2 x^2 + \alpha^2 y^2) \left[B_{m+2k}^m(\alpha) \cos(m\phi) + D_{m+2k}^m(\alpha) \sin(m\phi) \right] e^{-(\alpha^2 x^2 + \alpha^2 y^2)} \quad (17)$$

where:

$$B_{m+2k}^m(\alpha) = \int_{-\pi}^{\pi} \int_{-\infty}^{\infty} g(y', \xi, z_c) \cos(m\xi) H_{m+2k}^{(\alpha y')} dy' d\xi \quad (18)$$

$$D_{m+2k}^m(\alpha) = \int_{-\pi}^{\pi} \int_{-\infty}^{\infty} g(y', \xi, z_c) \sin(m\xi) H_{m+2k}^{(\alpha y')} dy' d\xi \quad (19)$$

Equations (17), (18), and (19) are the basic equations used to obtain the density distribution of a completely asymmetric flow field.

3. The Numerical Procedure

The calculation of the unknown coefficients $B_{m+2k}^m(\alpha)$ and $D_{m+2k}^m(\alpha)$ in the series representation of $f(x, y, z_c)$ as given by equation (17) is not analytically possible in general since the function $g(y', \xi, z_c)$ representing the variation of fringe number is an experimentally measured quantity and thus not explicitly given as a function of the co-ordinates of a field point. If the analytical procedure is to be used to obtain the density from experimental observations of the fringe numbers, therefore, it is necessary to evaluate

the double integrals in equations (18) and (19) numerically. This is achieved by first noting that for every $g(y', \xi, z_c)$ encountered experimentally, there is a circular domain outside which the fringe distribution is zero so that it is possible to replace the limits of integration of $+\infty$ and $-\infty$ in equations (18) and (19) by finite values. The function $g(y', \xi, z_c)$ is then approximated by constant step values over elemental areas into which the domain is partitioned. This results in the B and D coefficients being represented by the double series:

$$B_{m+2k}^m(\alpha) = \sum_{i=0}^{I-1} \sum_{j=0}^{J-1} g(\xi_j + \Delta \xi_j, x_i + \Delta x_i) \int_{\xi_j}^{\xi_{j+1}} \cos(m\xi) d\xi \int_{x_i}^{x_{i+1}} H_{m+2k}(\alpha x) dx \quad (20)$$

and

$$D_{m+2k}^m(\alpha) = \sum_{i=0}^{I-1} \sum_{j=0}^{J-1} g(\xi_j + \Delta \xi_j, x_i + \Delta x_i) \int_{\xi_j}^{\xi_{j+1}} \sin(m\xi) d\xi \int_{x_i}^{x_{i+1}} H_{m+2k}(\alpha x) dx \quad (21)$$

Using the derivative formula for Hermite polynomials, the following equations result:

$$B_{m+2k}^m(\alpha) = \left[\frac{1}{2\alpha m} (m+2k+1) \right] \sum_{i=0}^{I-1} \sum_{j=0}^{J-1} g(\xi_j + \Delta \xi_j, x_i + \Delta x_i) \cdot \left[\sin(m\xi_{j+1}) - \sin(m\xi_j) \right] \left[H_{m+2k+1}(\alpha x_{i+1}) - H_{m+2k+1}(\alpha x_i) \right] \quad (22)$$

$$D_{m+2k}^m(\alpha) = - \left[\frac{1}{2\alpha m} (m+2k+1) \right] \sum_{i=0}^{I-1} \sum_{j=0}^{J-1} g(\xi_j + \Delta \xi_j, x_i + \Delta x_i) \cdot \left[\cos(m\xi_{j+1}) - \cos(m\xi_j) \right] \left[H_{m+2k+1}(\alpha x_{i+1}) - H_{m+2k+1}(\alpha x_i) \right] \quad (23)$$

Since it is not possible to sum over an infinite number of terms, equation (17) is replaced by the sum of a finite series:

$$f(x, y, z) = \left(\frac{\alpha}{\pi}\right)^2 \sum_{k=0}^K \sum_{m=0}^M \epsilon_m (-i)^k \left[\frac{k!}{(m+2k)!} \right] (\alpha^2 x^2 + \alpha^2 y^2) L_k^m(\alpha^2 x^2 + \alpha^2 y^2) \\ \cdot \left[B_{m+2k}^m(\alpha) \cos(m\phi) + D_{m+2k}(\alpha) \sin(m\phi) \right] e^{-(\alpha^2 z^2 + \alpha^2 y^2)} \quad (24)$$

The accuracy of the representation depends on the values of K, M, $\Delta\xi$ and Δx chosen and convergence of the series is influenced by the parameter α .

B. THE FLOW AROUND A RIGHT CIRCULAR CONE

1. Axisymmetric Case

The problem of the supersonic flow around a cone has been extensively studied by several investigators ever since it was first opened up by Busemann, Bourquard and Taylor and Maccoll. The basic approach to the problem is outlined below but a detailed description may be found in References 12, 13, 14 and 17.

Starting with the equations of motion of inviscid flow in three dimensions expressed in spherical co-ordinates:

$$\left. \begin{aligned} u \frac{\partial u}{\partial r} + \frac{v}{r} \frac{\partial u}{\partial \theta} + \frac{w}{r \sin \theta} \frac{\partial u}{\partial \phi} + \frac{1}{\rho} \frac{\partial p}{\partial r} - \frac{v^2 + w^2}{r} &= 0 \\ u \frac{\partial v}{\partial r} + \frac{v}{r} \frac{\partial v}{\partial \theta} + \frac{w}{r \sin \theta} \frac{\partial v}{\partial \phi} + \frac{1}{\rho r} \frac{\partial p}{\partial \theta} + \frac{uw - w^2 \cot \theta}{r} &= 0 \\ u \frac{\partial w}{\partial r} + \frac{v}{r} \frac{\partial w}{\partial \theta} + \frac{w}{r \sin \theta} \frac{\partial w}{\partial \phi} + \frac{1}{\rho r \sin \theta} \frac{\partial p}{\partial \phi} + \frac{uw + vw \cot \theta}{r} &= 0 \end{aligned} \right\} \quad (1)$$

and the equation of continuity:

$$\frac{d}{dr} (r r^2 u \sin \epsilon) + \frac{d}{d\epsilon} (r r v \sin \epsilon) + \frac{d}{d\phi} (r r \omega) = 0 \quad (2)$$

the cylindrical symmetry of the cone allows one to eliminate the velocity component w and all terms dependant on ϕ . In addition, application of the condition that the flow be conical, that is, no variation of the flow parameters with r , reduces equations (1) to:

$$\left. \begin{aligned} \frac{du}{d\epsilon} - v &= 0 \\ \frac{dv}{d\epsilon} + u + \frac{1}{r} \frac{dr}{d\epsilon} &= 0 \end{aligned} \right\} \quad (3)$$

the first of these equations asserting that the flow must be irrotational. The equation of continuity similarly reduces to:

$$\frac{d}{d\theta} (r v \sin \epsilon) + 2 r u \sin \epsilon = 0 \quad (4)$$

Elimination of v between (3) and (4) yields:

$$\left\{ \frac{d^2 u}{d\epsilon^2} + u \right\} \frac{du}{d\epsilon} + \frac{1}{r} \frac{dr}{d\epsilon} = 0 \quad (5)$$

Setting:

$$\frac{dr}{d\theta} = \frac{dr}{d\epsilon} \frac{d\epsilon}{d\theta} = a^2 \frac{dr}{d\epsilon} \quad (6)$$

the following ordinary differential equation is obtained:

$$\frac{d^2 u}{d\epsilon^2} + u = \frac{a^2 (u + v \cot \epsilon)}{(v^2 - a^2)} \quad (7)$$

From the Bernoulli equation:

$$\int \frac{d\rho}{\rho} + \frac{1}{2} (u^2 + v^2) = \frac{1}{2} c^2 \quad (8)$$

and with assumption of a perfect gas satisfying the equation:

$$\frac{p}{\rho^\gamma} = k \quad (9)$$

the velocity of sound a can be expressed in terms of the velocity components as:

$$a^2 = \frac{1}{\gamma} (\gamma - 1) (c^2 - u^2 - v^2) \quad (10)$$

The density, pressure and temperature are then found to vary as:

$$\begin{aligned} (a) \quad \frac{\rho}{\rho_c} &= (c^2 - u^2 - v^2)^{\frac{\gamma}{\gamma-1}} \\ (b) \quad \frac{p}{p_c} &= \left(\frac{\rho}{\rho_c} \right)^{\frac{\gamma}{\gamma-1}} = (c^2 - u^2 - v^2)^{\frac{\gamma}{\gamma-1}} \\ (c) \quad \frac{T}{T_c} &= \left(\frac{a}{a_c} \right)^2 = (c^2 - u^2 - v^2) \end{aligned} \quad (11)$$

For the solution of the governing equation (7) to be physically meaningful, it is necessary to satisfy the boundary condition of no normal velocity at the cone surface and the jump conditions at the shock wave. The physical conditions on either side of a shock wave are given by the Rankine Hugoniot relations:

$$\left. \begin{aligned} \cos^2 \alpha &= \frac{(\gamma-1) + (\gamma+1) \left(\frac{x}{y} \right)}{2\gamma \left(\frac{U}{a_1} \right)^2} \\ \tan \beta &= \frac{(\gamma-1) + (\gamma+1) \left(\frac{x}{y} \right)}{(\gamma-1) \left(\frac{x}{y} \right) + (\gamma+1)} \\ \left(\frac{x}{y} \right)^{\frac{\gamma-1}{\gamma}} &= 1 + \frac{\gamma-1}{4\gamma \cos^2 \beta} \left\{ (\gamma-1) + (\gamma+1) \left(\frac{y}{x} \right) \right\} \end{aligned} \right\} \quad (12)$$

where, referring to Figure 11,

α = Angle between the normal to the shock wave and the streamlines in front of it.

β = Angle between the normal to the shock wave and the streamlines immediately behind it.

ϕ = Angle between the streamline at any point and the radius vector from the vertex of the cone.

U = Freestream velocity.

a = Velocity of sound in the freestream.

$\frac{x}{y} = p_w/p_1$

$\frac{x}{z} = p_w/p_o$

p_1 = Pressure of the undisturbed gas in front of the shock wave.

p_w = Pressure immediately behind the shock wave.

p_o = Stagnation pressure behind the shock wave.

The boundary condition at the shock wave thus reduces to the requirement that the ratio (x/z) defined by the Rankine Hugoniot relations be equal to the pressure ratio (p/p_o) defined by equation (11a). This together with equations (12) defines the physical characteristics of the shock wave.

Many schemes have been employed in order to numerically integrate the governing differential equation and to satisfy the boundary conditions to yield the complete solution of the flow field. Results of some of these are tabulated in References 6 and 14. For the purposes of this report, the more recent results in Reference 6 have been used.

2. Flow Around Cones with Small Yaw

The governing differential equation for the flow around a yawed cone is developed on similar lines as that for axisymmetric flow with the difference that in this case, the velocity components, pressure and density are expressed as a series representation about the axial flow values. A detailed description of the procedure may be found in References 13, 15 and 17. An examination of the results reveals that although the flow is no longer irrotational, the flow field can still be regarded as conical. Furthermore, the shock wave in this case is still a cone of the same semi-apex angle as in the no-yaw case with the difference that the shock wave is itself yawed at an angle which is proportional to the angle of yaw of the cone with respect to the freestream.

In Reference 6, the method employed to obtain the flow properties is basically one of iteration. An estimate is made of the shape of the shock wave and this shape is improved in such a way that the normal velocity at the surface of the cone is made close to zero. The results are presented in the co-ordinate system shown in Figure 12. Values of u , v , w , $\frac{\rho}{\rho_\infty}$, and p at various azimuthal angles ϕ are given for various non-dimensional distances between the body and the shock wave. Such results are tabulated for cones of different half-cone angles, Mach number and angle of attack at which the flow can no longer be considered conical. For the case of a 10 degree half-angle cone,

this limiting angle of attack is 10 degrees at a Mach number of 3.0 and 11 degrees at a Mach number of 2.0.

IV. DESCRIPTION OF THE EXPERIMENT

A. NUMERICAL SIMULATION OF THE EXPERIMENT

The suitability of the computer program HOLOFER for handling cases with discontinuities in slope had been investigated by means of various test function inputs into the program in Reference 3. The accuracy of the inversion in these cases was reported to be within 3.8 percent. In order to verify the applicability of the program to the present investigation, known values of the density along one line of sight, obtained from Reference 6 at a particular cross-section in the flow, were fed in as input and Mode 1 operation of the computer program utilized. In this mode, the program calculates the fringe number array that would result from the specified density distribution and then uses this data as the input for inversion to obtain the density distribution. One of the primary objectives of this investigation was to determine the effect of opaque objects introduced into the flow field and the presence of the shock wave on the resulting inversion. It was found that the effect of the presence of the cone could be reduced by the introduction of a fictitious density distribution in the area occupied by it of a constant value equal to the density at the cone surface.

B. EXPERIMENTAL PROCEDURE

1. Laboratory Techniques

It has been shown in Reference 10 that the transmitted intensity from a diffuse glass falls off below 30 percent of the incident intensity beyond viewing angles of ± 8 degrees. Thus this represents a limit on the field of view obtainable from a single hologram. For the flow around a right circular cone at incidence, there is planar symmetry and hence a 90 degree field of view is required for complete coverage of the total flow field. This coverage can be obtained by the simultaneous production of a number of holograms in various azimuthal positions as employed in Reference 3 or by a rotation of the viewing angle between each production of a single hologram. Taking advantage of the steadiness of the flow fields investigated, holograms covering various sectors of the flow field were obtained by rotating the cone to six positions in a 90 degree sector, one hologram being obtained in each case.

Complete angular coverage of the flow field was obtained by a rotation of the cone and spindle arrangement in the mount by an angle of 15 degrees between each hologram. Since it was desired to obtain the flow field at the same cross-section for the various angles of rotation, it was necessary to obtain the holographic interferograms in such a way that the line of sight was always perpendicular to the axis of the cone. For this purpose, a pair of grids were used, one on each wall of the test section, in which

the lines were designed to be parallel and perpendicular to the cone axis for a particular rotational position of the cone. The two grids were offset laterally with respect to each other in order to account for the rotation of the cone axis away from the central plane when the cone was rotated. On production of the holograms, the variable viewing property of light field holograms was utilized to line up the two grids thereby ensuring that the line of sight was normal to the axis of the cone. This would have involved a considerable amount of complexity and effort if a conventional Mach-Zehnder interferometer had been employed for the same purpose.

Since the coherence length of the pulsed laser was only about 2 cms. at the output used, it was necessary to maintain the optical path lengths in the reference and scene beams nearly equal. Since the scene beam path traversed 4 inches of plexiglas while the reference beam passed through two thick plano-convex lenses, it was necessary to compensate for this by making the reference beam path 3.5 inches longer than that of the scene beam. A reference to scene beam ratio of 4:1 was found to yield good holograms.

The holograms were obtained on Agfa-Gevaert 8E-75 holographic plates, 4" x 4" in size. Development was for 5 minutes in Kodak D-19 developer, thirty seconds in an acetic acid stop bath of standard dilution, five minutes in standard fixer, one minute water wash followed by immersion in a Kodak PhotoFlo wetting agent prior to drying. Reconstruction

of the scene was achieved by illuminating the hologram with the light from a helium-neon laser operating at a wavelength of 6328 Angstroms.

2. Photographic Techniques

To obtain reconstruction of the image from the hologram, various methods can be employed. In the usual method where the hologram is re-illuminated by a beam similar to the original reference beam as shown in Figure 13, each point on the photograph is produced by a series of non-parallel rays that appear to originate from various sources on the diffuse glass that was used to construct the hologram. An almost parallel set of rays can be selected by the positioning of a small aperture at the focal plane of the imaging lens as shown in Figure 14. A similar effect is achieved by illuminating the hologram by a conjugate beam of small diameter as depicted in Figure 15. Because of the small diameter of the reconstruction beam, the illuminated portion of the hologram represents a small aperture and thus the image produced has a large depth of field. This was of considerable advantage in the production of the interferograms from the holograms since it enabled the front and rear grids, the cone and the fringes to be simultaneously projected on a screen and thus made the task of obtaining the correct viewing angle and the interferogram quite easy to achieve. A photograph of the scene was obtained by focusing the camera at the desired plane in the test section, usually in such a manner so as to be in the plane of the fringes.

The lines of sight recorded on the photograph in this case represent the almost parallel pencil of rays from the diffuser that pass through the effective aperture in the hologram.

3. Data Reduction

To obtain photographic interferograms, the hologram was illuminated by the conjugate reference beam using a continuous wave laser operating at a wavelength of 6328 Angstroms. A camera back with viewingscreen was placed in the position of the real image as shown in Figure 13. By lining up the appropriate horizontal and vertical lines of the front and rear grids, the viewing angle corresponding to the particular line of sight desired was achieved. As the spacing of the lines on each grid was $\frac{1}{2}$ inch and the two grids were physically $7 \frac{7}{8}$ inches apart, a viewing angle of $3^{\circ}38'$ was obtained by lining up a line on one of the grids with the adjacent one on the other. A f7.7 lens with full aperture and an exposure time of 4 seconds was used to obtain workable holograms on Poloroid Type 55 P/N film. The reduction of fringe shift was obtained by projecting the negative in a photoenlarger and by tracing the fringes, the cone surface, the shock wave and the grid line at the desired station at which the reduction was to be performed, on a sheet of paper. Some judgement was usually necessary in locating the centre of the fringes but in general the light fringes were found to be narrower than the dark fringes and a location of the fringes to within ± 0.1 of the fringe spacing in the freestream could be obtained. The

fringes in the region outside the shock were extended towards the cone surface and the fringe shift read at the points of intersection of the displaced fringes with a number of rays from the cone vertex. The assumption of locally conical flow in the region within two to three fringes on either side of the section was made in order to obtain the fringe displacements at the section from those at the points of intersection of the rays from the cone vertex with the fringes on either side of the section. The distance between the cone tip and the section at which reduction was performed was measured from the projected image and, since the actual distance between these points was known, it was possible to calculate the factor by which the projected image was magnified as compared with its true size. This magnification factor was then used to determine the actual radial distances from the cone axis at which the fringe shifts were obtained. The radius of the inversion circle was selected such that the maximum distance of the shock from the cone axis was at 95 percent of the radius of the inversion circle. From the data so obtained, the radial variation of fringe number was plotted and a smooth curve drawn through the points. The fringe number at 201 equidistant points was then read off from the curve and utilized as the input into the computer program HOLOFER in Mode 3. This mode utilizes raw data taken at the proper interval and directly read into the G array in the program by Subroutine READ. Further details about the use of this computer

program are outlined in Appendix C. For the axisymmetric case, it was necessary to feed in the fringe data along one line of sight only and to obtain the density variation along one radial line. For the asymmetric case, fringe data was fed in along six lines of sight in a 90 degree field of view and the inverted density field obtained along 9 radial lines spanning a 180 degree field of view on one side of the axis of planar symmetry of the flow. A typical reduction of an interferogram to obtain the radial variation of fringe number at a section is shown in Appendix A.

V. EXPERIMENTAL RESULTS AND DISCUSSION

A. DENSITY FIELD OBTAINED EXPERIMENTALLY

1. Computer Simulation Results

The density distribution obtained from the AGARD 167 tables for the axisymmetric case was used as a test function in Computer program HOLOFER. The fringe distribution calculated from this density distribution was inverted to obtain the original density distribution. A plot of the original density distribution and that inverted by the program is shown in Figure 16. Since the Mach number for this inversion was 2.84, it was necessary to first interpolate the 13 values obtained from Reference 6 for a Mach number of 2.84, and then to obtain from these, the values at 201 equidistant points along a line of sight within the region of the inversion circle. This was done using Computer Program 1. As a side benefit obtained from a use of this program, the discontinuities in slope in the density distribution at the cone surface that would otherwise have resulted by assuming a constant value in the region occupied by the cone, were eliminated. Various values of K, M and interval size were experimented with to obtain the minimum deviation of the inverted density distribution from the input value in the region close to the shock wave. Increasing the value of K above 500 was found to have little effect on the accuracy, the maximum variation of the inverted density being 1.5

percent of the input density value at the point of inversion. The value of α was found to affect the total number of terms in the series representation of the B and D coefficients required for convergence within the value of ϵ specified. A value of $K = 2000$, $M = 5$, $\alpha = 2.5$ and an interval size of 0.01 was found to yield the minimum effect of the shock discontinuity.

2. Experimental Results

a. Axisymmetric Case

A photograph of the holographic interferogram obtained is shown in Figure 17(a). The fringe data obtained from a reduction of the two sides of the cone is shown in Figure 17(b). Since the flow was axisymmetric, an average of the two readings was taken and a curve plotted. The values at 201 equidistant points was read off, this being input into Subroutine READ of computer program HOLOFER as the G array. The density distribution obtained from the output of the inversion is shown in Figure 18. Also shown plotted is the density field obtained from the AGARD 167 tables interpolated for a Mach number of 2.84 by computer program 2, this being the Mach number of the tunnel obtained from pressure measurements. The pressure data obtained from the visicorder is shown in Figure 19. The value of Mach number calculated from these pressure measurements compares favorably with the value obtained in earlier experiments from shadowgraphs of the flow in the tunnel. A comparison of the density distributions from the AGARD tables

and those obtained from the experiment show good agreement, the maximum variation in overall density being 8 percent of the theoretical density value.

b. Asymmetric Case

The views along which holograms were taken for the cone at 10 degrees angle of attack are shown in Figure 20 and photographs of the interferograms obtained are shown in Figures 21 to 26. Except for the 67.5 degree and 82.5 degree angles of view, the perturbation to the flow on the leeward side of the cone was insufficient to enable either the shock position or the fringe displacements on this portion of the flow field to be obtained. The fringe shifts in this region were, therefore, taken as being zero. A comparison of the shock wave position obtained experimentally from the interferograms with that from the AGARD 167 tables interpolated for a Mach number of 2.84 is shown in Figure 27. The fringe data were input into computer program HOLOFER starting with the 82.5 degree fringe distribution in order to be consistent with the plane of symmetry for which that program was written. The resulting density distribution output from the program was along the lines of sight indicated in Figure 28. A comparison of the experimentally obtained radial distributions with those from the AGARD 167 tables interpolated for a Mach number of 2.84 are shown in Figures 29 to 35.

B. ERROR ANALYSIS

The errors in the final solution are mainly due to errors in the fringe data input into the computer program. One of the major sources of error was due to the difficulty in obtaining the slope of the fringe lines in the freestream to a very high degree of accuracy. From the results of the experiments conducted on a 10 degree half angle cone in Reference 18, it was apparent that the flow in regions close to the tip of the cone would be affected by the boundary layer on the cone whereas sections near the base of the cone would be affected by the wake and expansion of the flow. In order to obtain a flow which was locally nearly conical, it was thus necessary to reduce the interferograms at a section approximately 60 to 70 percent of the cone length downstream of the tip. At this section, however, the shock wave was about 1 inch from the axis of the cone and considering that the fringes in a region about $\frac{1}{4}$ inch adjacent to the tunnel walls were affected by the boundary layer, this left a region of about $\frac{3}{4}$ inch in which the fringes of the flow in the freestream were present. It was thus difficult to obtain the slope of the fringes very accurately and it is estimated that errors of approximately ± 1 mm. in the fringe data along any fringe could have resulted. However, since the fringe data along the section was obtained by interpolation between different fringes at varying radial distances from the cone axis, this would have resulted in a smoothing of the errors to about ± 0.5 mm. Since the maximum fringe shifts obtained

were in the region of 8 mm., an error of ± 0.5 mm. corresponds to an error of approximately ± 8 percent in the magnitudes of the fringe shifts obtained.

The errors between the experimental and theoretical density curves in Figure 18 reflect the above estimates of error quite well. The experimentally obtained density distribution is generally about 5% higher than the theoretical curve and this rises to a maximum of 8% close to the cone surface. Similar errors are apparent in general in Figures 29 to 35. However, in these curves the maximum error is somewhat higher probably due to the fact that reduction was performed at a section closer to the base of the cone than for the axisymmetric case. In so far as the general magnitude of the density is concerned, the experimentally obtained distribution follows the theoretical one fairly well. Except for the density distributions for $\phi = 0^\circ$ and $\phi = 22.5^\circ$, the density starts to rise above the freestream value at a normalized radial distance from the cone axis of about 0.7, then assumes a nearly constant value before rising steeply again at a radial distance closer to the cone axis. This appears to be inconsistent with the data input into the program in which the radial distance of the shock from the cone axis is seen to decrease with increasing values of ϕ .

V. SUMMARY

A. CONCLUSIONS

The finite fringe method for the production of holographic interferograms has been applied successfully to the determination of the three-dimensional density distribution of the flow around a 10 degree half angle cone. The method has been demonstrated to yield results within an accuracy of 8 percent for the axisymmetric case and within 13 percent for the asymmetric case. The magnitude of the errors are mainly a result of the constraints imposed by the existing wind tunnel size and the fact that the cone model used produced perturbations in the flow field of a fairly small magnitude so that small errors in measurement were reflected as relatively large percentage errors. The computer program HOLOFER has been evaluated for the effect of the shock and the cone and found to yield good results.

B. ACKNOWLEDGEMENTS

The writer wishes to gratefully acknowledge Dr. D. J. Collins for his most valuable guidance and assistance throughout the course of this investigation; the technical staff of the Department of Aeronautics under R. Besel and T. Dunton, particularly N. Leckenby, G. Gulbranson, G. Middleton, G. Teaby for the fabrication and assembly of the models and equipment used in these experiments and

D. Lawrence for the preparation of the necessary drawings;
and Mrs. C. Roper for her considerable effort in the final
preparation and typing of this report.

PORT IDENTIFICATION

STEPPER POWER SUPPLY

TRANSDUCER POWER SUPPLY

24 V DC FOR STEPPING SWITCH

2V DC FOR PORT IDENTIFICATION

3V DC FOR TRANSDUCER EXCITER

SCANIVALVE

PRESSURE SIGNAL

VALVE PORT IDENTIFICATION

I5 LEADS FROM MODEL PRESSURE PORTS

PLENUM TOTAL PRESSURE

10° HALF ANGLE CONE MODEL

A

B

C

D

E

F

G

H

I

J

K

L

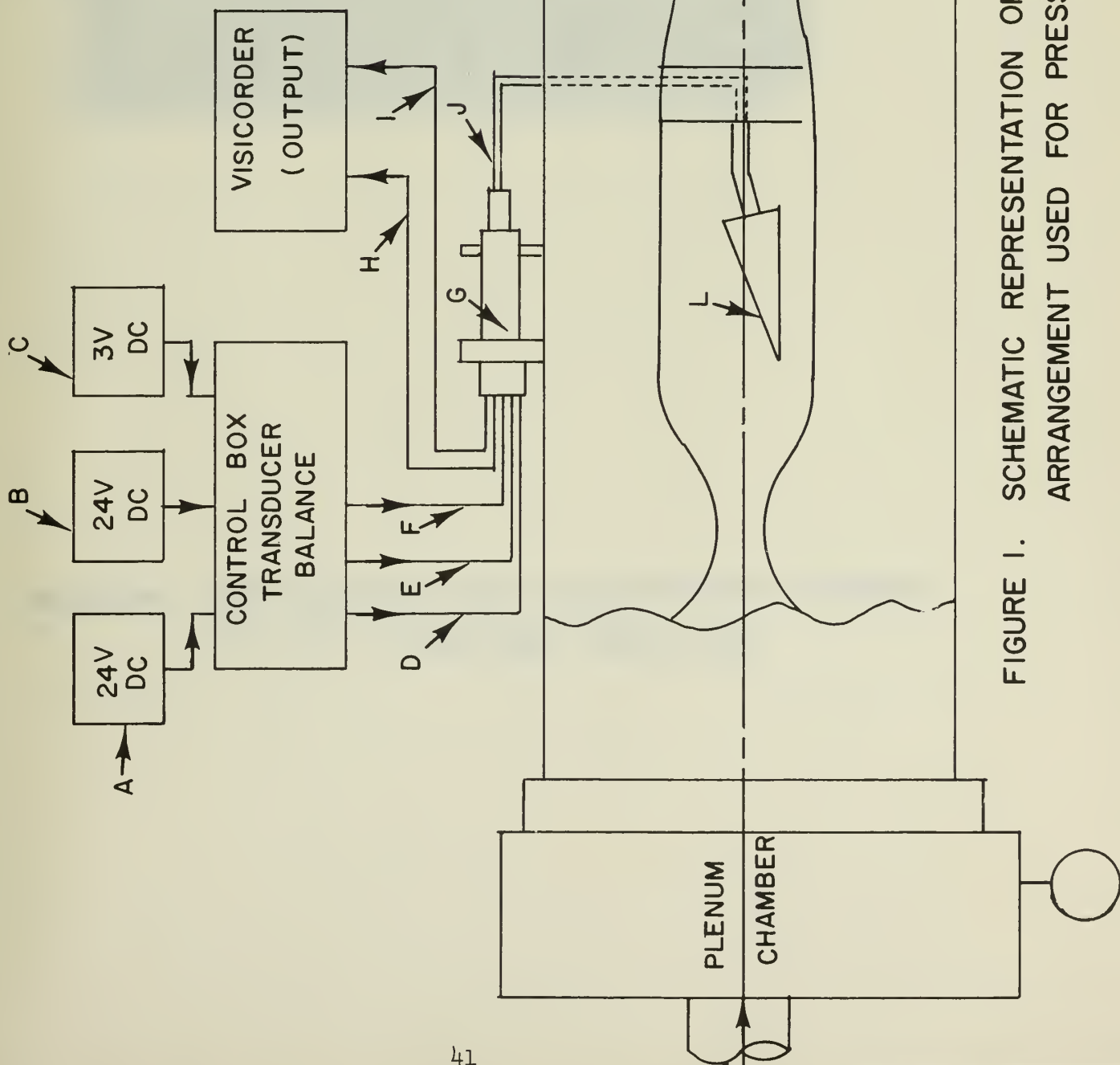


FIGURE 1. SCHEMATIC REPRESENTATION OF THE EQUIPMENT ARRANGEMENT USED FOR PRESSURE MEASUREMENT

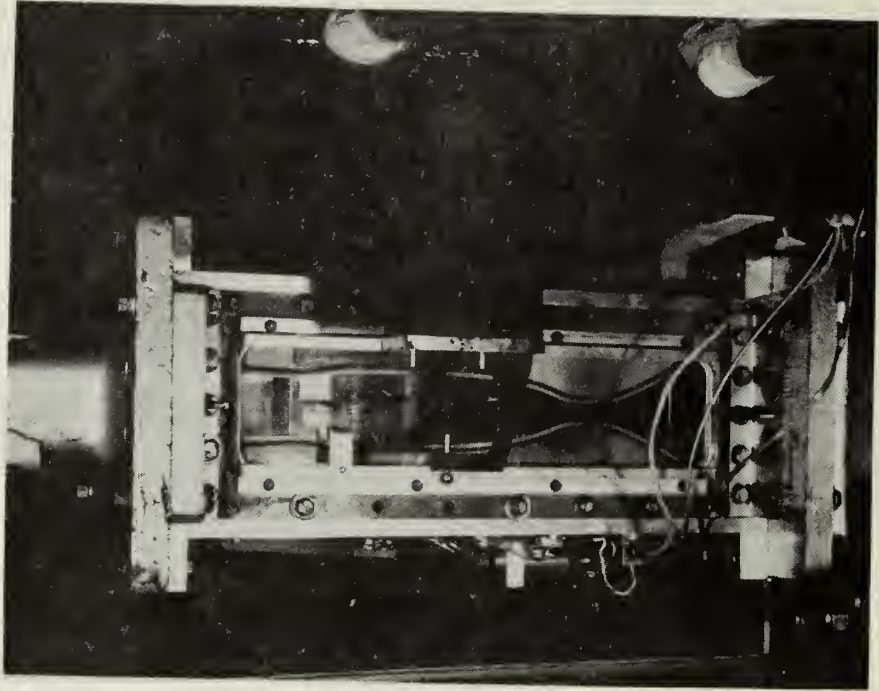


FIGURE 2. WIND TUNNEL TEST SECTION AND PRESSURE MEASURING EQUIPMENT

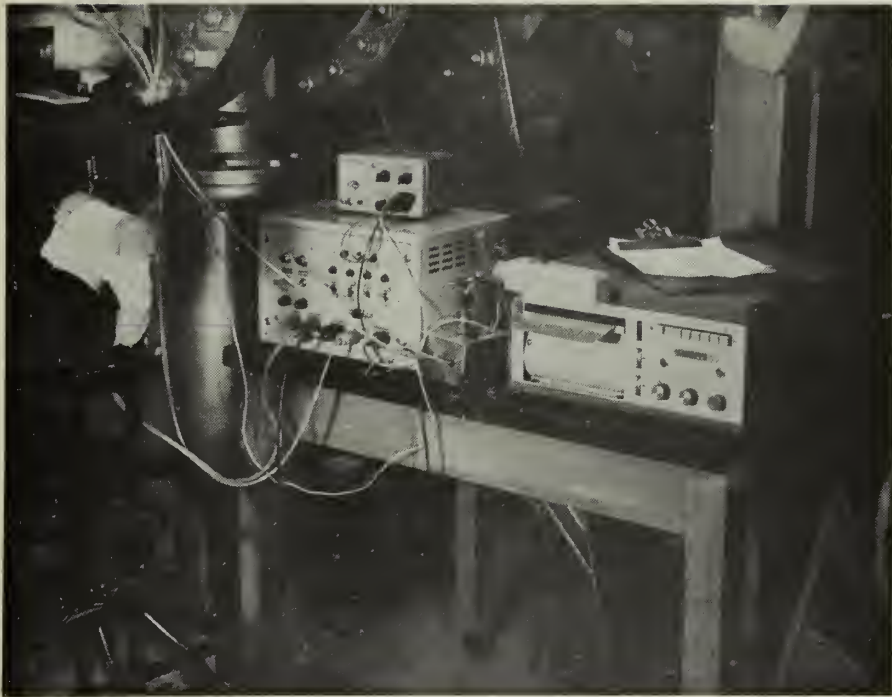


FIGURE 3. PRESSURE RECORDING EQUIPMENT, CONTROL BOX, AND POWER SUPPLIES

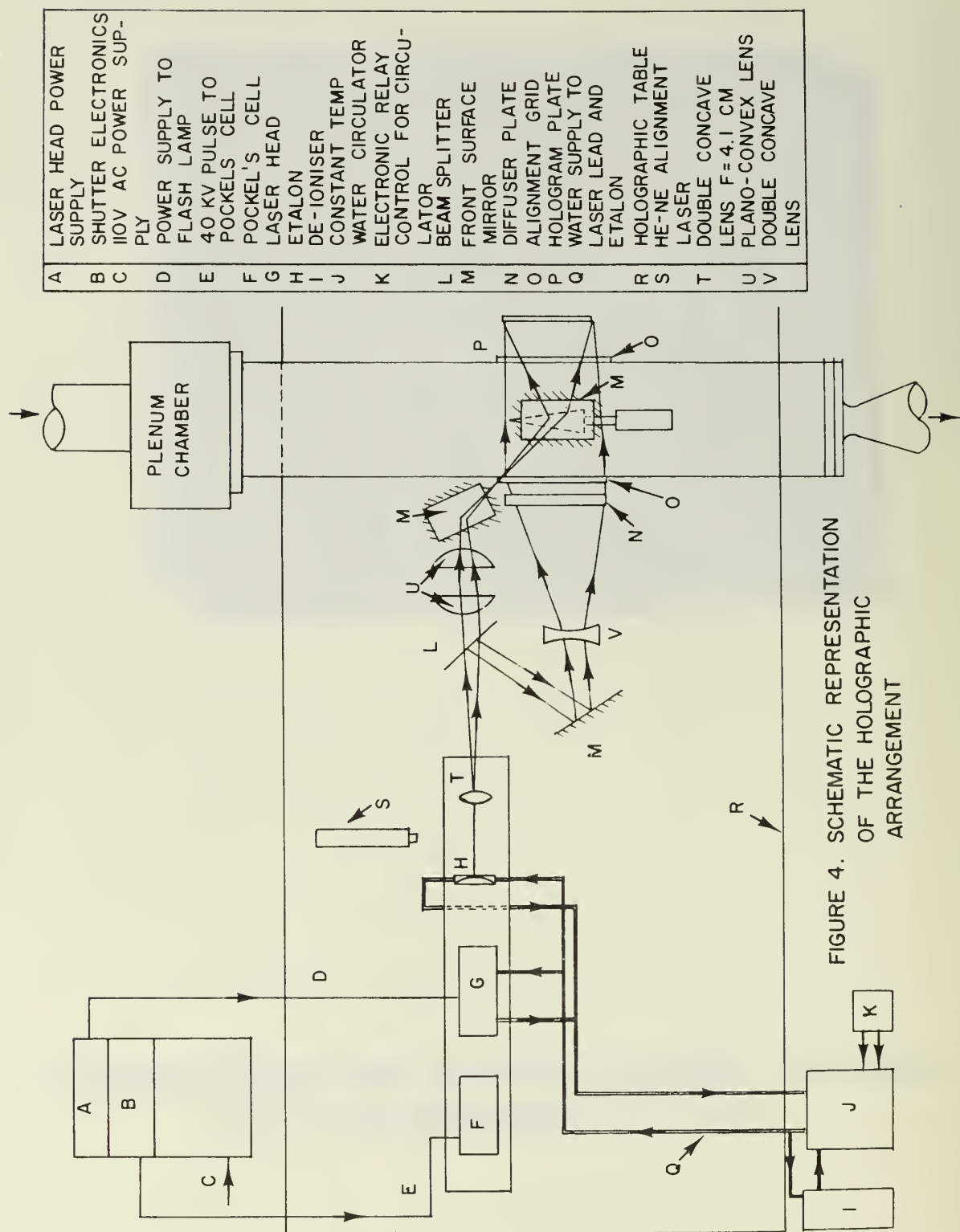


FIGURE 4. SCHEMATIC REPRESENTATION OF THE HOLOGRAPHIC ARRANGEMENT

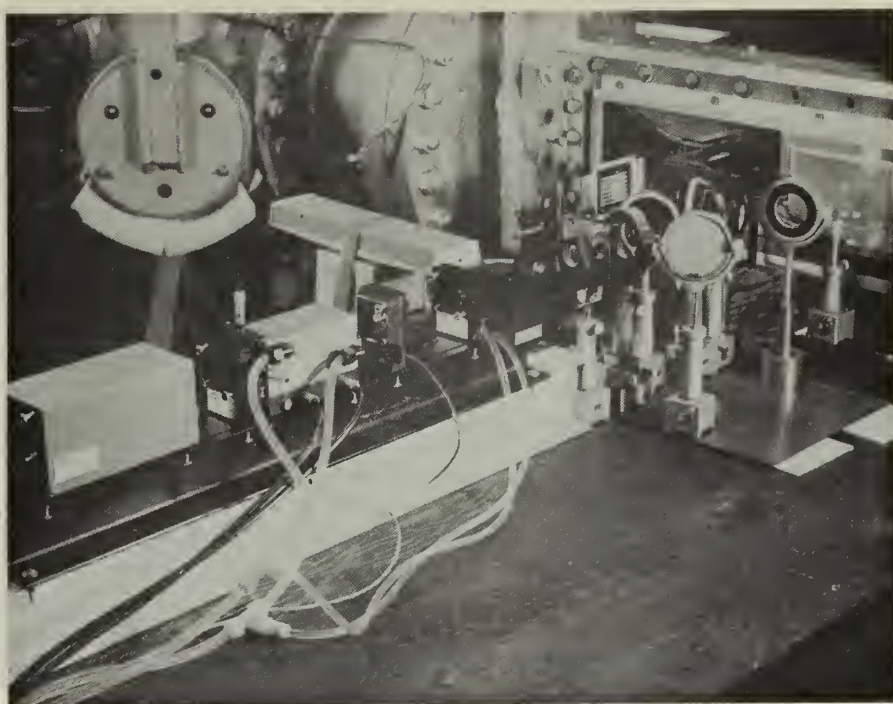


FIGURE 5a. HOLOGRAPHIC TABLE LASER CONTROL BOX
AND TEMPERATURE CONTROL EQUIPMENT

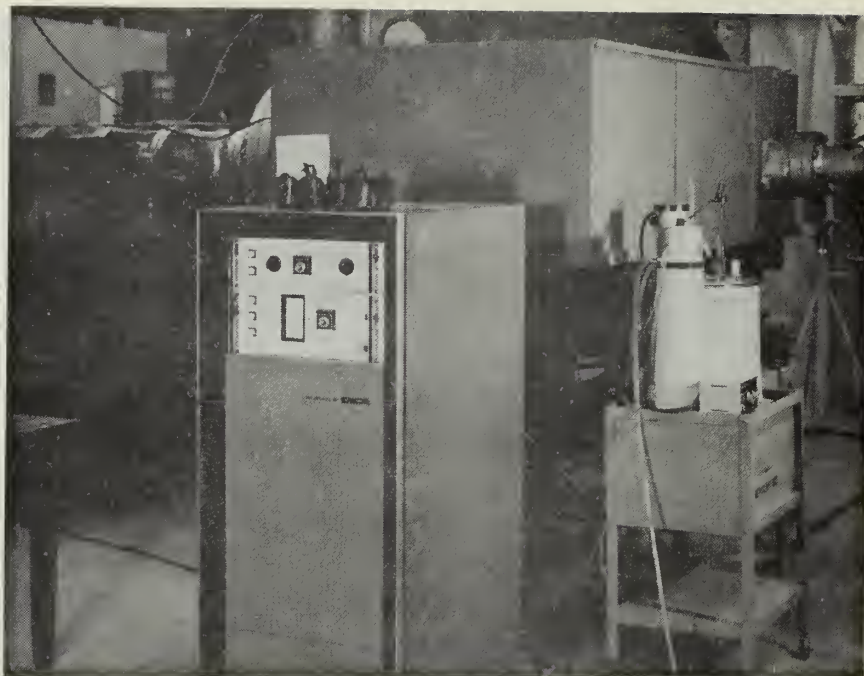


FIGURE 5b. DETAILS OF THE HOLOGRAPHIC ARRANGEMENT

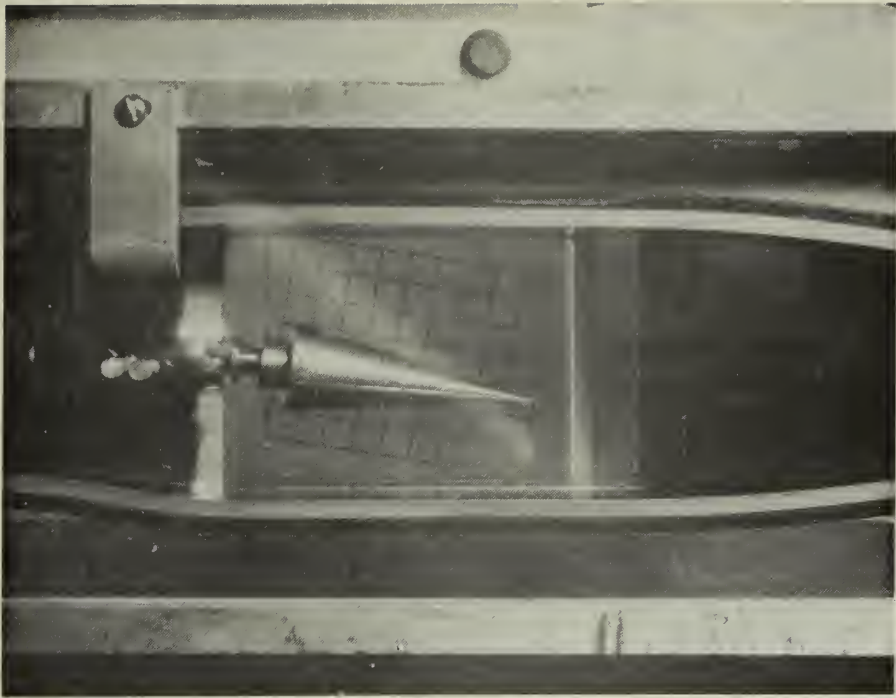
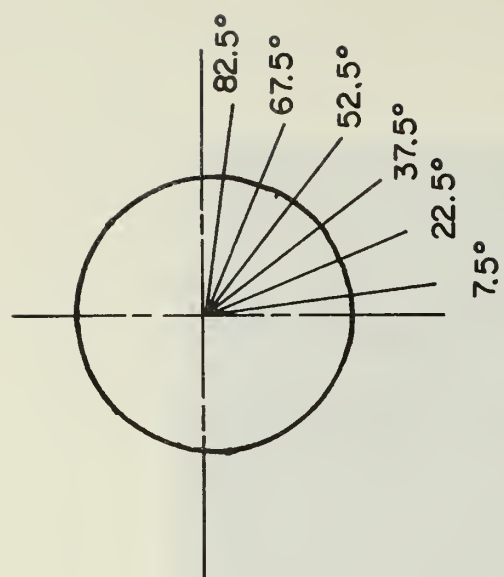
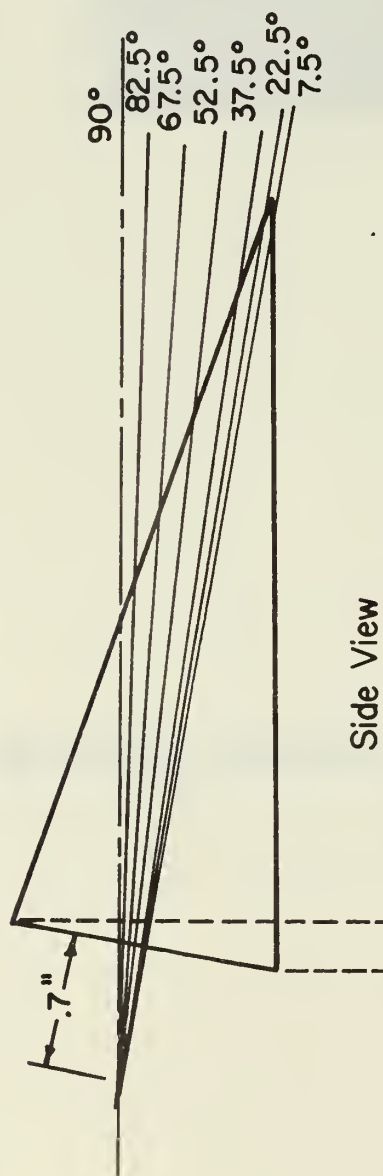


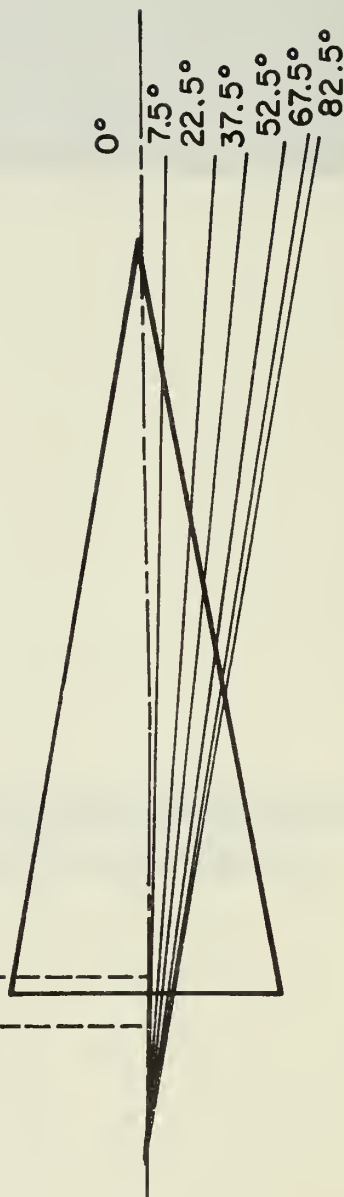
FIGURE 6. VIEW OF TEST SECTION SHOWING DETAILS OF
MODEL, MOUNT, AND GRID



End View



Side View



Bottom View

FIGURE 7a. POSITIONS OF THE CONE AXIS FOR VARIOUS ROTATIONAL POSITIONS OF THE CONE TIP

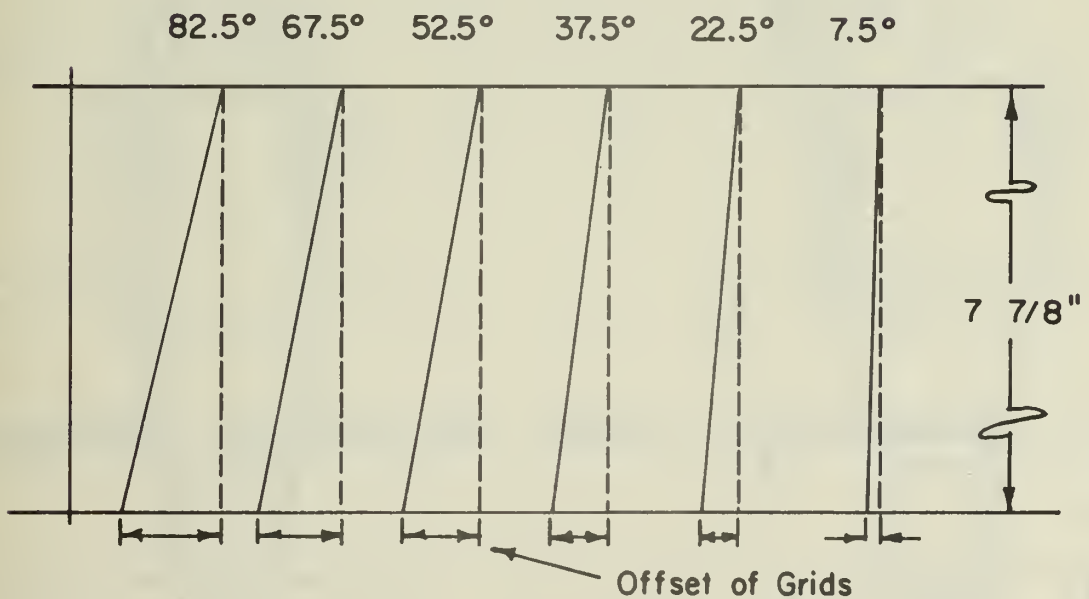
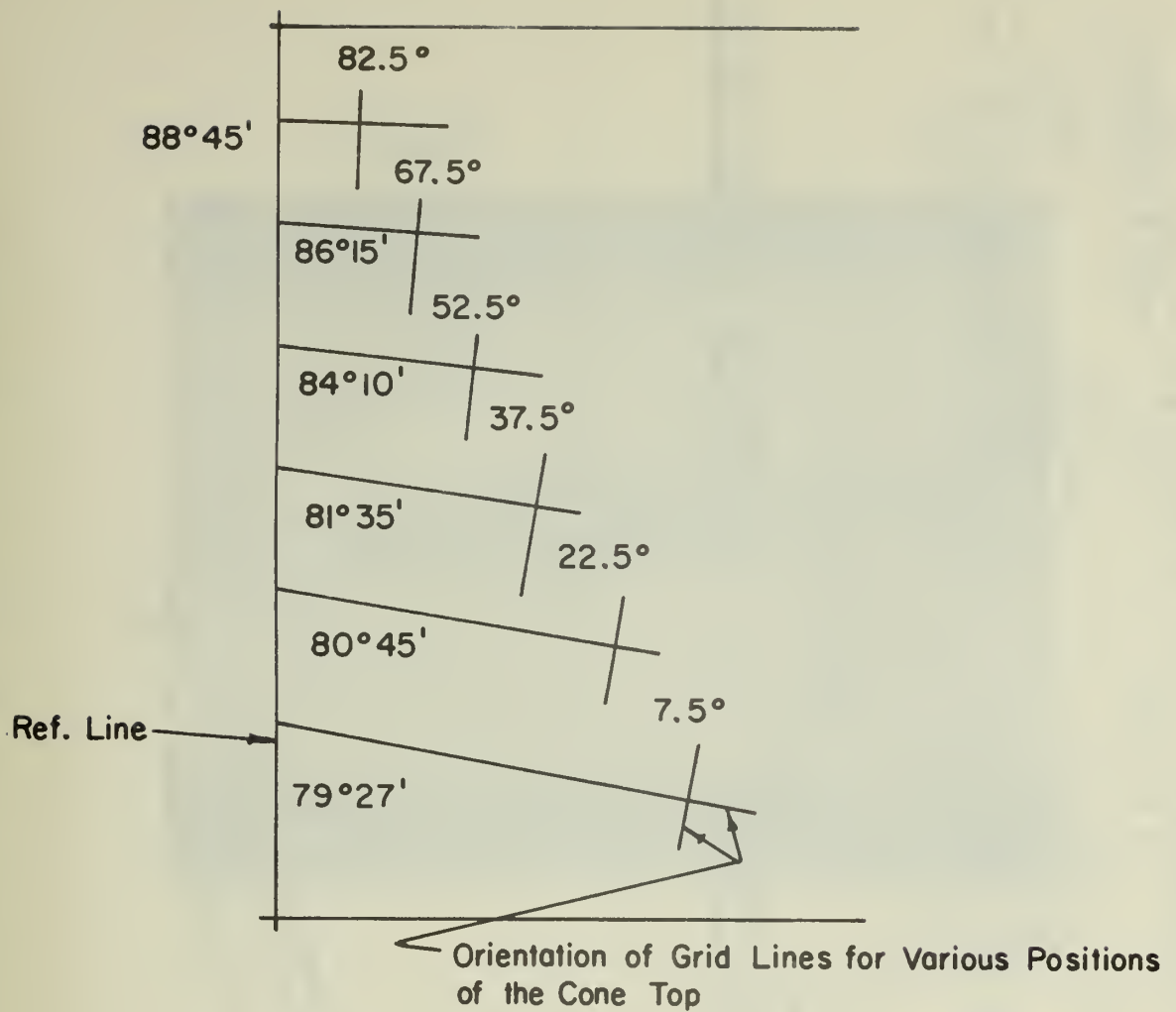


FIGURE 7b. ORIENTATION OF GRID LINES AND OFFSET OF THE GRIDS

ALL RADIALLY DRILLED HOLES .040 DIA

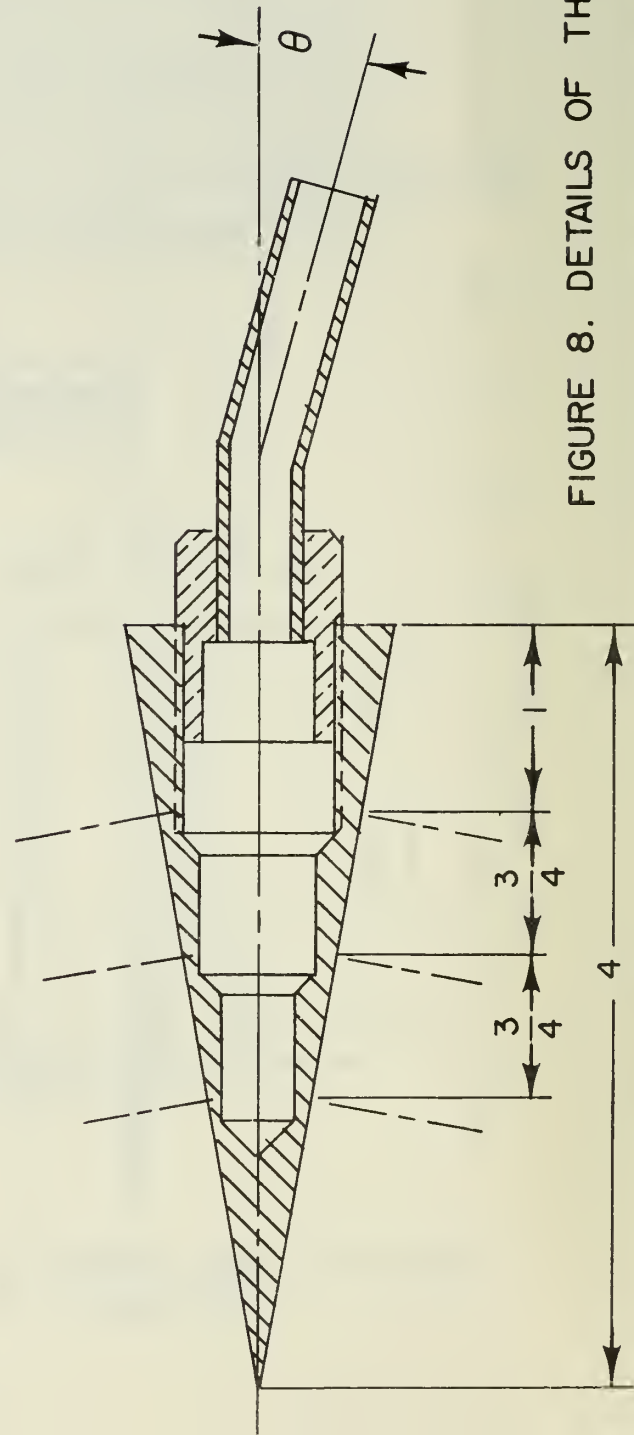
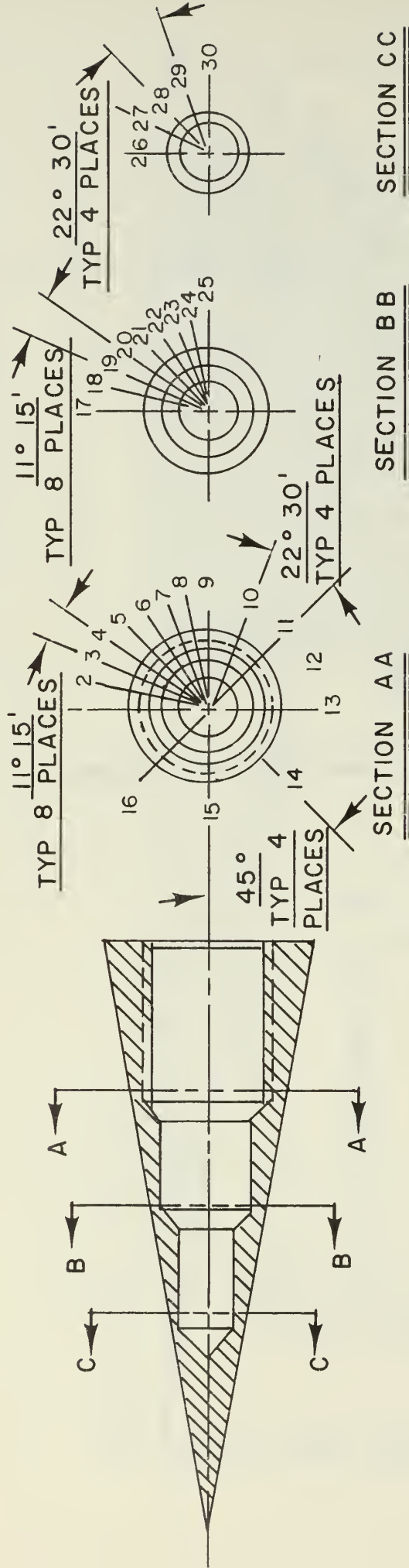


FIGURE 8. DETAILS OF THE CONE MODEL

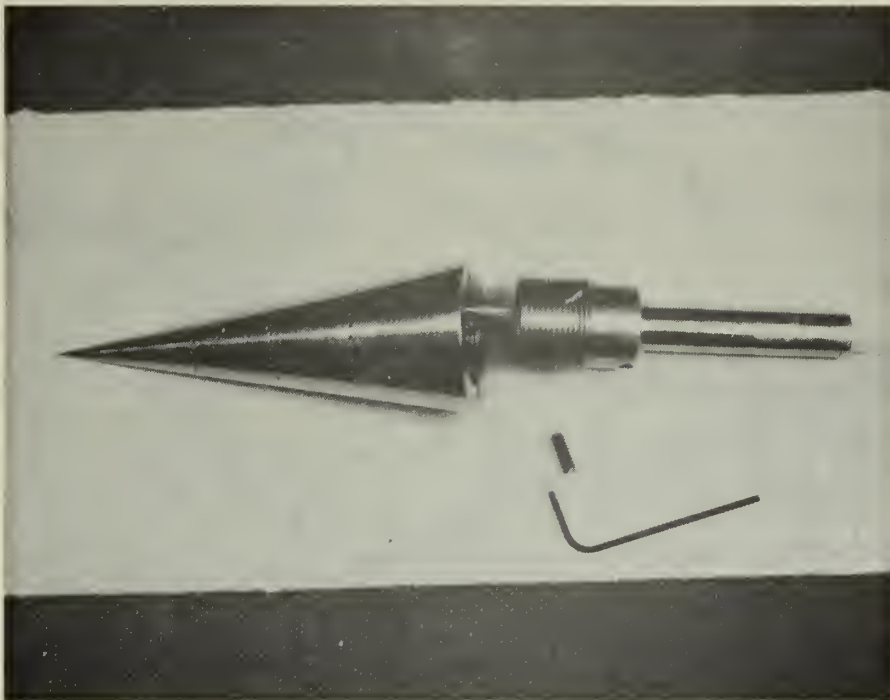


FIGURE 9. THE CONE AND SPINDLE ARRANGEMENT

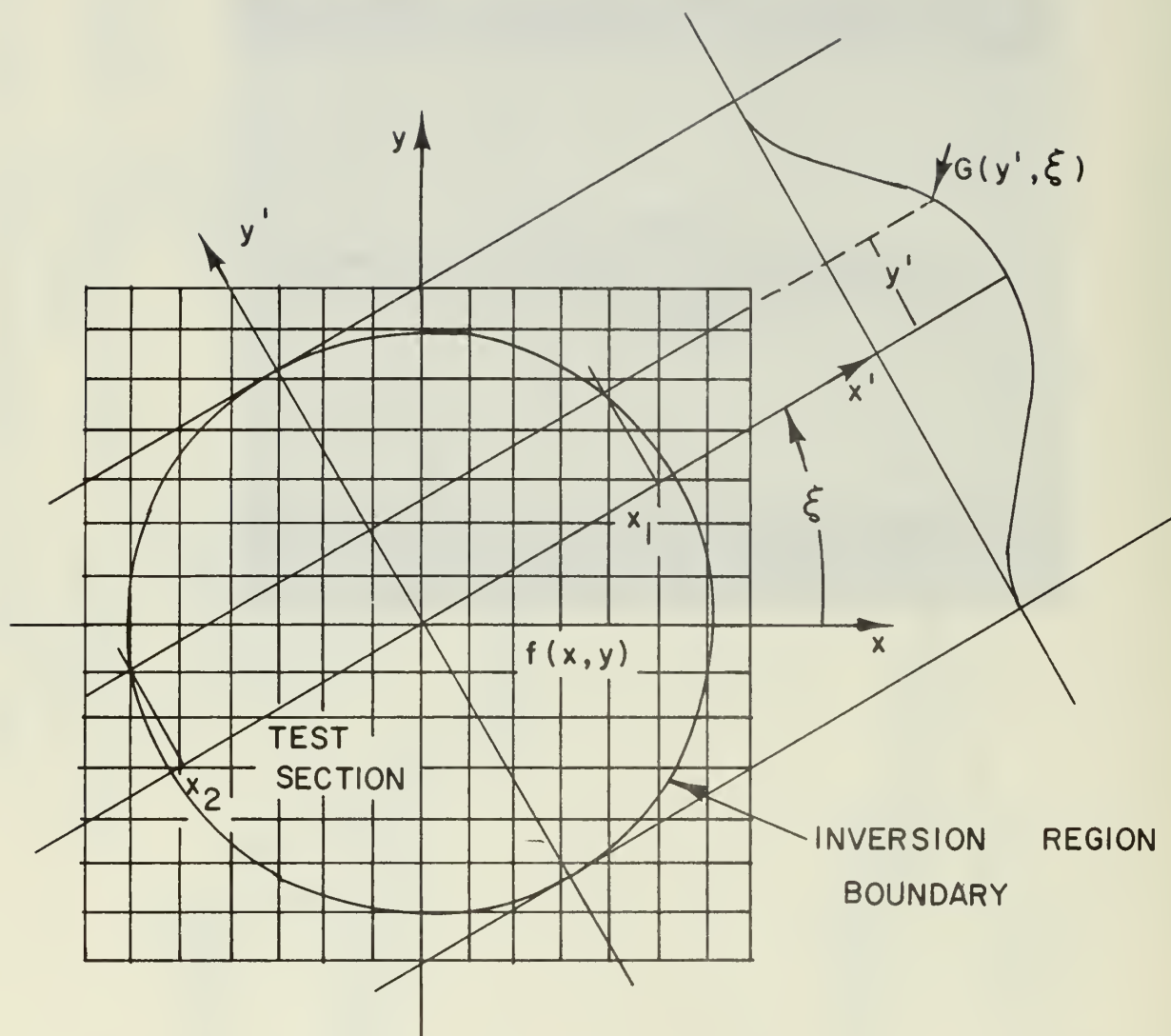


FIGURE 10. CO-ORDINATE SYSTEM USED FOR THE INVERSION OF FRINGE NUMBER TO DENSITY

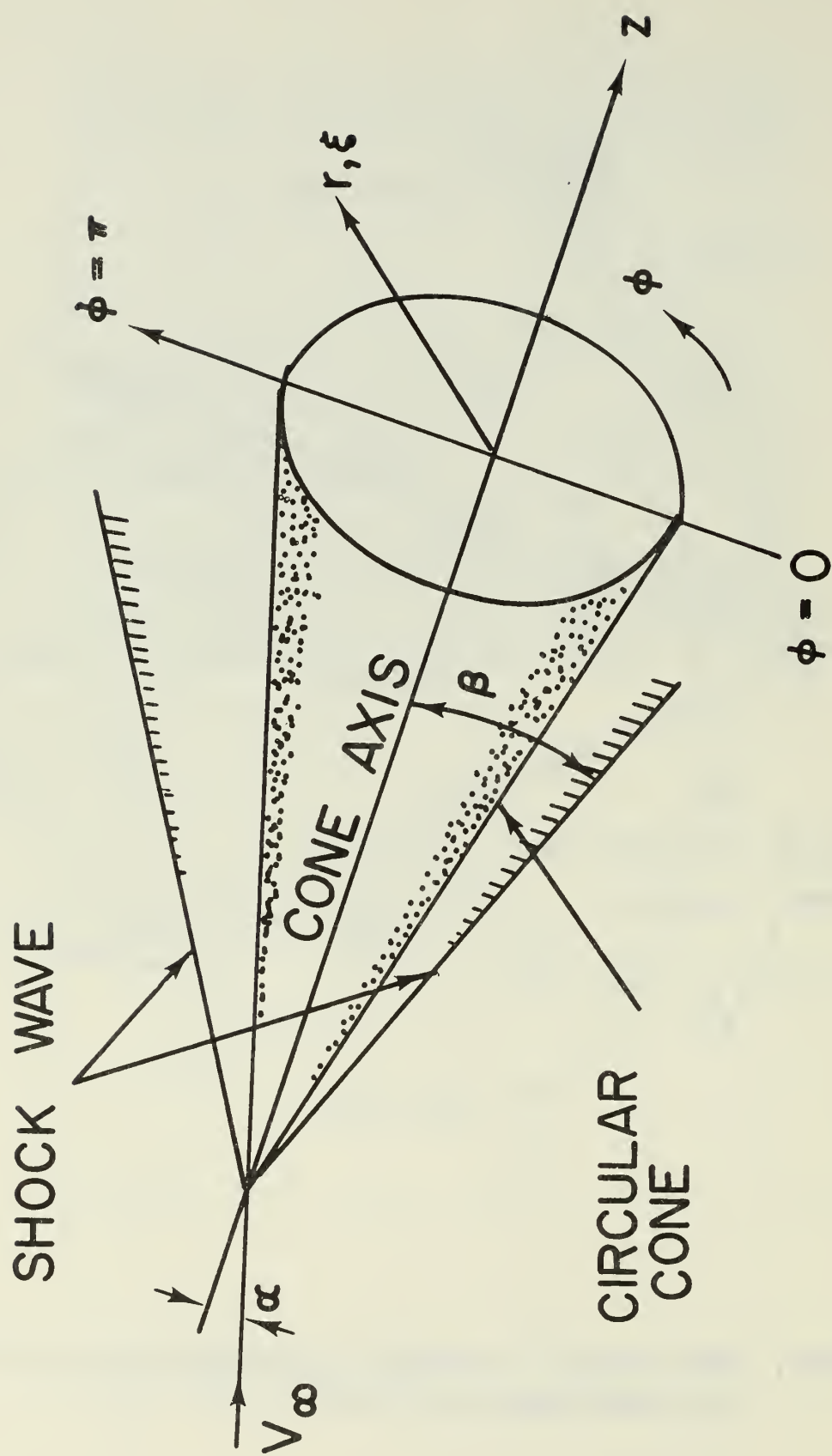


FIGURE 12. CO-ORDINATE SYSTEM USED IN REFERENCE 6

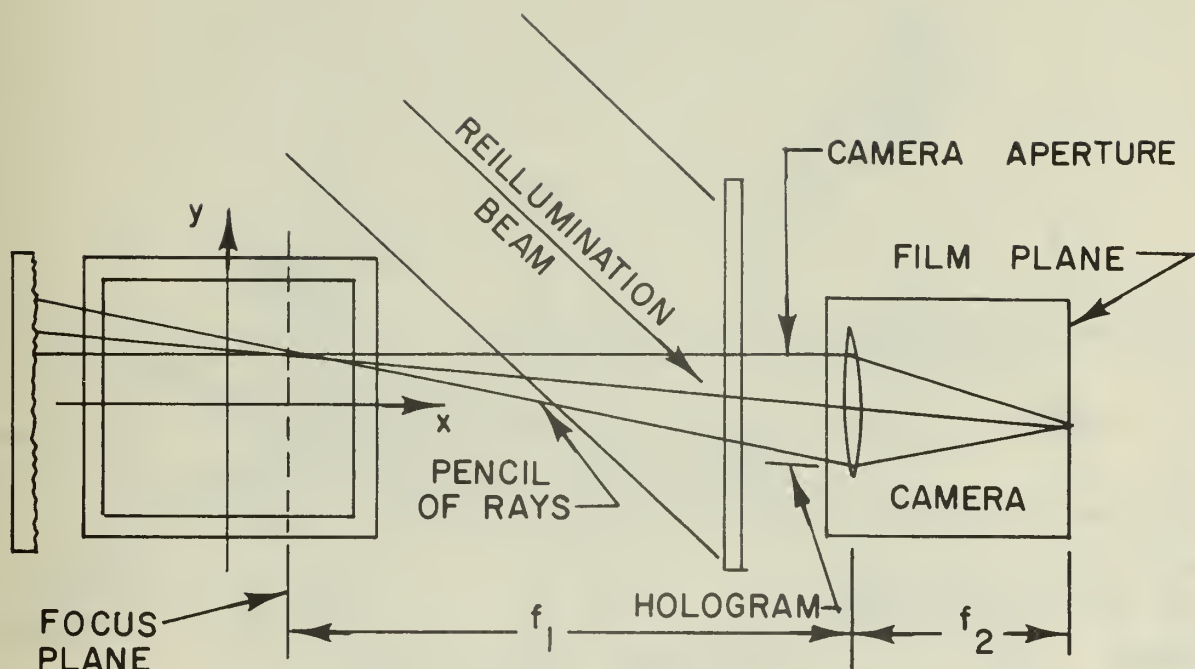


FIGURE 13. EFFECT OF APERTURE SIZE FOCUS PLANE POSITION ON THE PENCIL SIZE OF RAYS ABOUT A LINE OF SIGHT RECORDED BY CAMERA

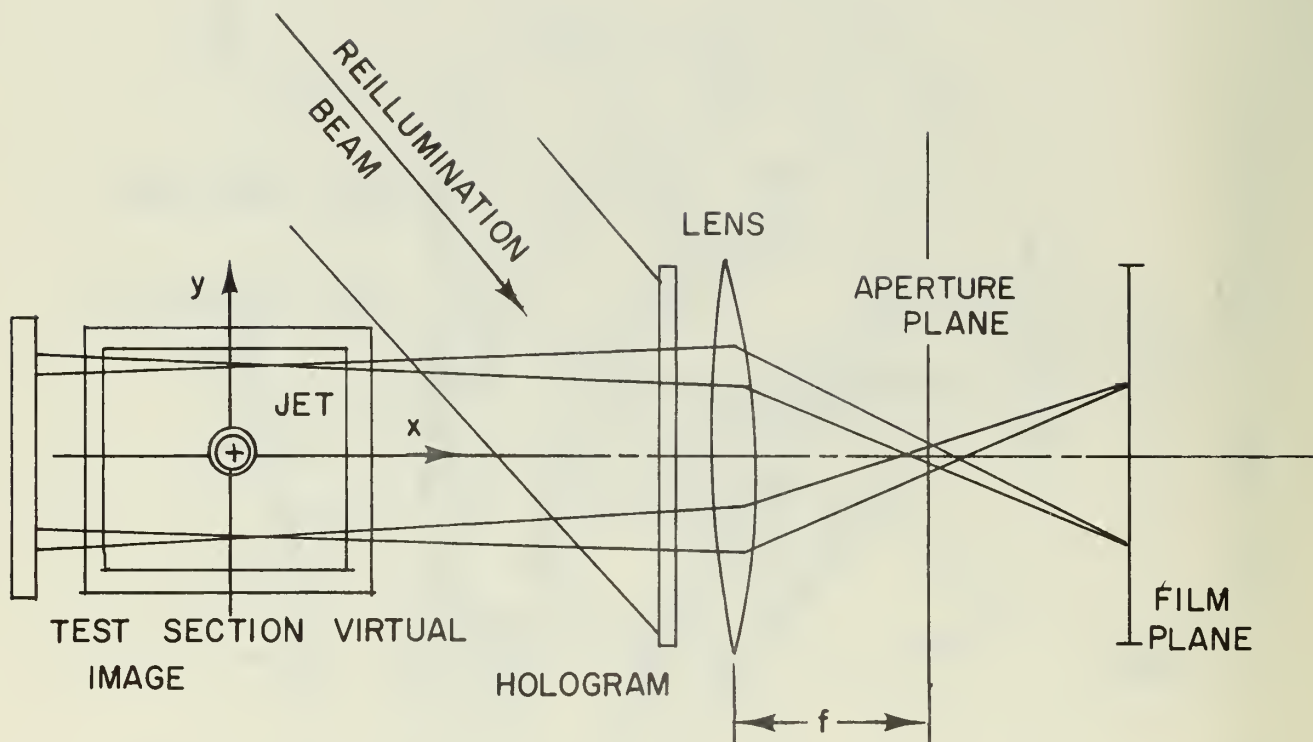


FIGURE 14. SPATIAL FILTERING TECHNIQUE FOR SELECTING PHOTOGRAPH OF CONSTANT ANGLE LINES OF LIGHT

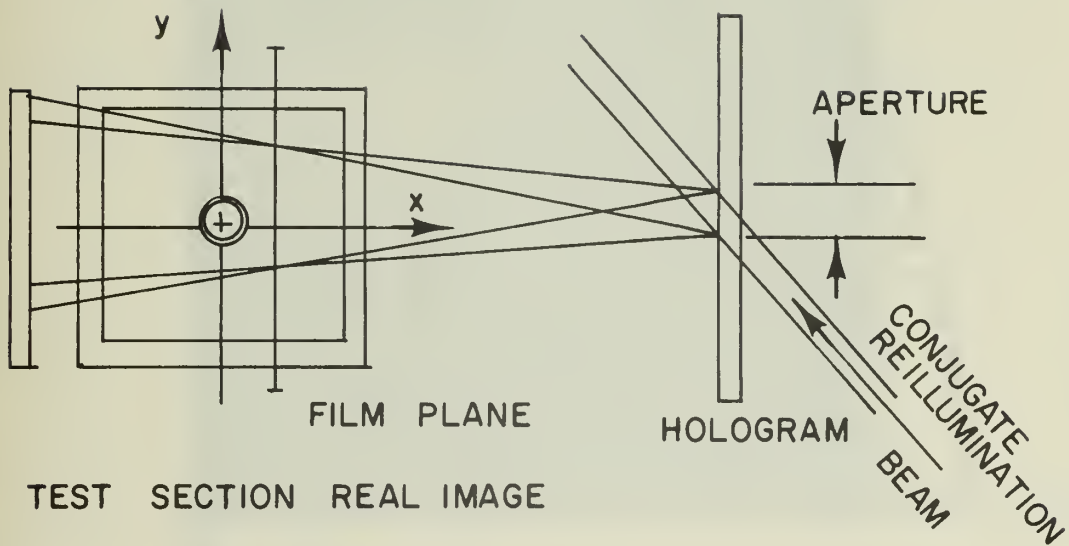


FIGURE 15. LENSLESS PHOTOGRAPHIC TECHNIQUE USING A CONJUGATE REFERENCE BEAM OF SMALL DIAMETER

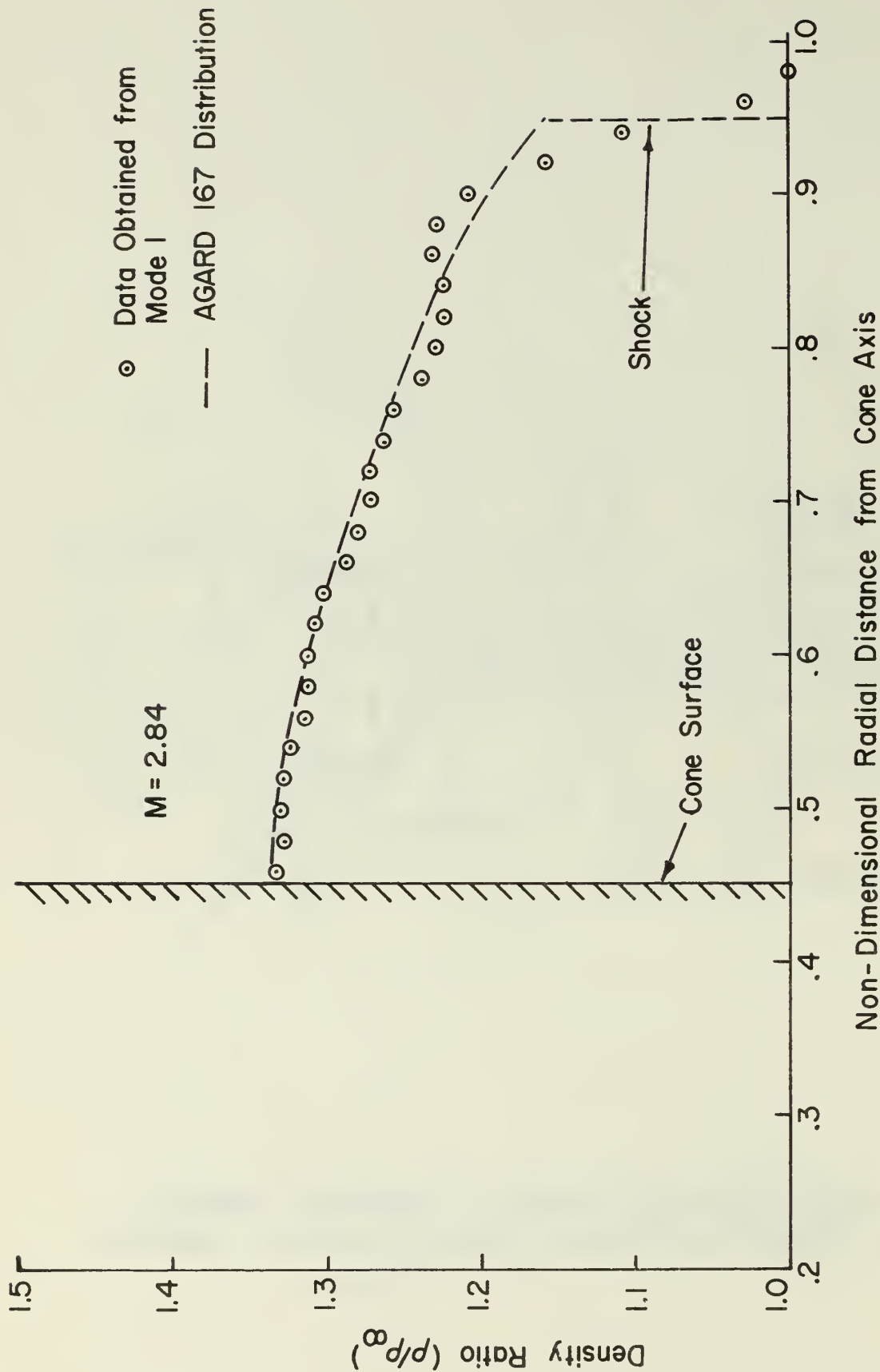


FIGURE 16
 COMPARISON OF THE RADIAL DENSITY DISTRIBUTION OBTAINED FROM MODE I
 WITH THE AGARD 167 RADIAL DENSITY DISTRIBUTION - AXI-SYMMETRIC CASE



FIGURE 17a. HOLOGRAPHIC INTERFEROGRAM OBTAINED FOR THE AXI-SYMMETRIC CASE

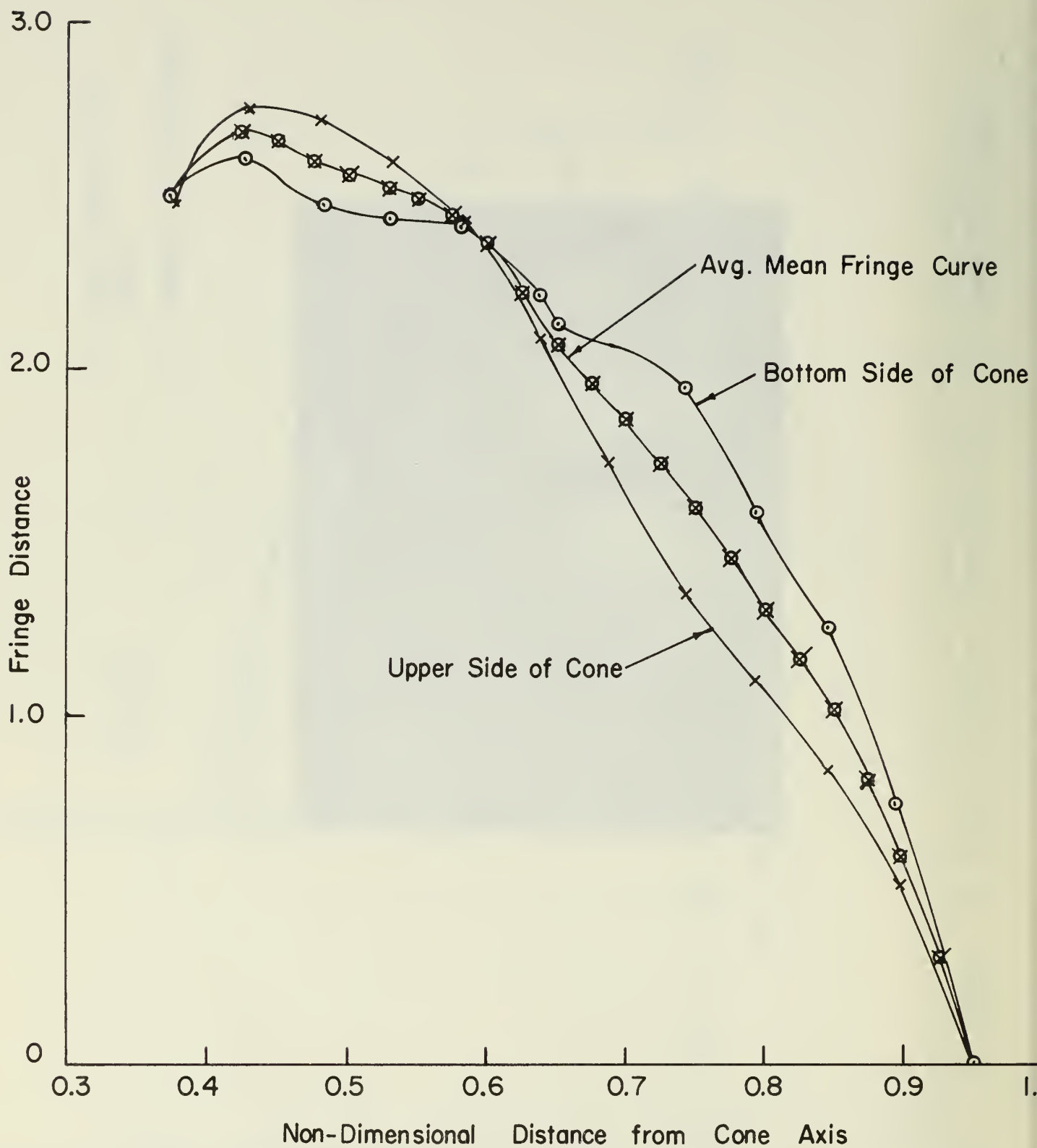


FIGURE 17b. RADIAL FRINGE DISTRIBUTION FROM A REDUCTION OF THE HOLOGRAPHIC INTERFEROGRAM FOR THE AXI-SYMMETRIC CASE

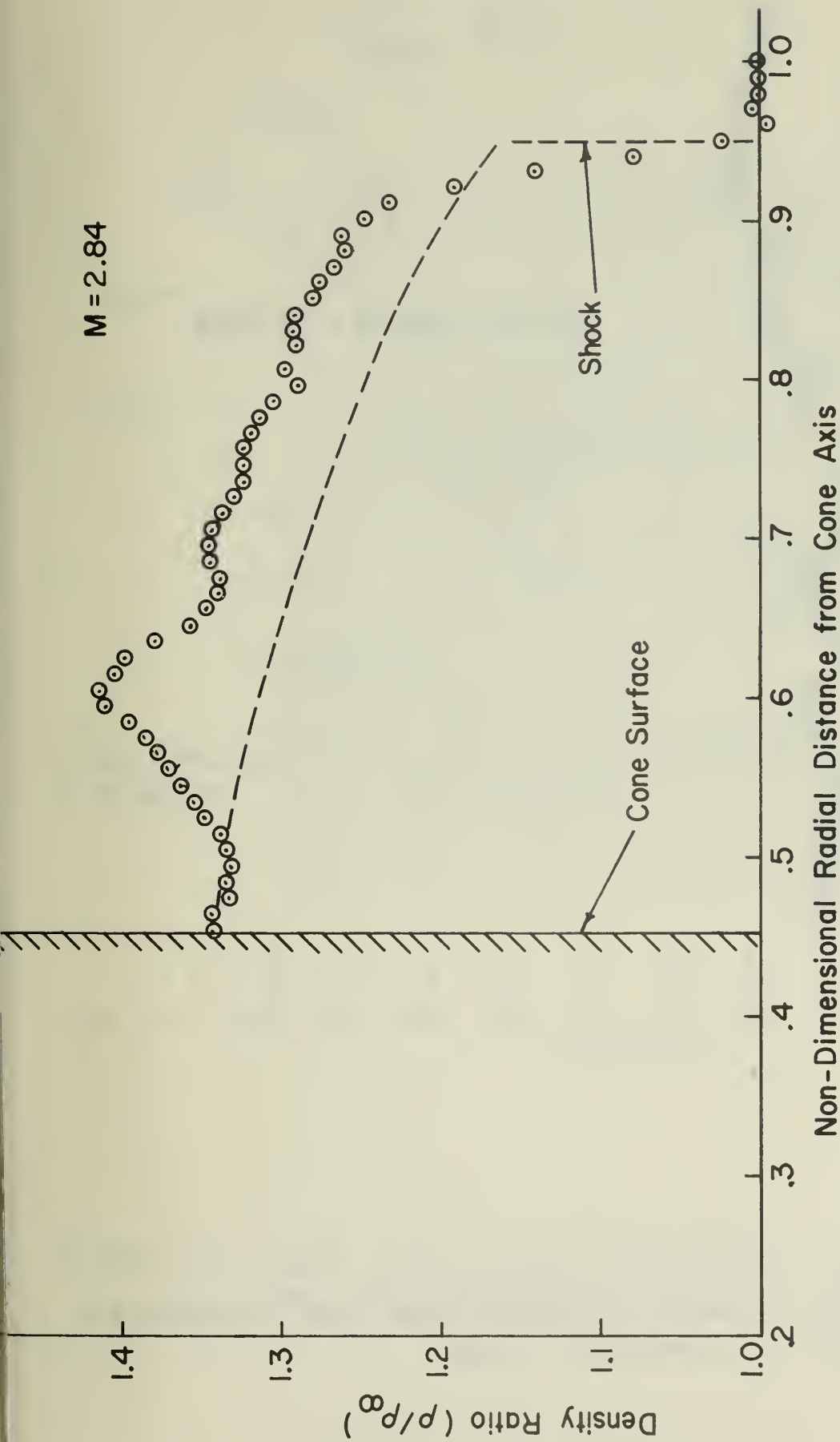


FIGURE 18.
COMPARISON OF THE RADIAL DENSITY DISTRIBUTION OBTAINED FROM
EXPERIMENT WITH THE AGARD 167 DISTRIBUTION - AXI-SYMMETRIC CASE

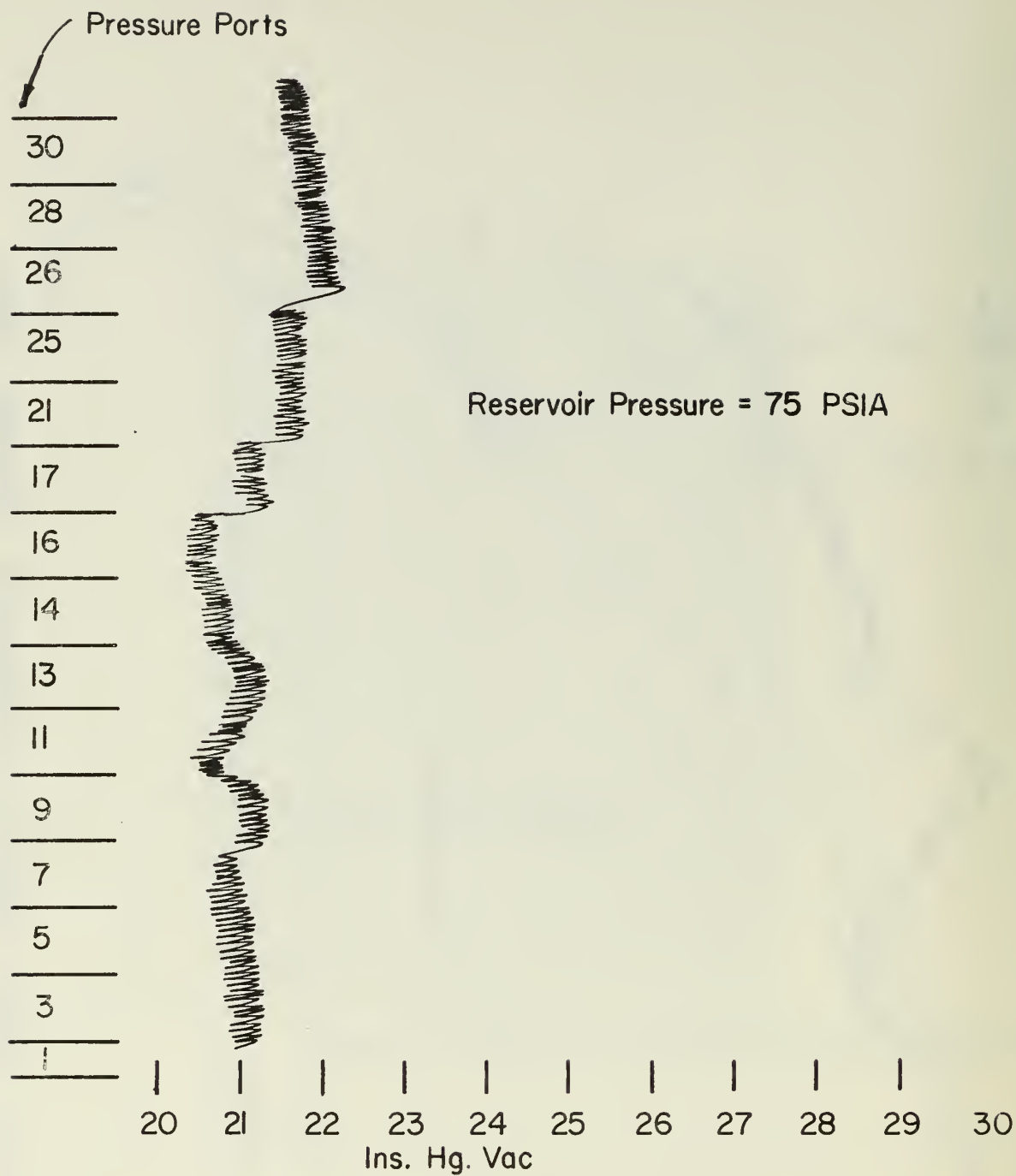


FIGURE 19. PRESSURE TRACE OBTAINED FROM THE VISCICORDER FOR THE AXI-SYMMETRIC CASE.

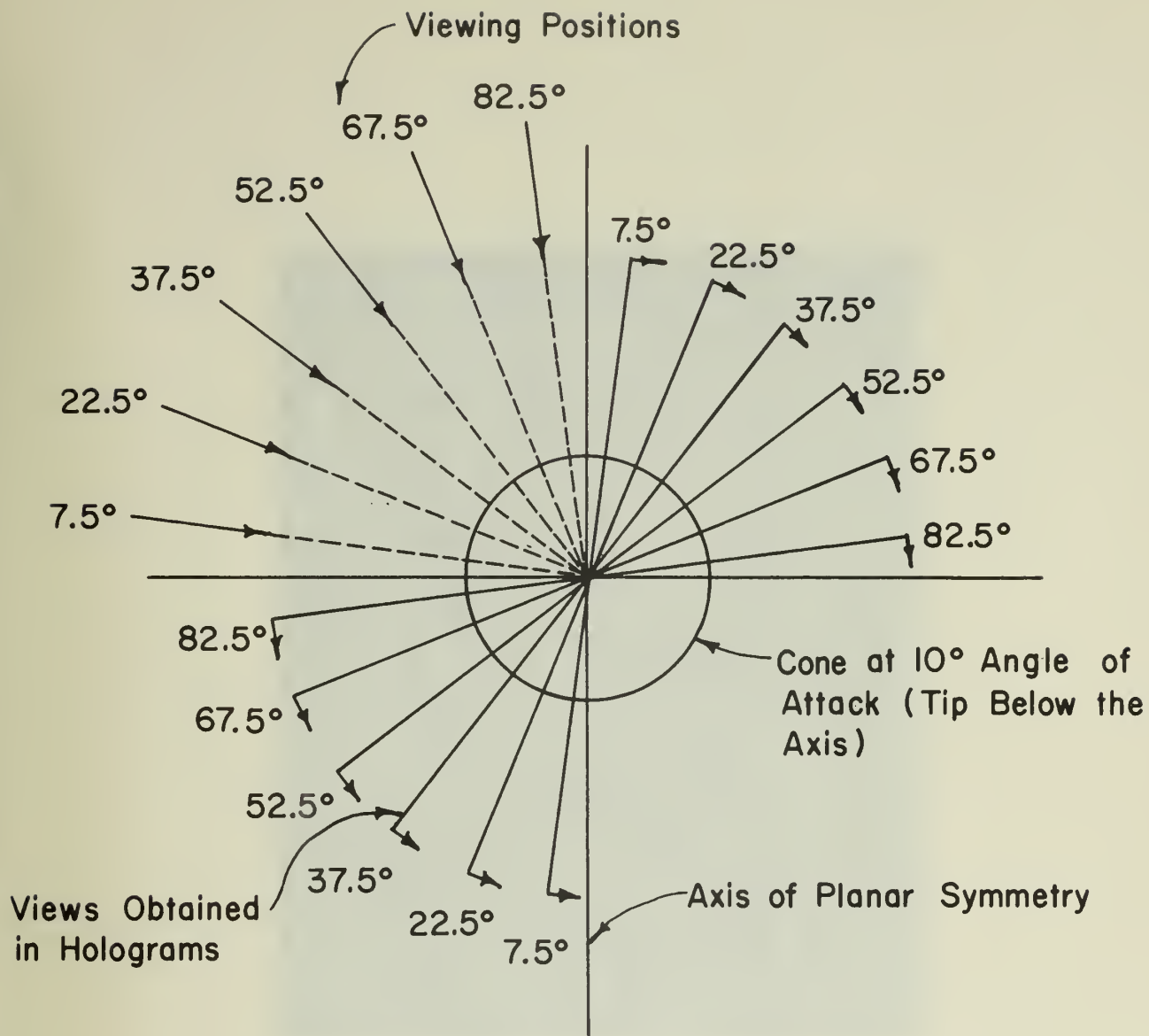


FIGURE 20. VIEWS ALONG WHICH HOLOGRAMS WERE OBTAINED FOR THE ASYMMETRIC CASE



FIGURE 21. HOLOGRAPHIC INTERFEROGRAM FOR 7.5°
ANGLE OF VIEW



FIGURE 22. HOLOGRAPHIC INTERFEROGRAM FOR 22.5°
ANGLE OF VIEW



FIGURE 23. HOLOGRAPHIC INTERFEROGRAM FOR 37.5°
ANGLE OF VIEW

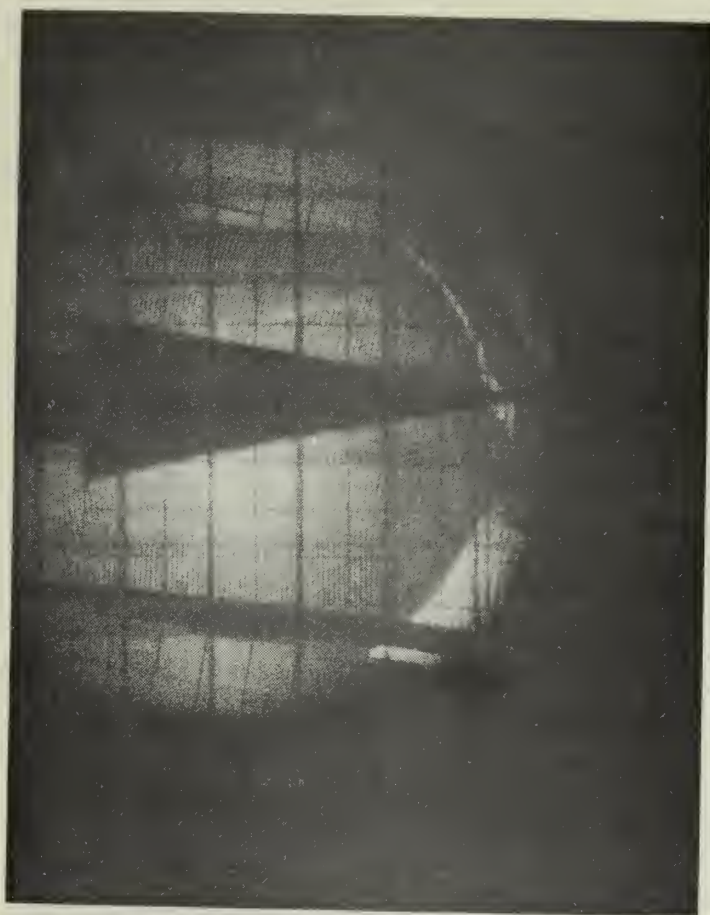


FIGURE 24. HOLOGRAPHIC INTERFEROGRAM FOR 52.5°
ANGLE OF VIEW



FIGURE 25. HOLOGRAPHIC INTERFEROGRAM FOR 67.5°
ANGLE OF VIEW



FIGURE 26. HOLOGRAPHIC INTERFEROGRAM FOR 82.5°
ANGLE OF VIEW

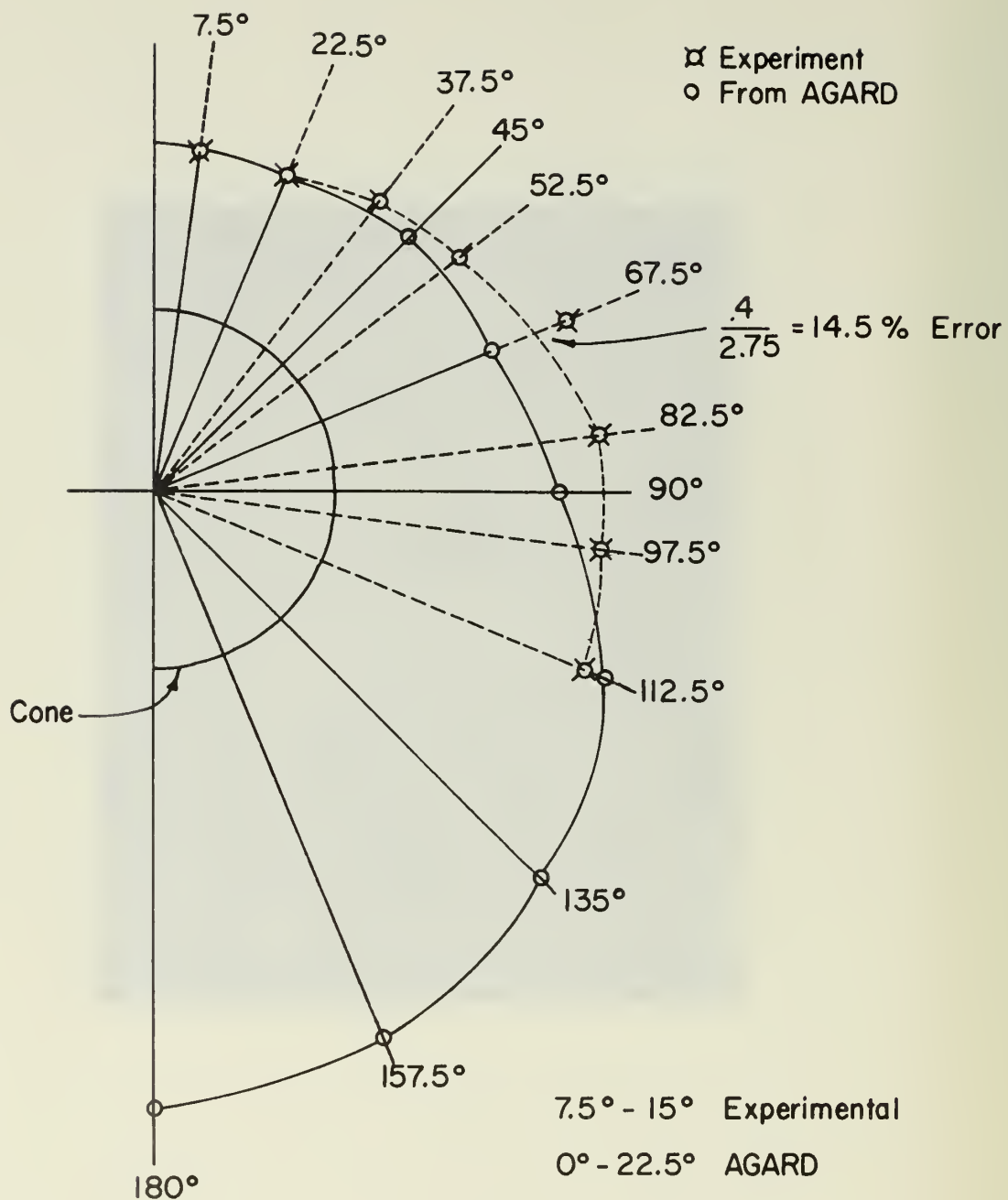


FIGURE 27. COMPARISON OF THE POSITION OF THE SHOCK WAVE OBTAINED EXPERIMENTALLY WITH THAT FROM AGARD 167 FOR $M = 2.84$, ASYMMETRIC CASE

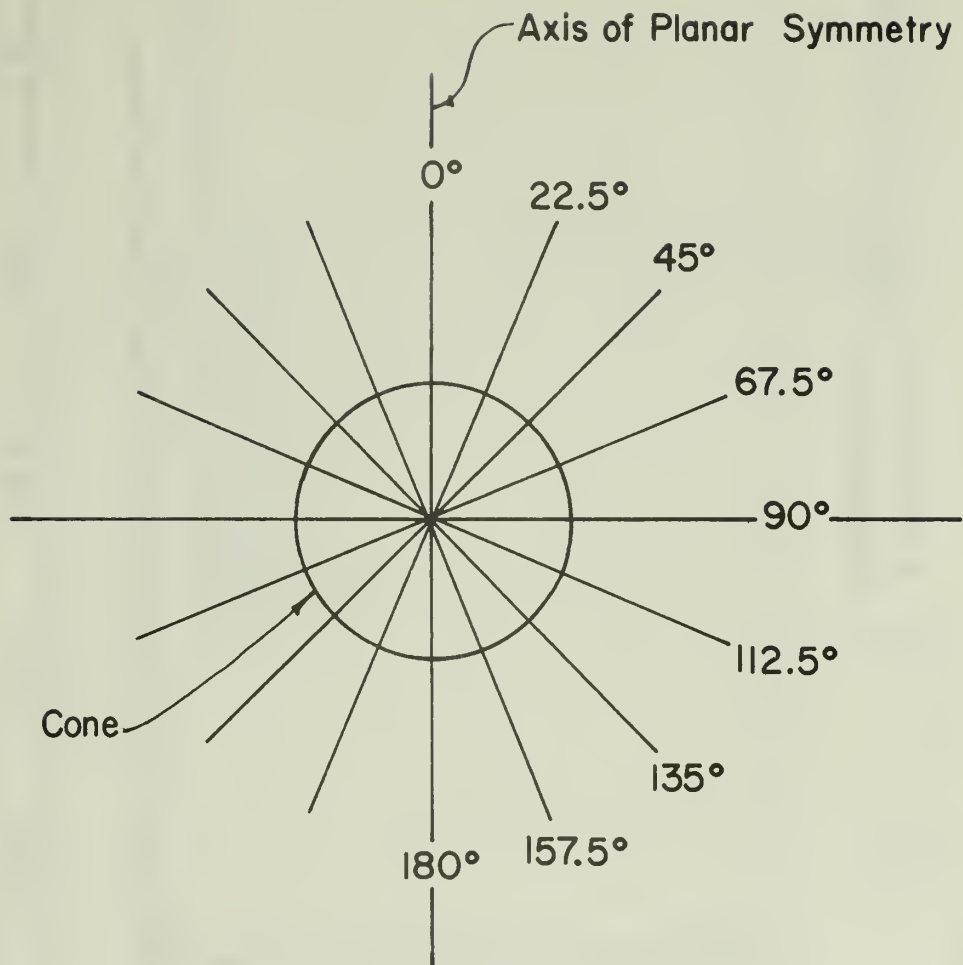


FIGURE 28. LINES OF SIGHT ALONG WHICH THE DENSITY FIELD WAS OBTAINED AFTER INVERSION, ASYMMETRIC CASE

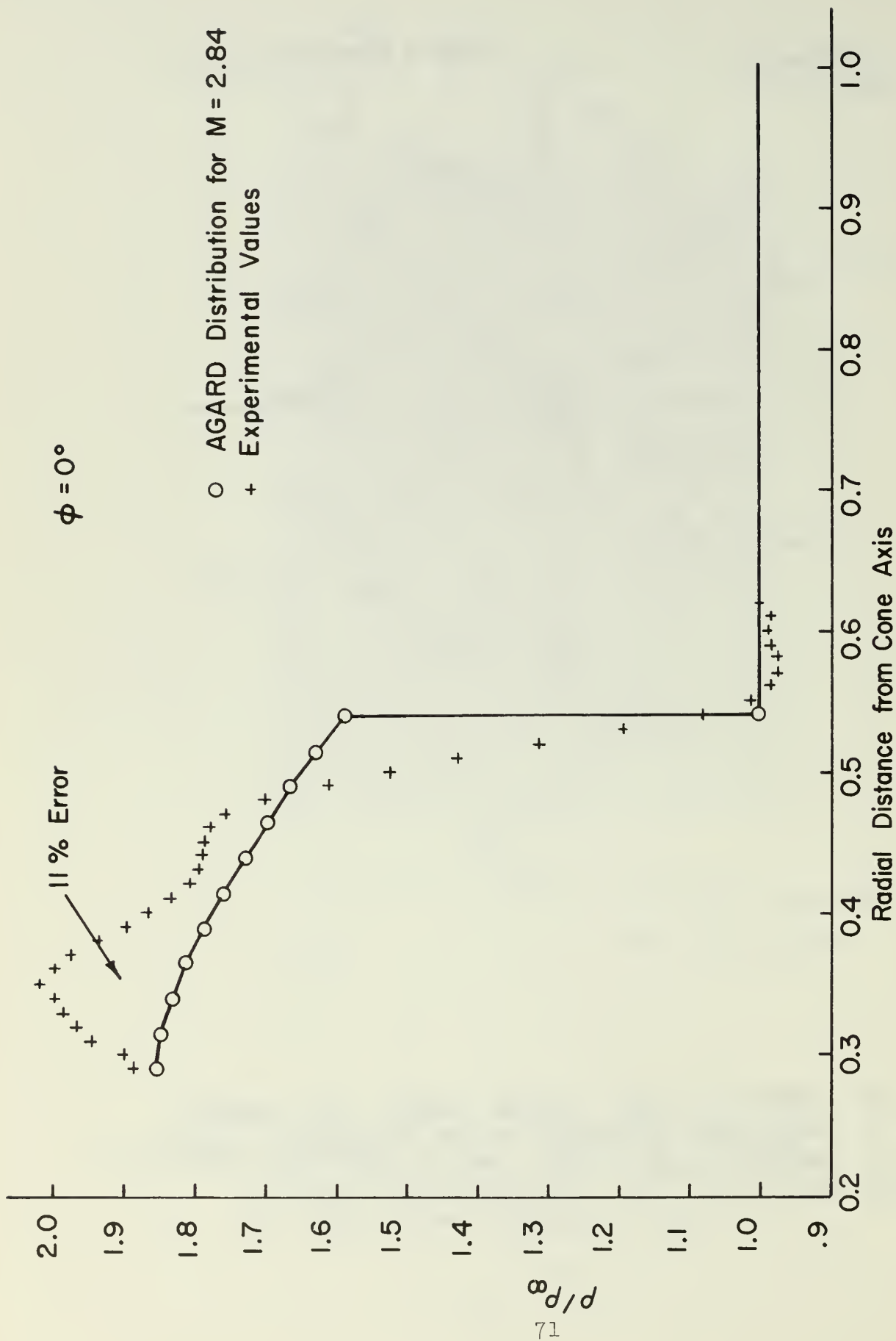


FIGURE 29. COMPARISON OF THE EXPERIMENTAL RADIAL DENSITY DISTRIBUTION WITH THE AGARD 167 DISTRIBUTION FOR THE ASYMMETRIC CASE AT $M = 2.84$, $\phi = 0^\circ$

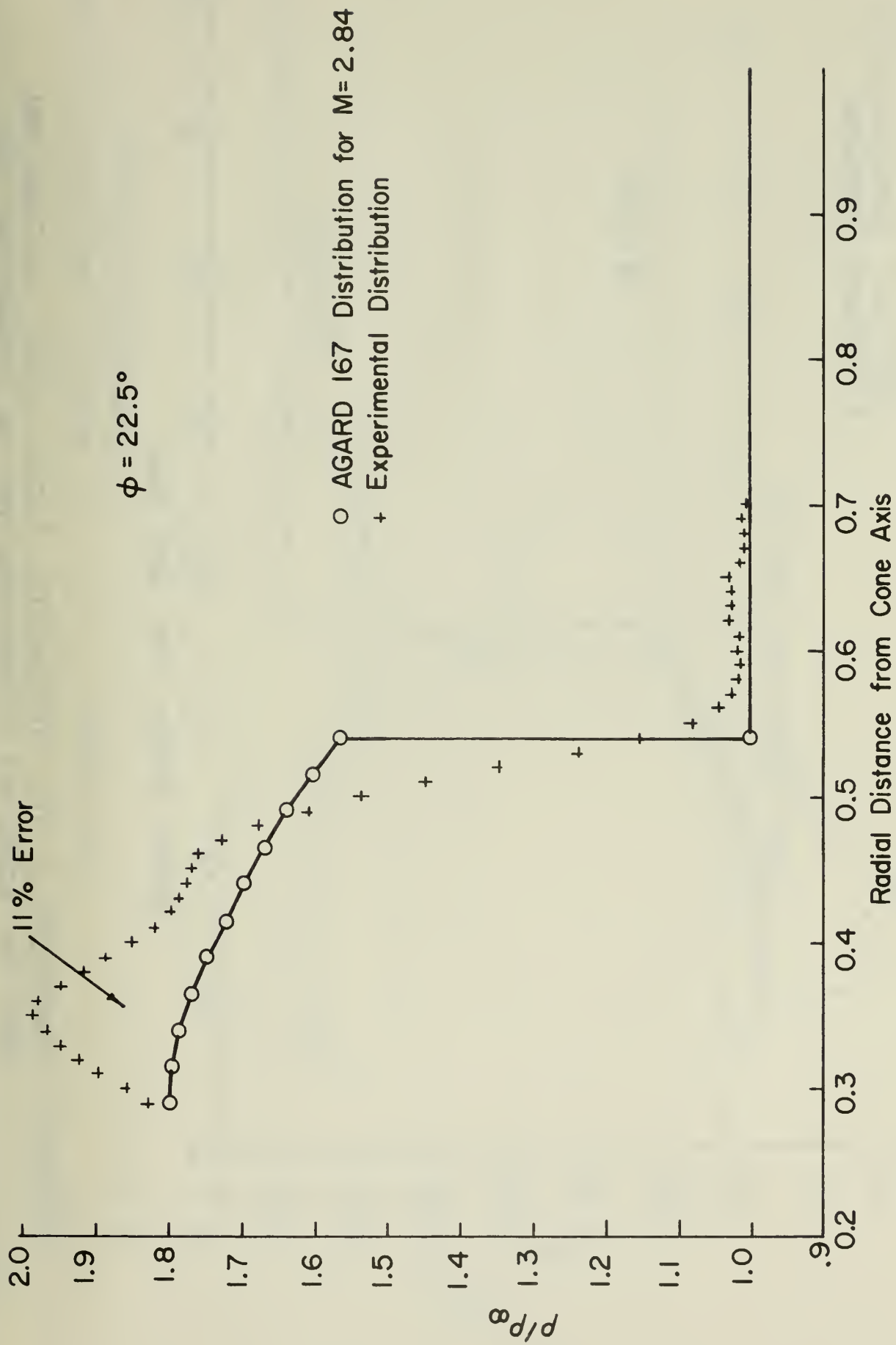


FIGURE 30. COMPARISON OF THE EXPERIMENTAL RADIAL DENSITY DISTRIBUTION WITH THE AGARD 167 DISTRIBUTION FOR THE ASYMMETRIC CASE AT $M=2.84$, $\phi = 22.5^\circ$

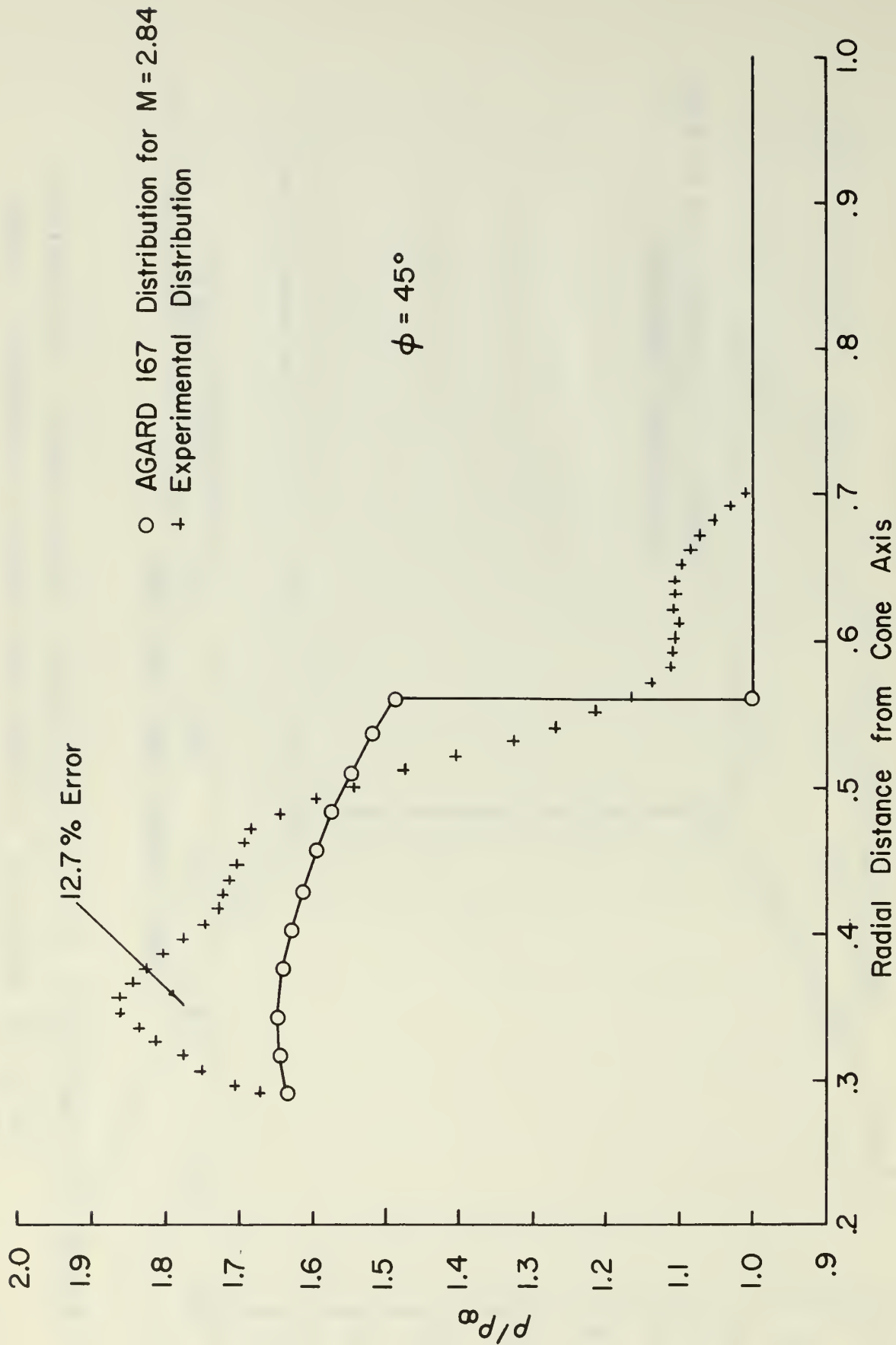


FIGURE 31. COMPARISON OF THE EXPERIMENTAL RADIAL DENSITY DISTRIBUTION WITH THE AGARD 167 DISTRIBUTION FOR THE ASYMMETRIC CASE AT $M=2.84$, $\phi = 45^\circ$

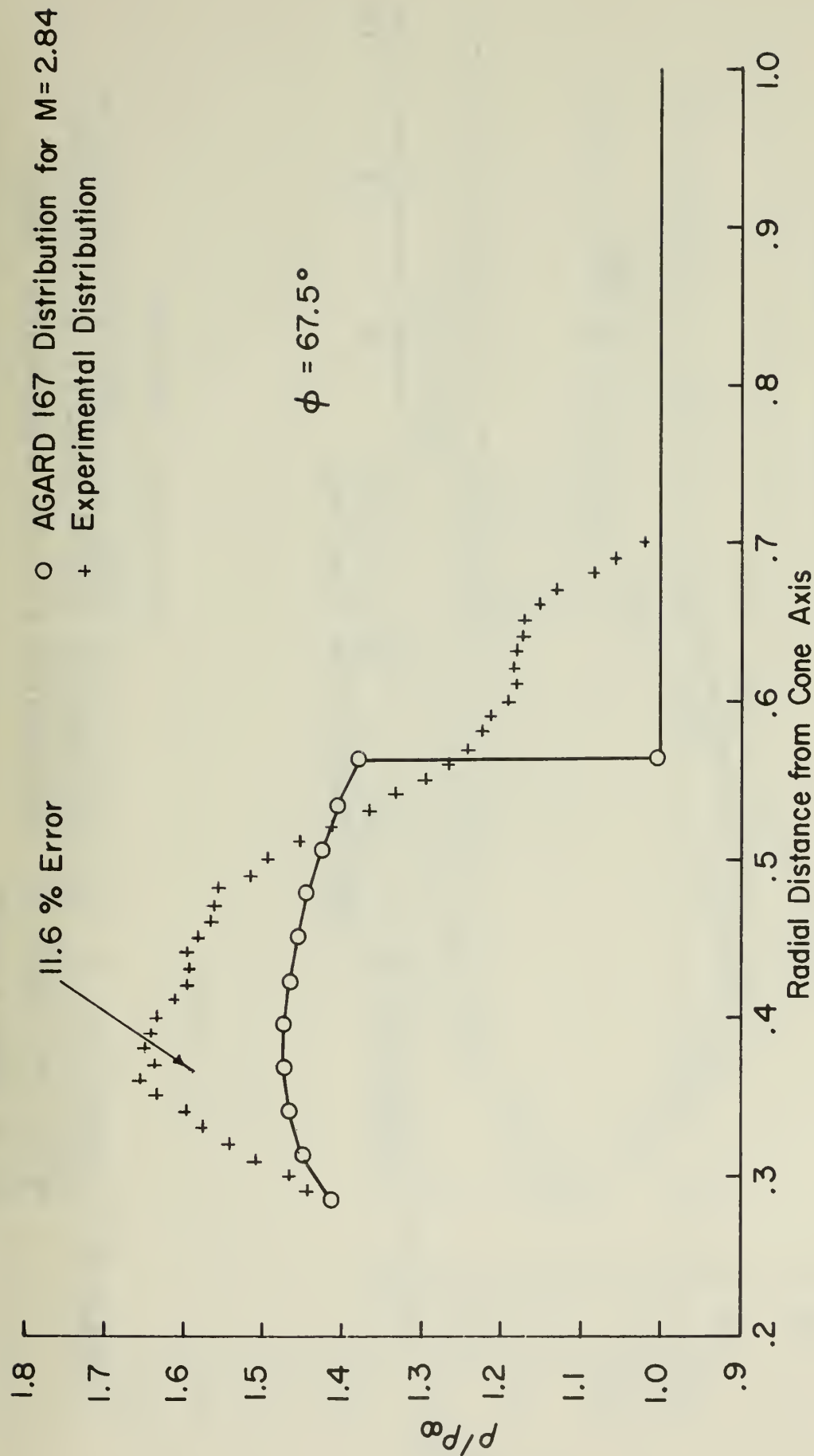


FIGURE 32. COMPARISON OF THE EXPERIMENTAL RADIAL DENSITY DISTRIBUTION WITH THE AGARD 167 DISTRIBUTION FOR THE ASYMMETRIC CASE AT $M = 2.84$, $\phi = 67.5^\circ$

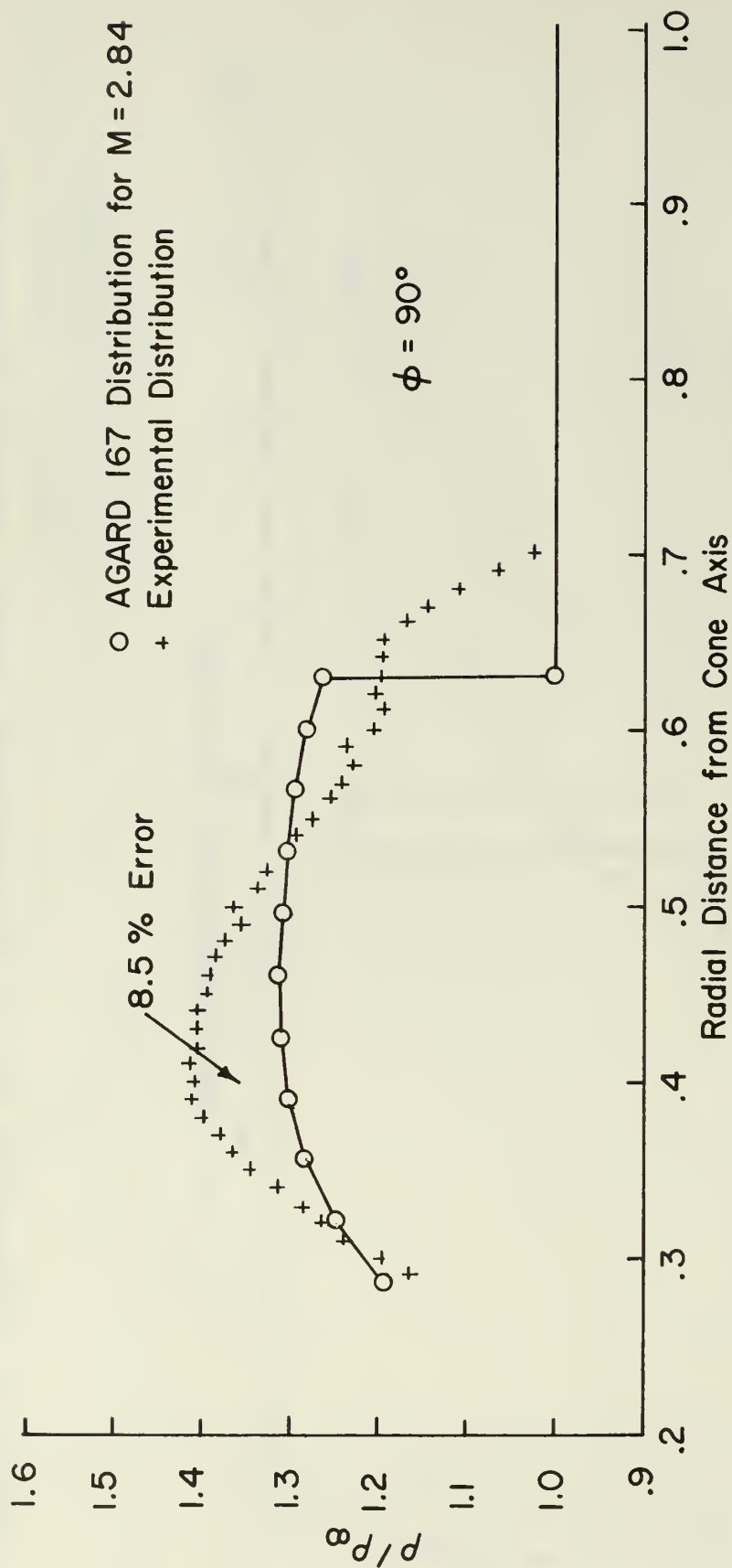


FIGURE 33. COMPARISON OF THE EXPERIMENTAL RADIAL DENSITY DISTRIBUTION WITH THE AGARD 167 DISTRIBUTION FOR THE ASYMMETRIC CASE AT $M = 2.84$, $\phi = 90^\circ$

○ AGARD 167 Distribution for $M = 2.84$
 + Experimental Distribution

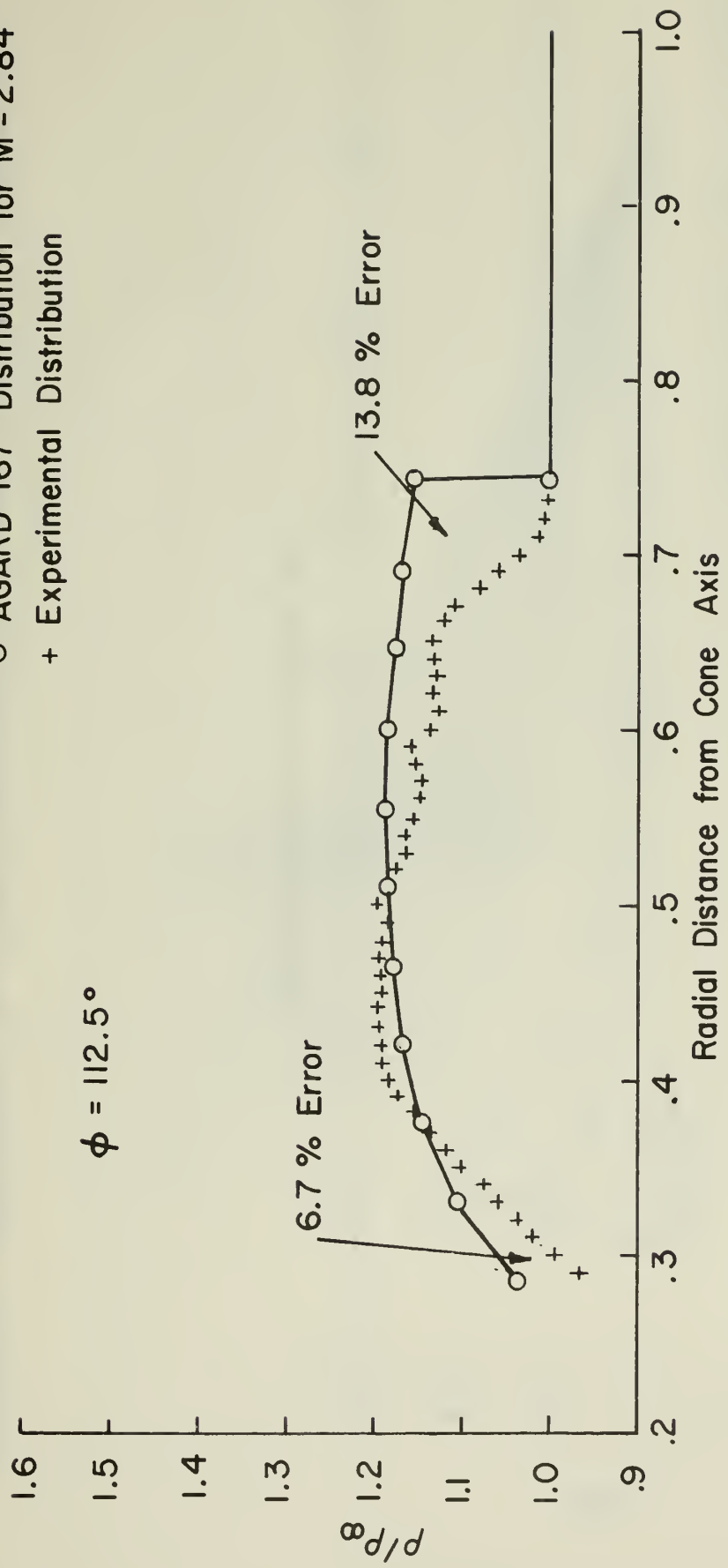


FIGURE 34. COMPARISON OF THE EXPERIMENTAL RADIAL DENSITY DISTRIBUTION WITH THE AGARD 167 DISTRIBUTION FOR THE ASYMMETRIC CASE AT $M = 2.84$, $\phi = 112.5^\circ$

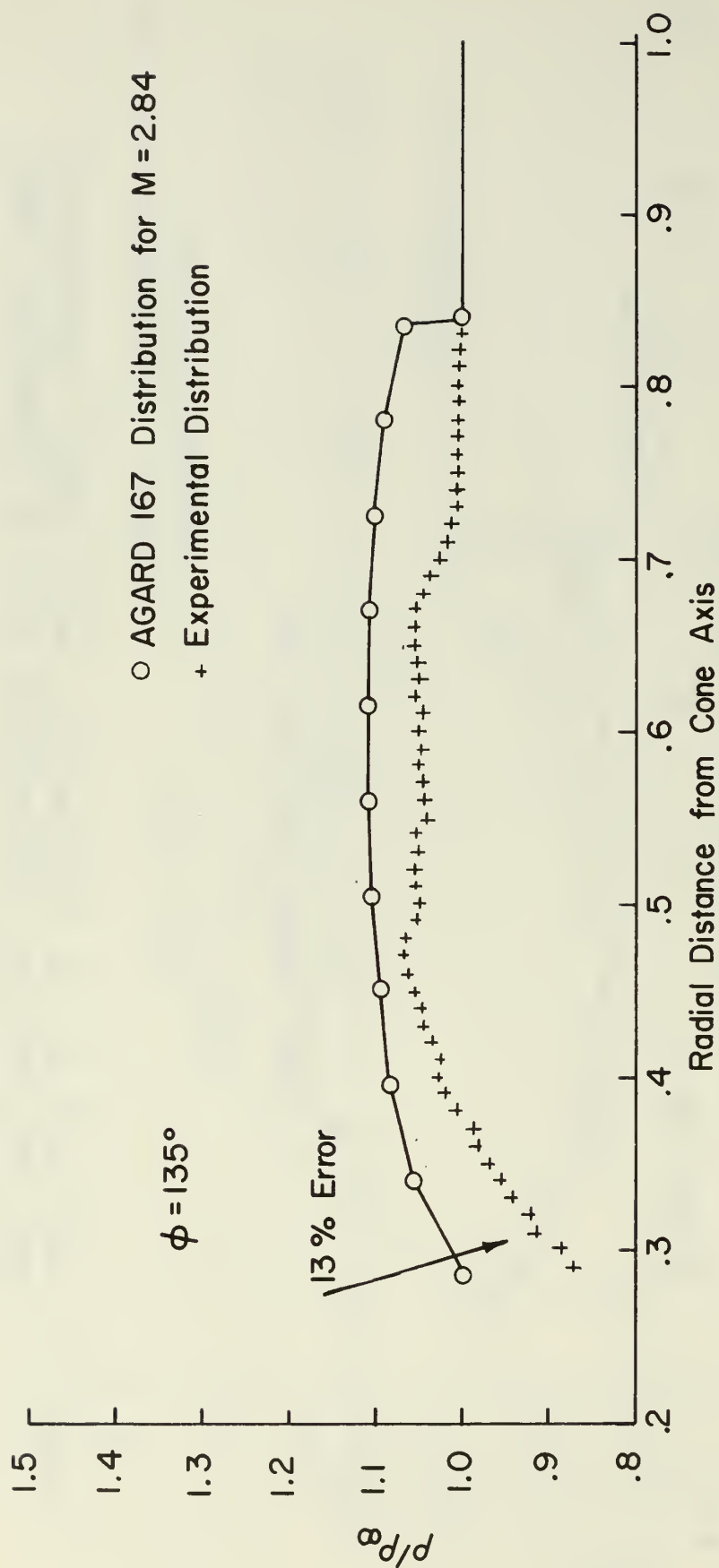
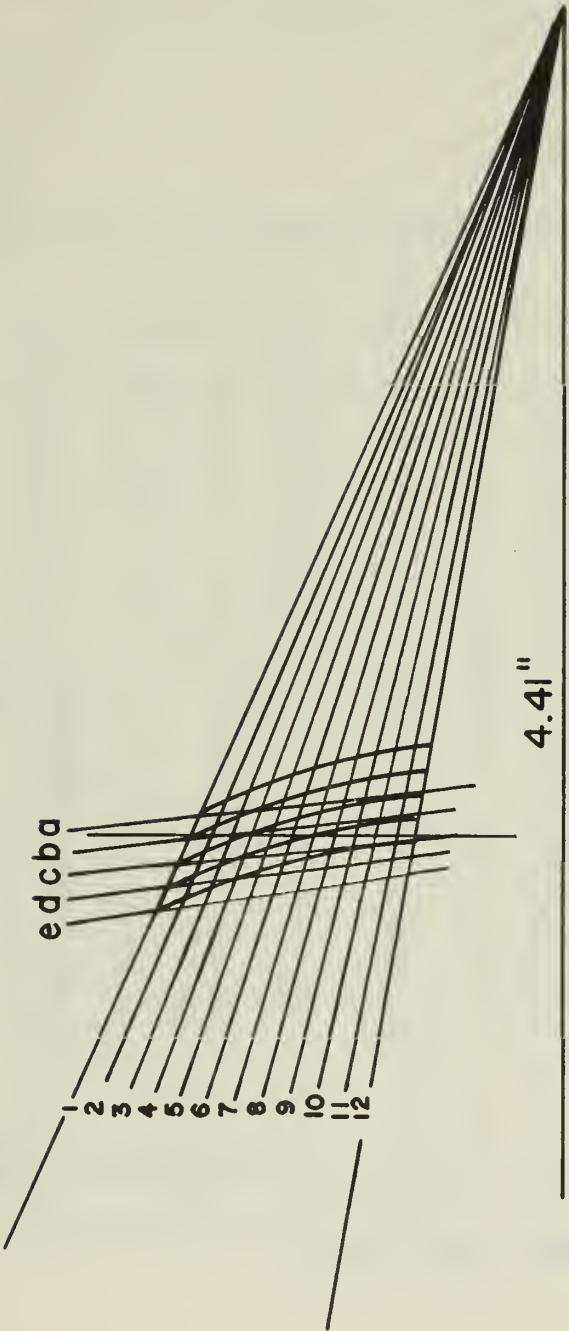


FIGURE 35. COMPARISON OF THE EXPERIMENTAL RADIAL DENSITY DISTRIBUTION WITH THE AGARD 167 DISTRIBUTION FOR THE ASYMMETRIC CASE AT $M = 2.84$, $\phi = 135^\circ$

$$\text{Avg. Fringe Dist.} = \frac{11.1}{4} = 2.775$$



$$\text{Magnif. Factor} = \frac{4.1''}{2.25''} = 1.8222''$$

FIGURE 36. TRACING OF THE PROJECTED IMAGE OF THE HOLOGRAPHIC INTERFEROGRAM FOR THE AXI-SYMMETRIC CASE

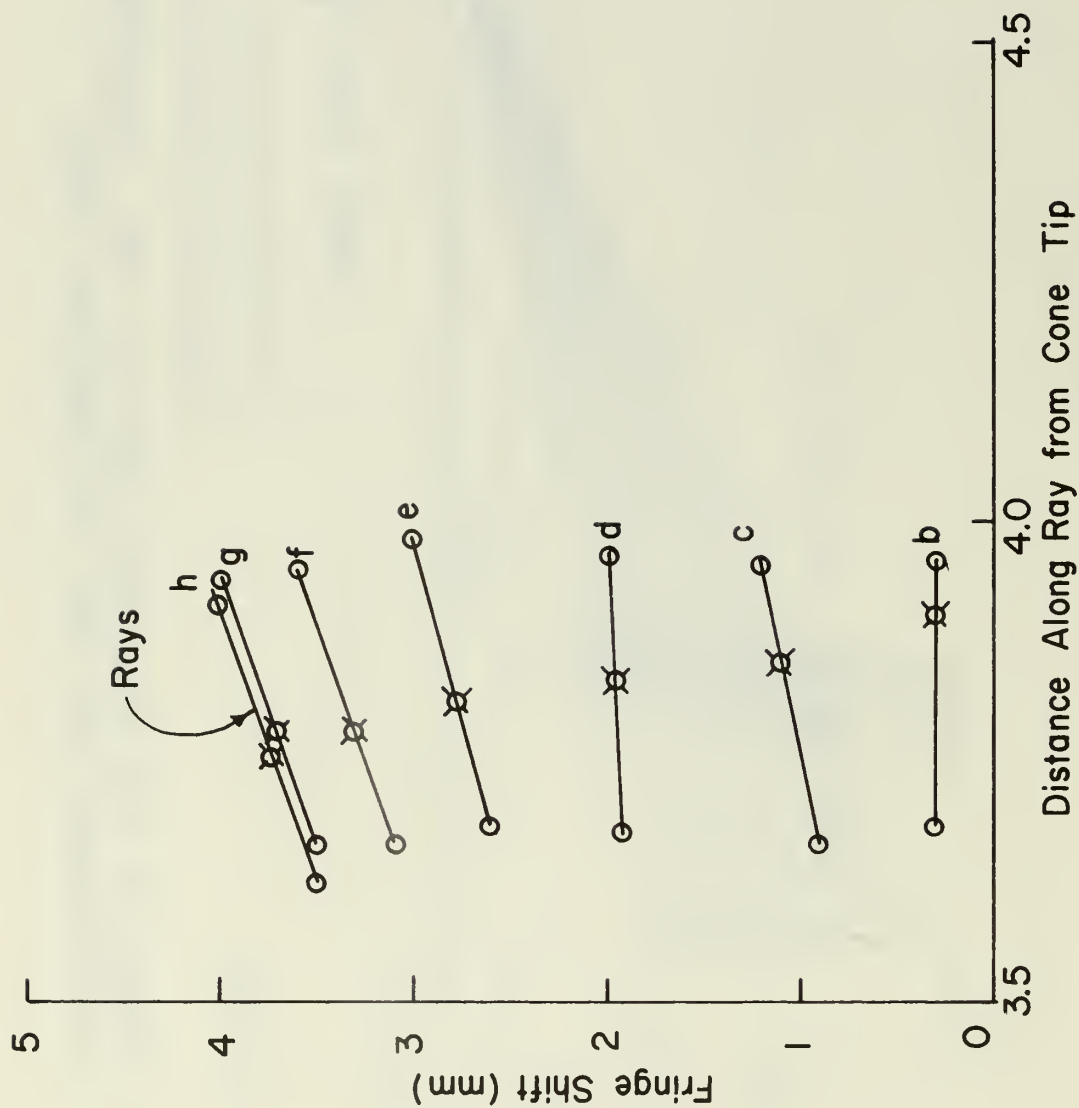


FIGURE 37. PLOT OF A TYPICAL FRINGE SHIFT VARIATION ALONG A RAY TO OBTAIN THE FRINGE SHIFT AT THE SECTION

TABLE I
VARIATION OF FRINGE SHIFT WITH DISTANCE
ALONG RAYS FROM THE CONE VERTEX

x = Fringe shift (mm.)

y = Distance from cone vertex along a ray (ins.)

Ray	Fringe 'a'		Fringe 'b'		Fringe 'c'		Fringe 'd'		Fringe 'e'		Section	
	x	y	x	y	x	y	x	y	x	y	x	y
1	0.0	4.50	0.0	4.63	0.0	4.75	0.0	4.89	0.0	5.0		4.48
2	2.0	4.37	2.1	4.49	1.9	4.63	1.7	4.77	1.0	4.92		4.44
3	3.3	4.26	5.5	4.40	3.6	4.50	3.2	4.64	2.1	4.78		4.40
4	4.1	4.17	4.4	4.29	4.4	4.41	4.1	4.53	3.5	4.68		4.36
5	4.9	4.08	4.9	4.21	5.4	4.32	5.0	4.43	4.7	4.58		4.32
6	5.5	4.02	5.6	4.13	6.1	4.24	5.5	4.35	5.6	4.48		4.28
7	6.0	3.95	6.1	4.08	6.6	4.18	6.0	4.29	6.4	4.14		4.26
8	6.4	3.91	6.8	4.03	7.2	4.13	6.7	4.22	6.9	4.34		4.23
9	6.6	3.87	7.2	3.97	7.7	4.08	6.6	4.18	7.4	4.28		4.21
10	6.6	3.84	7.3	3.92	7.8	4.03	6.6	4.14	7.7	4.23		4.18
11	6.5	3.80	7.1	3.91	7.2	4.0	6.5	4.10	7.7	4.19		4.15
12	6.3	3.79	6.4	3.90	7.1	3.99	6.3	4.08	7.3	4.17		4.14

TABLE II
RADIAL DISTANCE FROM THE CONE AXIS OF THE
INTERSECTION OF RAYS WITH THE SECTION

Ray	Distance from cone axis	Normalized distance from cone axis
1	1.83	0.95
2	1.72	0.89
3	1.63	0.846
4	1.53	0.794
5	1.43	0.742
6	1.33	0.69
7	1.23	0.639
8	1.12	0.581
9	1.02	0.53
10	0.92	0.478
11	0.82	0.426
12	0.72	0.374

TABLE III

CALCULATION OF THE RADIAL VARIATION
OF FRINGE NUMBER AT THE SECTION

Average fringe spacing in the freestream = 2.775 mm.

Ray	Normalized distance from cone axis	Fringe shift (mm.)	Fringe number
1	0.95	0.0	0.0
2	0.89	2.08	0.75
3	0.846	3.5	1.26
4	0.794	4.42	1.59
5	0.742	5.4	1.946
6	0.69	5.92	2.13
7	0.639	6.16	2.22
8	0.581	6.69	2.41
9	0.53	6.73	2.425
10	0.478	6.87	2.476
11	0.426	7.22	2.60
12	0.374	6.80	2.45

APPENDIX A

REDUCTION OF AN INTERFEROGRAM TO OBTAIN FRINGE SHIFT DATA

The reduction of only one side of the interferogram obtained for the axisymmetric case is indicated as an illustration of the procedure employed. After projection of the negative, the cone surface, the shock waves, the grid line at the section concerned and the fringes from the projected image were traced on a sheet of paper as shown in Figure 36. The distance between the cone surface and the shock at the section was divided into a convenient number of parts and rays drawn from the tip of the cone through these points. The fringe shift distances at the point of intersection of each displaced fringe and the rays were measured by means of a 7X PEAK scale magnifier as well as the average fringe spacing in the freestream. The radial distance from the cone axis to the intersection of each of the rays with the section was also measured as also the distance along each ray to the intersection with each fringe and with the section concerned. A tabulation of these results is shown in Tables 1, 2, and 3. For each ray, the fringe shift distance was then plotted against the distance along the ray as in Figure 37, and from these curves the fringe shift distance at the section was obtained. These fringe shift distances were divided by the average fringe spacing in the freestream to obtain the fringe numbers at the various

points concerned. From a measurement of the distance from the tip of the cone to the section on the projected image and comparison with the known distance, the magnification of the image with respect to the actual conditions existing in the wind tunnel was determined. The radius of the inversion circle was obtained by assuming the distance of the shock from the cone axis to be at 95% of the radius of the inversion circle. The distance from the cone axis of the various intersections of the rays from the cone vertex and the section were obtained as a fraction of the inversion circle radius. The fringe number at these points was then plotted against the non-dimensional distance from the cone axis as shown in Figure 17 and a smooth curve drawn through these points. The value of the fringe number in the region occupied by the cone was taken as a constant value equal to that at the cone surface. From the curve so obtained, values of the fringe number at 101 equidistant points were obtained on each side of the cone axis (including the value at the axis) so that a total of 201 data values resulted. This fringe data was read into Subroutine READ of computer program HOLOFER and inverted to obtain the required density field.

The use of 201 data points was essentially dictated by the necessity to be able to define the shock position accurately and to have the fringe distribution in the region between the shock and the cone described fairly well. Since

the fringe curve from which these points were obtained was plotted using only about 10 experimental fringe values, the use of 201 points does not imply a higher accuracy in the density distribution output from the computer program.

APPENDIX B
USE OF COMPUTER PROGRAM "HOLOFFER"

This computer program is designed to invert the array of fringe numbers to obtain the associated density field using the inversion first proposed by C. D. Maldonado and described in Section III of this report. The computer program can be run in basically 3 modes as described below:

(a) Mode 1

This mode provides the basic testing capability of the program and uses various test functions listed in Subroutine FUNCT in order to generate a G array which is then inverted back to obtain the original input function. Functions other than those specified in FUNCT can also be read in on cards by specifying a test function number of 8.0 in the original list of 42 parameters read in into the main program HOLOVERT. In this case the main program first calls Subroutine FREAD to read in the data cards. The first card in this data deck consists of two values indicating the total number of cards to be read in and the 'Z' section at which inversion is being performed and is input according to format 89 of the subroutine. Thence follows one point per card according to format 88 representing the numerical test function being input. This mode was employed in the present case for inverting the 201 points that were obtained from the AGARD tables by interpolation using Computer Program 1.

Apart from an evaluation of the effect of discontinuities due to the shock and the cone, this method provided advance information on the magnitude of the fringe numbers to be expected in the experimental results.

(b) Mode 2

This mode obtains the G array at regular intervals from irregularly spaced values of the fringe number function by utilizing Subroutine SHEET. The fringe data may also be simulated by specifying NCODE=1 in which case one of the functions in FUNCT may be used to generate the G array. This mode has not been applied to the present investigation.

(c) Mode 3

In this mode, the fringe numbers are read in directly at regularly spaced points by Subroutine READ which is called by Subroutine GARRAY. The various parameters in the first two cards of Subroutine READ serve to identify the symmetry of the fringe field. The following parameters have been used in the cases dealt with in this report:

<u>Parameter</u>	<u>Axisymmetric Case</u>	<u>Asymmetric Case</u>
NOF	Any value specifying the run number.	Any value specifying the run number
IMAX	201	201
JMAX	1	24
ISYM	2	1
JSYM	101	1
IMS	101	201
JMS	1	1
Z	The 'Z' section at which inversion is performed.	The 'Z' section at which inversion is performed.

<u>Parameter</u>	<u>Axisymmetric Case</u>	<u>Asymmetric Case</u>
XO	0.	0.
YO	0.	0.
PHISYM	0.	0.

Further details regarding the computer program are contained in Reference 3. A listing of the program is, however, included in this appendix for reference.


```

RLAMDA=AR(11)*1.E-8
BETA=AR(12)
NPTS=AR(15)
NLINS=AR(16)
SD=AR(18)
PHIZ=AR(19)
DELPHI=AR(20)
YPZERO=AR(21)
YPRNG=AR(22)
XPZERO=AR(23)
XPRNG=AR(24)
NOF=AR(25)
NAF=AR(26)
IPT=AR(27)
KPT=AR(28)
LPT=AR(29)
BND=AR(30)
A=AR(31)
B=AR(32)
C=AR(33)
D=AR(34)
E=AR(35)
P=AR(36)
S=AR(37)
T=AR(38)
U=AR(39)
V=AR(40)
W=AR(41)
Q=AR(42)
WRITE(6,90)
WRITE(6,98)
WRITE(6,91)
WRITE(6,92)
WRITE(6,93)
WRITE(6,94)
WRITE(6,95)
WRITE(6,96)
WRITE(6,97)
WRITE(6,98)
FORMAT(///), * IMAX * JMAX/2 * KLIMIT * MLIMIT * KEXTRA * SET00310
1, MEXTRA *, /3X, 6F10.0) * SIZE * EPS. * RHO-INF * LAMBDA * SET00340
1, BETA *, /3X, 2F10.3, F11.6, F11.6) * POINTS * LINES * DIAGNOS * SET
1, STD DEV *, /2X, 5F10.0, F10.3) * YPZERO * YPRANGE * XPZERO *
1, XPRANGE *, /4X, 6F10.3)

```

```

CAL00460
CAL00470
CAL00480
CAL00490
CAL00500
CAL00510
CAL00520
CAL00530
CAL00540
CAL00550
CAL00560
CAL00570
CAL00580
CAL00590
CAL00600
CAL00610
CAL00620
CAL00630
CAL00640
CAL00650
CAL00660
CAL00670
CAL00680
CAL00690
CAL00700
CAL00710
CAL00720
CAL00730
CAL00740

```



```

95  FORMAT (/5X,'* TST FUN * ADD FUN * GARRAY * GRAPH * LIN PRT *',SET00400
1  MAP BND *,/2X,6F10.0) *
96  FORMAT (/5X,'* A * B * C * D * E *',SET00420
1  P *,/4X,6F10.3) *
97  FORMAT (/5X,'* S * T * U * V * W *',SET00440
1  Q *,/4X,6F10.3) *
98  FORMAT (/3X,75A1)
    IF (DGN.GE.4) WRITE (6,89) (AR(I),I=1,42)
NNN=2
    IF (MODE.LT.0) NNN=1
    IF (MODE.GT.5) NNN=3
    IF (MODE.GT.5) MODE=MODE-10
NGP=0
    IF (KLIMIT.LT.KEXTRA) KEXTRA=KLIMIT
    IF (MLIMIT.LT.MEXTRA) MEXTRA=MLIMIT
    IF (IPT.LT.0) NGP=IPT
    IF (IPT.LT.0) IPT=-IPT
    ISYM=2.1-(FLOAT(JSYM)/2.-FLOAT(JSYM/2))*2
    IF (JSYM.EQ.0) ISYM=1
    IF (JSYM.GT.JMAX) ISYM=2
    IF (ISYM.EQ.1) JMAX=((JMAX+1)/2)*2
RJMX=JMAX
MSYM=JSYM
    IF ((MSYM.EQ.0).OR.(MSYM.GT.JMAX)) MSYM=1
FCU=ISYM*JSYM*JMAX
    IF ((JSYM.GT.JMAX).OR.(JSYM.EQ.0)) FCU=JMAX
QSYM=FCU/RJMX
IMS=(IMAX+ISYM-1)/ISYM
JMS=JMAX
    IF (ISYM.EQ.1) JMS=(JMAX/2+1)/2
    IF (JSYM.EQ.0) JMS=JMAX/2
MODE=ABS(AR(13))
XO=0.
YO=0.
ZD=0.
PHISYM=0.
HS=SIZE/2.
RHOS=1.286
BOX=RHOINF*BETA/RHOS/RLAMDA
RPTS=NPTS
XPR=0.
    IF (NPTS.GT.1) XPR=XPRNG/(RPTS-1.)/2.
XPM=-XPR
PIE=3.141592653589793
MONE=1
    WRITE (6,58) IMAX,JMAX,IMS,JMS,ISYM,JSYM,MSYM,QSYM,FCU
    FORMAT (3X,'IMAX,JMAX,IMS,JMS,ISYM,JSYM,MSYM,QSYM,FCU',/
1  7I5,2F7.3/)

```

58


```

NTWO=2
IX=IMAX+JMAX
NF=IN1
IF ((MODE.EQ.1.) .AND. (NOF.EQ.8) .AND. (DGN.GE.1.)) WRITE (6,69)
IF ((MODE.EQ.1.) .AND. (NOF.EQ.8)) CALL FREAD (NO,RO,NF,ZD)
Z=ZD
IF (DGN.GE.1.) WRITE (6,68)
CALL GARRAY (G,GA,NOF,DGN,MONE,XO,YO,PHISYM)
LM=1
IF ((LPT.EQ.0) .AND. (BND.EQ.0)) LM=0
IIMX=IMAX+1
JJMX=JMAX+1
IJMX=IMAX*JMAX
NBD=1
IF (JSYM.EQ.0) NBD=2
KBD=KLIMIT*NBD
DO 15 IJ=1,IJMX
GA(IJ)=0.
IF (NAF.EQ.0) GO TO 16
NF=IN2
IF ((NAF.EQ.8) .AND. (DGN.GE.1.)) WRITE (6,69)
IF (NAF.EQ.8) CALL FREAD (NA,RA,NF,ZD)
MST=MODE
MODE=1
IF (DGN.GE.1.) WRITE (6,68)
IF (NAF.NE.0) CALL GARRAY (GA,G,NAF,DGN,NTWO,XO,YO,PHISYM)
MODE=MST
DO 6 IJ=1,IJMX
G(IJ)=G(IJ)+GA(IJ)
RLINS=NLINS
IF (NAF.EQ.8) WRITE (6,88) NA,(RA(L),L=1,NA)
IF (NOF.EQ.8) WRITE (6,87) NO,(RO(I),I=1,NO)
IF (LM.EQ.0) GO TO 14
RB(1)=-1.
DO 1 I=2,7
RB(I)=RB(I-1)+.5
TPIE=2.*PIE
MPIE=-PIE
DYP=0.
DXP=0.
IF (NLINS.GT.1) DYP=YPRNG/(RLINS-1.)
IF (NLINS.GT.1) DXP=XPRNG/(RPTS-1.)
IF ((DGN.GE.1.) .AND. (NNN.EQ.2)) WRITE (6,64)
IF (NNN.EQ.2) CALL BDGEN (G,H,SCF,DGN,NBD,BDA,KBD)
DO 5 J=1,NLINS
IF (DGN.GE.1.) WRITE (6,67) J
RJM=J-1
PHI=PHIZ+DELPHI*RJM

```

CAL01160
 CAL01170
 CAL01180
 CAL01190
 CAL01200
 CAL01210
 CAL01220
 CAL01230
 CAL01240
 CAL01250
 CAL01260
 CAL01270
 CAL01280
 CAL01290
 CAL01300
 CAL01310
 CAL01320
 CAL01330
 CAL01340
 CAL01350
 CAL01360
 CAL01370
 CAL01380
 CAL01390
 CAL01400
 CAL01410
 CAL01420
 CAL01430
 CAL01440
 CAL01450
 CAL01460
 CAL01470
 CAL01480
 CAL01490
 CAL01500
 CAL01510
 CAL01520
 CAL01530
 CAL01540
 CAL01550
 CAL01560
 CAL01570
 CAL01580
 CAL01590
 CAL01600
 CAL01610
 CAL01620
 CAL01630

15

6
16

1

```

YP(J)=YPZERO+DYP*RJM
PSI=(PHI+90.)*PIE/180.
TAU=PSI-PHISYM
IF (LPT.EQ.0) GO TO 9
IF (LPT.LE.1) WRITE (6,78) (ST,I=1,124)
IF (LPT.GT.1) WRITE (6,74) (ST,I=1,95)
IF ((CMS.EQ.1.).AND.(LPT.GT.1)) READ (5,79) ZZ
WRITE (6,86)
WRITE (6,85) Z,PHI,YP(J)
WRITE (6,76)
IF (MODE.EQ.1) WRITE (6,83) (RB(I),I=1,7)
IF (MODE.GT.1) WRITE (6,80) (RB(I),I=1,7)
WRITE (6,81) (DH,I=1,54),(PL,I=1,13)
IC=0
DO 3 I=1,NPTS
RIM=I-1
THEO(I,J)=0.
CA(I)=0.
FA(I,J)=0.
ERR(I)=0.
CALC(I,J)=0.
RHO(I)=0.
XP(I)=XPZERO+DXP*RIM
XPI=ABS(XP(I))
IF (XPI.LT.1.E-10) XP(I)=0.
RS=SQRT(XP(I)**2+YP(J)**2)/HS
IF (RS.GT.1.) GO TO 13
THT=ATANM(YP(J),XP(I))
IF (XPI.EQ.0.) THT=0.
SIG=TAU-PIE/2.+THT
IF (SIG.GT.PIE) SIG=SIG-TPIE
IF (SIG.LT.MPIE) SIG=SIG+TPIE
SIGI=SIG
XS=RS*COS(SIG)
IF (DGN.GE.1.) WRITE (6,44) SIG
FORMAT (1,SIG=,E10.3)
YS=RS*SIN(SIG)
IF (DGN.GE.5) WRITE (6,57) PHI,DELPHI,PSI,TAU,THT,SIG,SIGI,XS,YS
IF (DGN.GE.5) WRITE (6,57) PHI,DELPHI,PSI,TAU,THT,SIG,SIGI,XS,YS
RI=1
F=0.
IF (DGN.GE.2.) WRITE (6,66) I
CALL FUNCT (XS,YS,FA(I,J),NAF,DGN,NTWO)
IF (MODE.EQ.1) CALL FUNCT (XS,YS,F,NOF,DGN,MONE)
THEO(I,J)=F
IF (NNN.GE.2) REWIND 3
IF (NNN.GE.2) CALL FIELD (RS,SIGI,SOLN,NBD,BDA,DGN,KBD)
IF (NNN.GE.2) CALL FIELD2 (RS,SIGI,SOLN,G,H,SCF,DGN)

```

9

44

57

CAL02120
CAL02130
CAL02140
CAL02150
CAL02160
CAL02170
CAL02180
CAL02190
CAL02200
CAL02210

```

CA(I)=SOLN/BOX/HS
CALC(I,J)=CA(I)-FA(I,J)
RHO(I)=RHOINF*(CALC(I,J)+1.)
ERR(I)=CA(I)
IF (MODE.EQ.1) ERR(I)=(CALC(I,J)-THEO(I,J))
IF (MODE.GT.1) THEO(I,J)=FA(I,J)
IF (LPT.EQ.0) GO TO 3
LC=0
TL(1)=BL
TTL=0
IF ((XP(I).GT.XPM).AND.(XP(I).LT.XPR)) TTL=1.
IF (IC.EQ.5) IC=0
IF (IC.EQ.0) TL(1)=PL
DO 2 L=2,62
  TL(L)=BL
  IF ((I.EQ.1).OR.(TTL.EQ.1).OR.(I.EQ.NPTS)) TL(L)=PL
  IF (LC.EQ.10) LC=0
  IF ((IC.EQ.0).AND.(LC.EQ.0)) TL(L)=PL
  LC=LC+1
  TL(2)=PL
  TL(22)=PL
  TL(62)=PL
  IC=IC+1
  RLW=(CA(I)+1.)*20.+2.5
  LW=RLW
  IF (LW.GT.62) LW=62
  IF (LW.LT.2) LW=2
  TL(LW)=SC
  RLY=(FA(I,J)+1.)*20.+2.5
  LY=RLY
  IF (LY.GT.62) LY=62
  IF (LY.LT.2) LY=2
  IF (NAF.NE.0) TL(LY)=ST
  RLX=(THEO(I,J)+1.)*20.+2.5
  LX=RLX
  IF (LX.GT.62) LX=62
  IF (LX.LT.2) LX=2
  IF (MODE.EQ.1) TL(LX)=OH
  RLZ=(CALC(I,J)+1.)*20.+2.5
  LZ=RLZ
  IF (LZ.GT.62) LZ=62
  IF (LZ.LT.2) LZ=2
  TL(LZ)=EX
  WRITE (6,82) MOUT, INDEX, THEO(I,J), ERR(I), CALC(I,J), RHO(I),
1XP(I), (TL(L),L=1,62)
  IF ((NPTS.LE.20).AND.(I.NE.NPTS)) WRITE (6,79)
  CONTINUE
  IF (LPT.NE.0) WRITE (6,81) (DH,I=1,54), (PL,I=1,13)

```

13

CAL02260
CAL02270
CAL02280
CAL02290
CAL02300
CAL02310
CAL02320
CAL02330
CAL02340
CAL02350
CAL02360
CAL02370
CAL02380
CAL02390
CAL02400
CAL02410
CAL02420
CAL02430
CAL02440
CAL02450
CAL02460
CAL02470
CAL02480
CAL02490
CAL02500
CAL02510
CAL02520
CAL02530
CAL02540
CAL02550
CAL02560
CAL02570
CAL02580
CAL02590

2

3

```

TMAX=0.
TMIN=0.
IE=0.
EB=0.
DO 4 I=1,NPTS
  TH=THEO(I,J)
  IF (TH.GT.TMAX) TMAX=TH
  IF (TH.LT.TMIN) TMIN=TH
  ER=ABS(CALC(I,J)-TH)
  IF (ER.LE.BE) GO TO 4
  BE=ER
  IE=I
CONTINUE
TMM=TMAX-TMIN
EB=RHOINF*(CALC(IE,J)-THEO(IE,J))
IF (TMM.NE.0.) BE=(CALC(IE,J)-THEO(IE,J))*100./TMM
IF ((MODE.EQ.1).AND.(LPT.NE.0)) WRITE (6,75) EB,XP(IE),BE
IF (DELPHI.NE.0.) YP(J)=PHI
CONTINUE
IF (BND.EQ.0.) GO TO 14
IF (LPT.EQ.1) WRITE (6,78) (ST,I=1,124)
IF (LPT.GT.1) WRITE (6,74) (ST,I=1,95)
IF ((CMS.EQ.1).AND.(LPT.GT.1)) READ (5,79) ZZ
IF (DGN.GE.1.) WRITE (6,63)
CALL MAP (NPTS,NLINS,CALC,NOF,Z,BND)
IF (NAF.EQ.0) GO TO 10
NAO=10*NOF+NAF
IF ((DGN.GE.1).AND.(NGP.EQ.-3)) WRITE (6,62)
IF (NGP.EQ.-3) CALL GPUNCH (Z,XO,YO,PHISYM,NAO,IMAX,JMAX,G)
DO 7 IJ=1,IJMX
  G(IJ)=G(IJ)-GA(IJ)
  IF ((IPT.LE.0) GO TO 11
  IF ((IPT.EQ.1).OR.(IPT.EQ.3)) WRITE (6,78) (ST,I=1,124)
  IF ((IPT.EQ.2).OR.(IPT.GE.4)) WRITE (6,74) (ST,I=1,95)
  IF ((CMS.EQ.1).AND.(IPT.EQ.2).OR.(IPT.GE.4)) READ (5,79) ZZ
  CALL GPRINT (G,MONE)
  IF (NGP.EQ.-1) CALL GPUNCH (Z,XO,YO,PHISYM,NOF,IMAX,JMAX,G)
  IF (IPT.EQ.3) WRITE (6,78) (ST,I=1,124)
  IF (IPT.GE.4) WRITE (6,74) (ST,I=1,95)
  IF ((CMS.EQ.1).AND.(IPT.GE.4)) READ (5,79) ZZ
  IF (IPT.GE.3) CALL GPRINT (GA,NTWO)
  IF (KPT.LE.0) GO TO 12
  IF ((KPT.EQ.1).OR.(KPT.EQ.3)) WRITE (6,78) (ST,I=1,124)
  IF ((KPT.EQ.2).OR.(KPT.GE.4)) WRITE (6,74) (ST,I=1,95)
  IF ((CMS.EQ.1).AND.(KPT.EQ.2).OR.(KPT.GE.4)) READ (5,79) ZZ
  IF (DGN.GE.1.) WRITE (6,61)
  CALL GPLOT (G,GA,JMS)

```

```

CAL02600
CAL02610
CAL02620
CAL02630
CAL02640
CAL02650
CAL02660
CAL02670
CAL02680
CAL02690
CAL02700
CAL02710
CAL02720
CAL02730
CAL02740
CAL02750
CAL02760
CAL02770
CAL02780
CAL02790
CAL02800
CAL02810
CAL02820
CAL02830
CAL02840
CAL02850
CAL02860
CAL02870
CAL02880
CAL02890
CAL02900
CAL02910
CAL02920
CAL02930
CAL02940
CAL02950
CAL02960
CAL02970
CAL02980
CAL02990
CAL03000
CAL03010
CAL03020
CAL03030
CAL03040
CAL03050
CAL03060
CAL03070

```


Line	Code	Text
12	WRITE (6,78) (EX,I=1,124)	CAL03080
	AGAIN=ST	CAL03090
	IF (CMS.NE.1.) READ(5,60) AGAIN	CAL03100
	IF (AGAIN.EQ.BL) GO TO 20	CAL03110
	WRITE (6,77)	CAL03120
89	FORMAT (6F12.7)	CAL03130
88	FORMAT (/)	CAL03140
	1. POINTS) WAS: /7(11F10.3//)	CAL03150
87	1. POINTS) WAS: /7(11F10.3//)	CAL03160
	1. POINTS) WAS: /7(11F10.3//)	CAL03170
86	FORMAT (1H1//)	CAL03180
85	FORMAT (10X,'Z =',F8.3,' CM./10X,' PHI=',F8.3,' DEGREES'/10X,	CAL03190
	14HY' =,F8.3,' CM./10X,' PHI=',F8.3,' DEGREES'/10X,	CAL03200
	270X,'* = F8.3,' CM./10X,' PHI=',F8.3,' DEGREES'/10X,	CAL03210
84	FORMAT (/)	CAL03220
83	1. POINTS) WAS: /7(11F10.3//)	CAL03230
	1. POINTS) WAS: /7(11F10.3//)	CAL03240
	1. POINTS) WAS: /7(11F10.3//)	CAL03250
82	FORMAT (1X,12,1X,13,1X,14,1X,F9.4,2X,F7.3,1X,F9.4,1X,F7.3,	CAL03260
81	1F7.3,1X,62A1)	CAL03270
80	FORMAT (3X,54A1,2X,A1,12(4X,A1))	CAL03280
	1. POINTS) WAS: /7(11F10.3//)	CAL03290
	1. POINTS) WAS: /7(11F10.3//)	CAL03300
	1. POINTS) WAS: /7(11F10.3//)	CAL03310
79	FORMAT (1X,16F10.1)	CAL03320
78	FORMAT (1X,124A1)	CAL03330
77	FORMAT (1X//)	CAL03340
76	FORMAT (4X,'FUNCTION = (RHO/RHO-INFINITY)-1.0',33X,' : = THE'	CAL03350
	1. POINTS) WAS: /7(11F10.3//)	CAL03360
75	1. POINTS) WAS: /7(11F10.3//)	CAL03370
	1. POINTS) WAS: /7(11F10.3//)	CAL03380
74	FORMAT (1X,47A1,1X,47A1,1X,47A1)	CAL03390
69	FORMAT (1X,47A1,1X,47A1,1X,47A1)	CAL03400
68	FORMAT (1X,47A1,1X,47A1,1X,47A1)	CAL03410
67	FORMAT (1X,47A1,1X,47A1,1X,47A1)	CAL03420
66	FORMAT (1X,47A1,1X,47A1,1X,47A1)	CAL03430
65	FORMAT (1X,47A1,1X,47A1,1X,47A1)	CAL03440
64	FORMAT (1X,47A1,1X,47A1,1X,47A1)	CAL03450
63	FORMAT (1X,47A1,1X,47A1,1X,47A1)	CAL03460
62	FORMAT (1X,47A1,1X,47A1,1X,47A1)	CAL03470
61	FORMAT (1X,47A1,1X,47A1,1X,47A1)	CAL03480
60	FORMAT (1X,47A1,1X,47A1,1X,47A1)	CAL03490
	STOP	CAL03500
	END	CAL03510
		CAL03520
		SUB000010
		SUB000020

```

C      SUBROUTINE BDGEN (G,H,SCF,DGN,NBD,BDA,KBD)
C      BDGEN EVALUATES THE B AND D COEFFICIENTS FOR ALL M AND K, AND WRITES
C      THE ARRAY LINEARLY ON DISK.
C
C      COMMON IMAX,JMAX,IIMX,JJMX,IJMX,ALPHA,SIZE,EPS,MODE,BOX,SD,IX,Z
C      COMMON /TAB/ INDEX,KEXTRA,MEXTRA,KLIMIT,MLIMIT,KOUT,MOUT
C      COMMON /SYM/ ISYM,JSYM,MSYM,FCU,IMS,JMS,QSYM
C      DIMENSION G(IJMX),H(IIMX,5),SCF(JJMX,6),BDA(KBD)
C      INITIALIZE THE VALUES:
C      INDEX=0
C      KL2=NBD*KLIMIT
C      REWIND 3
C      JJMX6=JJMX*6
C      IIMX2=(IIMX+1)/2
C      PIE=3.141592653589793
C      RIMAX=IMAX
C      KLMP=KLIMIT+1
C      DX=2./RIMAX
C      RJMAX=JMAX
C      DXI=2.*PIE/FCU
C      INITIALIZE THE MODIFIED HERMITE POLYNOMIAL ARRAY; VECTORS:
C      (1)=H1, (2)=H2, (3)=ALPHA*X(I), (4)=HM+2 STORED, (5)=HM+1 STORED
C      DO 1 I I=1,IIMX2
C      RI=I
C      IIM=IIMX-I+1
C      H(I,I,3)=ALPHA*(RI*DX-DX-1.)
C      H(IIM,3)=-H(I,I,3)
C      H(I,I,1)=2.*H(I,I,3)
C      H(I,I,2)=(H(I,I,3)*H(I,I,1)-1.)/3.
C      H(IIM,1)=-H(I,I,1)
C      H(IIM,2)=H(I,I,2)
C      H(I,I,5)=H(I,I,2)
C      H(IIM,5)=H(I,I,2)
C      H(I,I,4)=H(I,I,1)
C      H(IIM,4)=H(IIM,1)
C      SIGN=1.
C      INITIALIZE THE SIN/COS ARRAY:
C      DO 2 J=1,JJMX
C      RJM=J-1
C      SCF(J,1)=0.
C      SCF(J,2)=1.
C      SCF(J,3)=SIN(RJM*DXI-PIE/2.)
C      SCF(J,4)=COS(RJM*DXI-PIE/2.)
C      SCF(J,5)=0.
C      SCF(J,6)=0.
C      MS=0
C      COMMENCE THE M LOOP:

```

```

SUB000030
SUB000040
SUB000050
SUB000060
SUB000070
SUB000080
SUB000090
SUB000100
SUB000110
SUB000120
SUB000130
SUB000140
SUB000150
SUB000160
SUB000170
SUB000180
SUB000190
SUB000200
SUB000210
SUB000220
SUB000230
SUB000240
SUB000250
SUB000260
SUB000270
SUB000280
SUB000290
SUB000300
SUB000310
SUB000320
SUB000330
SUB000340
SUB000350
SUB000360
SUB000370
SUB000380
SUB000390
SUB000400
SUB000410
SUB000420
SUB000430
SUB000440
SUB000450
SUB000460
SUB000470
SUB000480
SUB000490
SUB000500

```



```

DO 7 MP=1,MLIMIT
M=MP-1
RM=M
SIGN=-SIGN
IF (DGN.LE.-4) WRITE (6,88) SCF(1,1),SCF(2,1),SCF(1,2),SCF(2,2)
C TEST FOR SYMMETRY SKIPS:
IF (MS.EQ.MSYM) MS=0
TOTAL=0.
MS=MS+1
IF (MS.NE.1) GO TO 6
C COMMENCE THE K LOOP:
DO 5 KP=1,KLIMIT
K=KP-1
PK=KP
RK=K
INDEX=INDEX+1
C CALL THE B & D COEFFICIENTS AND WRITE THEM ON DISK:
CALL BD (M,K,G,H,SCF,B,D,JJMX6)
IF (DGN.EQ.3.) WRITE(6,89) M,K,B,D
IF (DGN.LE.-2) WRITE (6,89) M,K,B,D
IF (DGN.LE.-4) WRITE (6,88) H(1,1),H(1,2),H(1,4),H(1,5)
KK=K*NBD+1
K2=KP*NBD
BDA(K2)=D
BDA(KK)=B
C GENERATE THE NEXT ORDER OF THE SET OF HERMITE POLYNOMIALS FOR NEW K:
ORDER=M+2*KP+1
HA=SQRT(PK*(PK+RM))/ORDER
HB=2.*SQRT((PK+1.)*(RM+PK+1.))/(ORDER+1.)/(ORDER+2.)
DO 5 II=1,IIMX2
IIM=IIMX-II+1
H(II,1)=2.*(H(II,3)*H(II,2)-HA*H(II,1))
H(II,1)=SIGN*H(II,1)
H(II,2)=HB*(H(II,3)*H(II,1)-ORDER*H(II,2))
C ADVANCE THE SIN/COS ARRAY FOR THE NEXT M:
DO 3 J=1,JJMX
IF (DGN.LE.-5) WRITE (6,87) (SCF(J,NT),NT=1,6)
FORMAT (10 SIN/COS MXI:8E10.3)
STEMP=SCF(J,1)
SCF(J,1)=SCF(J,4)+SCF(J,2)*SCF(J,3)
SCF(J,2)=SCF(J,2)*SCF(J,4)-STEMP*SCF(J,3)
DO 4 J=1,JJMAX
SCF(J,5)=SCF(J+1,1)-SCF(J,1)
SCF(J,6)=SCF(J+1,2)-SCF(J,2)
WRITE (3) (BDA(I),I=1,KBD)
IF (DGN.LE.-3) WRITE (6,88) (BDA(I),I=1,10)
IF (JSYM.GT.JMAX) RETURN
RM=RM+1
6

```

SUB000510
SUB000520
SUB000530
SUB000540
SUB000550
SUB000560
SUB000570
SUB000580
SUB000590
SUB000600
SUB000610
SUB000620
SUB000630
SUB000640
SUB000650
SUB000660
SUB000670
SUB000680

SUB000690
SUB000700
SUB000710
SUB000720
SUB000730
SUB000740
SUB000750
SUB000760
SUB000770
SUB000780
SUB000790
SUB000800
SUB000810
SUB000820
SUB000830
SUB000840
SUB000850
SUB000860
SUB000870
SUB000880
SUB000890
SUB000900
SUB000910
SUB000920
SUB000930
SUB000940
SUB000950
SUB000960
SUB000970

SUB01440
SUB01450
SUB01460
SUB01470
SUB01480
SUB01490
SUB01500
SUB01510
SUB01520
SUB01530
SUB01540
SUB01550
SUB01560
SUB01570
SUB01580
SUB01590
SUB01600
SUB01610
SUB01620
SUB01630
SUB01640
SUB01650
SUB01660
SUB01670
SUB01680
SUB01690
SUB01700
SUB01710
SUB01720
SUB01730
SUB01740
SUB01750
SUB01760
SUB01770
SUB01780
SUB01790
SUB01800
SUB01810
SUB01820
SUB01830
SUB01840
SUB01850
SUB01860
SUB01870
SUB01880
SUB01890
SUB01900
SUB01910

```

16 RJMAX=JMAX
   SIGN=1.
   STK(1)=0.
   STM(1)=0.
   SMS=0.
   CMS=1.
   SMI= SIN(SIG)
   CMI= COS(SIG)
   MEP= ME XTRA+1
   DO 16 MB=1,MEP
     STM(MB)=0.
     FM=1.
     MS=0
   C  COMMENT THE M LOOP:
   2   SIGN=-SIGN
     K=0
     RK=K
     RM=M
     ARM=1. NE.0) ARM=AR**M
     IF (M.
     KTIMER=0
     KEP=KEXTRA+1
     DO 15 KB=1,KEP
       STK(KB)=0.
       SIGNK=-1.
   15  C  COMPUTE THE K=0 & K=1 ORDERS OF LAGUERRE POLYNOMIAL FOR GIVEN M:
       PM=0.
       PP=SQRT(1./FM)*SQRT(1./FM/(RM+1.))
   C  TEST FOR SYMMETRY SKIPS:
       IF (MS.EQ.MSYM) MS=0
       MS=MS+1
       IF (MS.NE.1) GO TO 7
   C  READ A LINE OF B & D COEFFICIENTS FOR GIVEN M:
       READ (3) (BDA(I),I=1,KBD)
       IF (DGN.LE.-6) WRITE (6,88) (BDA(I),I=1,10)
   C  COMMENT THE K LOOP:
   3   INDEX=INDEX+1
       SIGNK=-SIGNK
   C  COMPUTE THE M,K SUMMATION TERM:
       KK=K*NBD+1
       B=BDA(KK)
       D=0.
       IF (NBD.EQ.2) D=BDA(KK+1)
       BRACKET=B
       IF (RM.EQ.0.) GO TO 4
       BRACKET=B*CMS+D*SMS
       ADD=SIGNK*BRACKET*P*ARM
   4

```

```

TOTAL=TOTAL+ADD
IF (DGN.GT.-5) GO TO 5
STOT=TOTAL*EXPON*APP/BOX/SIZE
WRITE (6,89) M,K,STOT,ADD,BRAKET,P,ARM,B,CMS,D,SMS
ESTABLISH CHECK AS THE RELATIVE SIZE OF THE M,K TERM OF THE SERIES:
5 CHECK=ABS(ADD)
IF (TOTAL.GT.EPS) CHECK=ABS(ADD/TOTAL)
C ADVANCE THE K INDEX:
K=K+1
RK=K
DO 10 KA=1,KEXTRA
KB=KEXTRA-KA+1
STK(KB+1)=STK(KB)
STK(2)=TOTAL
ORDER=M+2*K+1
C GENERATE THE NEXT ORDER OF LAGUERRE POLYNOMIAL FOR NEW K:
PM=P
P=PP
PP=P*(ORDER-ARG)-PM*SQRT(RK*(RM+RK))
PP=PP/SQRT((RK+1.)*(RM+RK+1.))
C SET K TIMER TO PROVIDE EXTRA K TERMS AFTER CHECK < EPS:
KTIMER=KTIMER+1
IF (K.GE.KLIMIT) GO TO 6
IF (CHECK.GE.EPS) KTIMER=0
IF (KTIMER.LE.KEXTRA) GO TO 3
GO TO 7
6 KOUT=KOUT+1
IF (KEXTRA.EQ.0) GO TO 7
TOTAL=0.
DO 11 KA=1,KEXTRA
TOTAL=TOTAL+STK(KA+1)
11 RKX=KEXTRA
TOTAL=TOTAL/RKX
C END OF K LOOP; ADVANCE M:
M=M+1
RM=M
STP=SMS
SMS=SMS*CMI+CMS*SMI
SMS=SMS*CMI-STP*SMI
CMS=CMS*CMI-STP*SMI
IF (K.GT.KMAX) KMAX=K
FM=FM+RM
DO 12 MA=1,MEXTRA
MB=MEXTRA-MA+1
STM(MB+1)=STM(MB)
12 STM(2)=TOTAL
SET M TIMER FOR EXTRA M TERMS:
C IF (MS.EQ.1) MTIMER=MTIMER+1
IF (JSYM.GT.JMAX) GO TO 9

```

SUB01920
SUB01930
SUB01940
SUB01950
SUB01960
SUB01970
SUB01980
SUB01990
SUB02000
SUB02010
SUB02020
SUB02030
SUB02040
SUB02050
SUB02060
SUB02070
SUB02080
SUB02090
SUB02100
SUB02110
SUB02120
SUB02130
SUB02140
SUB02150
SUB02160
SUB02170
SUB02180
SUB02190
SUB02200
SUB02210
SUB02220
SUB02230
SUB02240
SUB02250
SUB02260
SUB02270
SUB02280
SUB02290
SUB02300
SUB02310
SUB02320
SUB02330
SUB02340
SUB02350
SUB02360
SUB02370
SUB02380
SUB02390

Line	Code	Text	Address
1	C	DH=H(I,I)-H(I)	SUB02850
	C	B=B+G(I,J)*S*DH	SUB02860
	C	B=B*QSYM/2.	SUB02870
	C	RETURN	SUB02880
2	C	DO 3 J=1,JMAX	SUB02890
	C	JS=J+JJMX4	SUB02900
	C	S=SCF(JS)/RM	SUB02910
	C	DO 3 I=1,IMAX	SUB02920
	C	II=I+1	SUB02930
	C	IJ=IMAX*(J-1)+I	SUB02940
3	C	DH=H(I,I)-H(I)	SUB02950
	C	B=B+G(I,J)*S*DH	SUB02960
	C	B=B*QSYM	SUB02970
	C	RETURN	SUB02980
4	C	IF (M.NE.O) GO TO 6	SUB02990
	C	S=DXI	SUB03000
	C	DO 5 J=1,JMAX	SUB03010
	C	DO 5 I=1,IMAX	SUB03020
	C	II=I+1	SUB03030
	C	IJ=IMAX*(J-1)+I	SUB03040
	C	DH=H(I,I)-H(I)	SUB03050
	C	B=B+G(I,J)*S*DH	SUB03060
	C	B=B/2.	SUB03070
	C	RETURN	SUB03080
6	C	DO 7 J=1,JMAX	SUB03090
	C	JS=J+JJMX4	SUB03100
	C	J2=JS+JJMX	SUB03110
	C	S=SCF(JS)/RM	SUB03120
	C	C=SCF(J2)/RM	SUB03130
	C	DO 7 I=1,IMAX	SUB03140
	C	II=I+1	SUB03160
	C	IJ=IMAX*(J-1)+I	SUB03170
	C	DH=H(I,I)-H(I)	SUB03180
	C	B=B+G(I,J)*S*DH	SUB03190
66	C	FORMAT ('BD:',4I5,10F6.2)	SUB03200
7	C	D=D-G(I,J)*C*DH	SUB03210
	C	RETURN	SUB03220
	C	END	SUB03230
	C	C000004	SUB03240
	C	C	
	C	SUBROUTINE FIELD2 (RS,SIG,SOLN,G,H,SCF,DGN)	SUB03250
	C	FIELD2 COMPUTES THE SAME INVERSION AS SUBROUTINE FIELD, EXCEPT THAT	SUB03260
	C	THE COEFFICIENTS B AND D ARE COMPUTED INDIVIDUALLY AS USED BY	SUB03270
	C	CALLING BD. DISK STORAGE IS NOT REQUIRED, BUT COMPUTING TIME IS	SUB03280
	C	MUCH GREATER. FIELD2 IS UTILIZED BY SPECIFYING A NEGATIVE MODE ON	SUB03290
	C		SUB03300


```

C THE INPUT PARAMETER.
C FIELD EVALUATES THE VALUE OF THE FIELD FUNCTION AT A PARTICULAR
C POINT DESIGNATED IN CYLINDRICAL COORDINATES, BY USING THE INVERSION
C EQUATION OF MALDONADO, ET AL. FIELD CALLS SUBROUTINES BD & GARRAY.
C
COMMON IMAX, JMAX, IIMX, JJMX, IJMX, ALPHA, SIZE, EPS, MODE, BOX, SD, IX, Z
COMMON /TAB/ INDEX, KEXTRA, MEXTRA, KLIMIT, MLIMIT, KOUT, MOUT
COMMON /SYM/ ISYM, JSYM, MSYM, FCU, IMS, JMS, QSYM
DIMENSION G(IJMX), H(IIMX,5), SCF(JJMX,6)
C INITIALIZE THE VALUES:
INDEX=0
MTIMER=0
KOUT=0
MOUT=0
MMAX=0
KMAX=0
TOTAL=0
JJMX6=JJMX*6
IIMX2=(IIMX+1)/2
AR=ALPHA*RS
ARG=AR**2
EXPON=EXP(-ARG)
PIE=3.141592653589793
APP=ALPHA/PIE/PIE
M=0
RM=M
RIMAX=IMAX
DX=2./RIMAX
RJMAX=JMAX
DXI=2.*PIE/FCU
C INITIALIZE THE MODIFIED HERMITE POLYNOMIAL ARRAY; VECTORS:
C (1)=H1, (2)=H2, (3)=ALPHA*X(I), (4)=HM+2 STORED, (5)=HM+1 STORED
DO 1 I I=1, IIMX2
RI I=I
IIM=IIMX-I+1
H(I I,3)=ALPHA*(RI I*DX-DX-1.)
H(I I,3)=-H(I I,3)
H(I I,1)=2.*H(I I,3)
H(I I,2)=(H(I I,3)*H(I I,1)-1.)/3.
H(I I,1)=-H(I I,1)
H(I I,2)=H(I I,2)
H(I I,5)=H(I I,2)
H(I I,5)=H(I I,2)
H(I I,4)=H(I I,1)
H(I I,4)=H(I I,1)
SIGN=1.
FM=1.
C INITIALIZE THE SIN/COS ARRAY:

```

SUB033310
SUB033320
SUB033330
SUB033340
SUB033350
SUB033360
SUB033370
SUB033380
SUB033390
SUB033400
SUB033410
SUB033420
SUB033430
SUB033440
SUB033450
SUB033460
SUB033470
SUB033480
SUB033490
SUB033500
SUB033510
SUB033520
SUB033530
SUB033540
SUB033550
SUB033560
SUB033570
SUB033580
SUB033590
SUB033600
SUB033610
SUB033620
SUB033630
SUB033640
SUB033650
SUB033660
SUB033670
SUB033680
SUB033690
SUB033700
SUB033710
SUB033720
SUB033730
SUB033740
SUB033750
SUB033760
SUB033770
SUB033780

```

11 DO 11 J=1,JMX
    RJM=J-1
    SCF(J,1)=0.
    SCF(J,2)=1.
    SCF(J,3)=SIN(RJM*DXI-PIE)
    SCF(J,4)=COS(RJM*DXI-PIE)
    SCF(J,5)=0.
    SCF(J,6)=0.
    MS=0
    COMMENCE THE M LOOP:
    2 SIGN=-SIGN
      K=0
      RK=K
      ARM=1.
      IF (M.NE.0) ARM=AR**M
      KTIMER=0
      SIGNK=-1.
      C COMPUTE THE K=0 & K=1 ORDERS OF LAGUERRE POLYNOMIAL FOR GIVEN M:
        PM=0.
        P=SQRT(1./FM)*SQRT(1.-FM/(RM+1.))
        PP=(RM+1.-ARG)*SQRT(1.-FM/(RM+1.))
        C ADVANCE THE SIN/COS ARRAY FOR NEW M:
          DO 12 J=1,JMX
            SCF(J,1)=SCF(J,1)*SCF(J,4)+SCF(J,2)*SCF(J,3)
            SCF(J,2)=SCF(J,2)*SCF(J,4)-SCF(J,1)*SCF(J,3)
            DO 13 J=1,JMAX
              SCF(J,5)=SCF(J+1,1)-SCF(J,1)
              SCF(J,6)=SCF(J+1,2)-SCF(J,2)
            C TEST FOR SYMMETRY SKIPS:
              IF (MS.EQ.MSYM) MS=0
              TOTAL=0.
              MS=MS+1
              IF (MS.NE.1) GO TO 7
              RMS=RM*SIG
              CMS=COS(RMS)
              SMS=SIN(RMS)
              C COMMENCE THE K LOOP:
                INDEX=INDEX+1
                SIGNK=-SIGNK
                C CALL THE B & D COEFFICIENTS AND COMPUTE THE M,K SUMMATION TERM:
                  CALL BD (M,K,G,H,SCF,B,D,JMX6)
                  IF (DGN.LE.-2.) WRITE (6,89) M,K,B,D
                  BRACKET=B
                  IF (RM.EQ.0.) GO TO 4
                  BRACKET=B*CMS+D*SMS
                  ADD=SIGNK*BRACKET*P*ARM
                  TOTAL=TOTAL+ADD
                  C ESTABLISH CHECK AS THE RELATIVE SIZE OF THE M,K TERM OF THE SERIES:

```

SUB03790
 SUB03800
 SUB03810
 SUB03820
 SUB03830
 SUB03840
 SUB03850
 SUB03860
 SUB03870
 SUB03880
 SUB03890
 SUB03900
 SUB03910
 SUB03920
 SUB03930
 SUB03940
 SUB03950
 SUB03960
 SUB03970
 SUB03980
 SUB03990
 SUB04000
 SUB04010
 SUB04020
 SUB04030
 SUB04040
 SUB04050
 SUB04060
 SUB04070
 SUB04080
 SUB04090
 SUB04100
 SUB04110
 SUB04120
 SUB04130
 SUB04140
 SUB04150
 SUB04160
 SUB04170
 SUB04180
 SUB04190
 SUB04200
 SUB04210
 SUB04220
 SUB04230
 SUB04240
 SUB04250
 SUB04260

```

      CHECK=ABS(ADD)
      IF (TOTAL.GT.EPS) CHECK=ABS(ADD/TOTAL)
      ADVANCE THE K INDEX:
      K=K+1
      RK=K
      ORDER=M+2*K+1
      GENERATE THE NEXT ORDER OF LAGUERRE POLYNOMIAL FOR NEW K:
      PM=P
      P=PP
      PP=PP*(ORDER-ARG)-PM*SQRT(RK*(RM+RK))
      PP=PP/SQRT((RK+1.)*(RM+RK+1.))
      GENERATE THE NEXT ORDER OF THE SET OF HERMITE POLYNOMIALS FOR NEW K:
      HA=SQRT(RK*(RK+RM))/ORDER
      HB=2.*SQRT((RK+1.)*(RM+RK+1.))/(ORDER+1.)/(ORDER+2.)
      DO 5 II=1, IIMX2
      IIM=IIMX-II+1
      H(II,1)=2.*H(II,3)*H(II,2)-HA*H(II,1)
      H(II,1)=SIGN*H(II,1)
      H(II,2)=HB*(H(II,3)*H(II,1)-ORDER*H(II,2))
      SET K TIMER TO PROVIDE EXTRA K TERMS AFTER CHECK < EPS:
      KTIMER=KTIMER+1
      IF (K.GE.KLIMIT) GO TO 6
      IF (CHECK.GE.EPS) KTIMER=0
      IF (KTIMER.LE.KEXTRA) GO TO 3
      GO TO 7
      END OF K LOOP; ADVANCE M AND COMPUTE NEW TOTAL:
      KOUT=KOUT+1
      M=M+1
      IF (K.GT.KMAX) KMAX=K
      RM=M
      FM=FM*RM
      REGENERATE THE HERMITE ARRAY FOR NEW M, K=0:
      DO 8 II=1, IIMX2
      IIM=IIMX-II+1
      H(II,2)=H(II,4)*SQRT(RM)/(RM+1.)
      H(II,1)=H(II,5)*(RM+2.)
      H(II,1)=-SIGN*H(II,1)
      H(II,2)=2.*SQRT(RM+1.)*(H(II,3)*H(II,1)-(RM+1.)*H(II,2))
      H(II,2)=H(II,2)/(RM+2.)/(RM+3.)
      H(II,4)=H(II,1)
      H(II,5)=H(II,2)
      SET M TIMER FOR EXTRA M TERMS:
      MS=MS*(MS.EQ.1) MTIMER=MTIMER+1
      IF (JSYM.GT.JMAX) GO TO 9
      IF (K.GT.KEXTRA) MTIMER=0
      IF (M.GE.KLIMIT) GO TO 9
      IF (MTIMER.LE.MEXTRA) GO TO 2
      END OF M LOOP; COMPUTE OUTPUT SOLN.

```

SUB04270
 SUB04280
 SUB04290
 SUB04300
 SUB04310
 SUB04320
 SUB04330
 SUB04340
 SUB04350
 SUB04360
 SUB04370
 SUB04380
 SUB04390
 SUB04400
 SUB04410
 SUB04420
 SUB04430
 SUB04440
 SUB04450
 SUB04460
 SUB04470
 SUB04480
 SUB04490
 SUB04500
 SUB04510
 SUB04520
 SUB04530
 SUB04540
 SUB04550
 SUB04560
 SUB04570
 SUB04580
 SUB04590
 SUB04600
 SUB04610
 SUB04620
 SUB04630
 SUB04640
 SUB04650
 SUB04660
 SUB04670
 SUB04680
 SUB04690
 SUB04700
 SUB04710
 SUB04720
 SUB04730
 SUB04740

SUB000390
SUB000400
SUB000410
SUB000420
SUB000430
SUB000440
SUB000450
SUB000460
SUB000470
SUB000480
SUB000490
SUB000500
SUB000510
SUB000520
SUB000530
SUB000540
SUB000550
SUB000560
SUB000570
SUB000580
SUB000590
SUB000600
SUB000610
SUB000620

```

DO 1 I=1,IMS
RI=I
II=IMAX+1-I
R=(RI-.5)*DELR-HS
CALL GOLF (R,XI,GIJ,NOF,DGN,NUMB)
G(I,J)=GIJ
IF (ISYM.EQ.2) G(II,J)=GIJ
IF (ISYM.EQ.2) GO TO 1
G(II,J3)=GIJ
IF (JSYM.EQ.0) GO TO 1
G(I,J2)=GIJ
G(II,J4)=GIJ
CONTINUE
GO TO 4
IF (MODE.GT.2) GO TO 3
CALL SHEET (G,GA,XO,YO,PHISYM,NOF)
GO TO 4
CALL READ (Z,XO,YO,PHISYM,NOF,IMAX,JMAX,G)
IF (DGN.GE.2) WRITE (6,39)
RETURN
FORMAT (' GARRAY RETURNS')
END
C000006
C

```

SUB000630
SUB000640
SUB000650
SUB000660
SUB000670
SUB000680
SUB000690
SUB000700
SUB000710
SUB000720
SUB000730
SUB000740
SUB000750
SUB000760
SUB000770
SUB000780
SUB000790
SUB000800
SUB000810
SUB000820
SUB000830
SUB000840

```

SUBROUTINE GOLF (R,XI,GIJ,NOF,DGN,NUMB)
C
C GOLF COMPUTES THE FUNCTION G(R,XI) FOR A PARTICULAR LINE OF SIGHT
C FROM A KNOWN FUNCTION CONTAINED IN SUBROUTINE FUNCT.
C
COMMON IMAX,JMAX,IIMX,JJMX,IJMX,ALPHA,SIZE,EPS,MODE,BOX,SD,IX,Z
ZERO=0.
LMAX=IMAX*3
RLMAX=LMAX
DELXP=SIZE/RLMAX
SXI=SIN(XI)
CXI=COS(XI)
DELS=DELXP*CXI
DELYS=DELXP*SXI
XP=DELS*5-SIZE/2.
XS=XP*CXI-R*SXI
YS=XP*SXI+R*CXI
G(I,J)=0.
DO 1 L=1,LMAX
RL=L
CALL FUNCT(XS,YS,F,NOF,DGN,NUMB)
GIJ=GIJ+F

```

SUB000850
SUB000860
SUB000870
SUB000880
SUB000890
SUB000900
SUB000910
SUB000920
SUB000930
SUB000940
SUB000950
SUB000960
SUB000970
SUB000980

```

1  XS=XS+DELS
   YS=YS+DELS
   IF (GIJ.NE.0.) GIJ=GIJ*DELP*BOX
   IF ((SD.EQ.0.) .OR. (NUMB.EQ.1)) GO TO 2
   IF (DGN.GE.3) WRITE (6,28) IX
   CALL GAUSS (IX,SD,ZERO,RV)
   GIJ=GIJ+RV
   IF (DGN.GE.3) WRITE (6,29) R,XI,GIJ
2  RETURN
29  FORMAT (' R=',F8.3,' XI=',F8.3,' GIJ=',F8.3)
28  FORMAT (' GAUSS, IX=',I8)
   END
C000007
C

```

SUB000990
SUB01000

```

C  SUBROUTINE FUNCT (XS,YS,F,NOF,DGN,NUMB)
C
C  CP67USERID 1095BOXJ
C
C  FUNCT EVALUATES AS INPUT FUNCTION AT POSITION (X,Y) IN THE TEST
C  SECTION COORDINATE SYSTEM. NOF IDENTIFIES THE EQUATION USED.
C
COMMON IMAX,JMAX,IIMX,IJMX,ALPHA,SIZE,EPS,MODE,BOX,SD,IX,Z
COMMON /EQPARA/ A,B,C,D,E,P,Q,S,T,U,V,W,RO,RA,NO,NA,N1,N2
DIMENSION RO(101),RA(101)
AA=A
BB=B
CC=C
DD=D
EE=E
PP=P
IF (NUMB.LE.1) GO TO 50
AA=S
BB=T
CC=U
DD=V
EE=W
PP=Q
PIE=3.141592653589793
HS=SIZE/2.
R=SQRT(XS**2+YS**2)/HS
F=0.
IF (R.GT.1.) GO TO 11
IF (NOF.LE.0) GO TO 11

```

SUB01020
SUB01030
SUB01040
SUB01050
SUB01060
SUB01070
SUB01080
SUB01090
SUB01100
SUB01110
SUB01120
SUB01130
SUB01140
SUB01150
SUB01160
SUB01170
SUB01180
SUB01190
SUB01200
SUB01210
SUB01220
SUB01230
SUB01240
SUB01250
SUB01260
SUB01270
SUB01280

1. AXISYMMETRIC GAUSSIAN:

1	IF (NOF.GT.1) GO TO 2	SUB01290
C	F=AA*EXP(-1.*(R*HS/BB)**2)	SUB01300
C	GO TO 11	SUB01310
2	2. ADJUSTABLE RECTANGULAR STEP FUNCTION:	SUB01320
C	IF (NOF.GT.2) GO TO 3	SUB01330
C	F=PP	SUB01340
C	IF ((ABS(XS-DD).LE.BB).AND.(ABS(YS-EE).LE.CC)) F=AA	SUB01350
C	GO TO 11	SUB01360
3	3. DISPLACABLE ELLIPTICAL GAUSSIAN:	SUB01370
C	IF (NOF.GT.3) GO TO 4	SUB01380
C	F=AA*EXP(-1.*(((XS-DD)/BB)**2+((YS-EE)/CC)**2))	SUB01390
C	GO TO 11	SUB01400
4	4. CONSTANT:	SUB01410
C	IF (NOF.GT.4) GO TO 5	SUB01420
C	F=AA	SUB01430
C	GO TO 11	SUB01440
5	5. ADJUSTABLE AND DISPLACABLE ELLIPTIC RAMP FUNCTION:	SUB01450
C	IF (NOF.GT.5) GO TO 6	SUB01460
C	RBC=SQRT(((XS-DD)/BB)**2+((YS-EE)/CC)**2)	SUB01470
C	F=0.	SUB01480
C	IF (RBC.LT.1.) F=AA*({1.-RBC)**PP)	SUB01490
C	GO TO 11	SUB01500
6	6. DISPLACABLE ELLIPTIC STEP FUNCTION:	SUB01510
C	IF (NOF.GT.6) GO TO 7	SUB01520
C	RBC=SQRT(((XS-DD)/BB)**2+((YS-EE)/CC)**2)	SUB01530
C	F=0.	SUB01540
C	IF (RBC.LT.1.) F=AA	SUB01550
C	GO TO 11	SUB01560
7	7. CIRCULAR COSINE-SQUARED FUNCTION OF BB MAXIMA:	SUB01570
C	IF (NOF.GT.7) GO TO 8	SUB01580
C	F=AA*COS((2.*BB-1.)*PIE*R/2.))**2	SUB01590
C	GO TO 11	SUB01600
8	8. NUMERICAL FUNCTION: REQUIRES AN INPUT ARRAY READ IN BY	SUB01610
C	SUBROUTINE FREAD; N FOLLOWED BY N POINT VALUES. (101 MAX)	SUB01620
C	A CONSTANT VALUE AA	SUB01630
C	IF (NOF.GT.8) GO TO 9	SUB01640
C	IF (NUMB.LE.1) N=NO	SUB01650
C	IF (NUMB.GT.1) N=NA	SUB01660
C	NM=N-1	SUB01670
C	MM=N-2	SUB01680
C	RN=N	SUB01690
8		SUB01700
		SUB01710
		SUB01720
		SUB01730
		SUB01740
		SUB01750
		SUB01760


```

SUBROUTINE SHEET (G,D,XO,YO,PHISYM,NOF)
SHEET READS IRREGULARLY SPACED VALUES OF THE LINE INTEGRAL, AS
OBTAINED FROM HOLOGRAPHIC INTERFEROGRAMS. THE INTEGRAL LINES MAY BE
DEFINED EITHER BY GRID INTERCEPT POSITIONS, OR BY ANGLE AND RADIUS
ABOUT THE CENTER OF THE LABORATORY COORDINATE SYSTEM CENTER. LINES
MUST BE ENTERED IN CONSECUTIVE ORDER FROM LOWEST (NEG.) TO HIGHEST
(POS.) RADIUS. DATA MAY BE SIMULATED BY SPECIFYING NCODE=1,
FOLLOWED BY APERTURE POSITIONS FOR A FUNCTION NUMBER IN 'SUBFUNCT'.
SUB02170
SUB02180
SUB02190
SUB02200
SUB02210
SUB02220
SUB02230
SUB02240
SUB02250
SUB02260
SUB02270
SUB02280
SUB02290
SUB02300
SUB02310
SUB02320
SUB02330
SUB02340
SUB02350
SUB02360
SUB02370
SUB02380
SUB02390
SUB02400
SUB02410
SUB02420
SUB02430
SUB02440
SUB02450
SUB02460
SUB02470
SUB02480
SUB02490
SUB02500
SUB02510
SUB02520
SUB02530
SUB02540
SUB02550
SUB02560
SUB02570
SUB02580
SUB02590
SUB02600
SUB02610
SUB02620
SUB02630
SUB02640

SUBROUTINE SHEET (G,D,XO,YO,PHISYM,NOF)
SHEET READS IRREGULARLY SPACED VALUES OF THE LINE INTEGRAL, AS
OBTAINED FROM HOLOGRAPHIC INTERFEROGRAMS. THE INTEGRAL LINES MAY BE
DEFINED EITHER BY GRID INTERCEPT POSITIONS, OR BY ANGLE AND RADIUS
ABOUT THE CENTER OF THE LABORATORY COORDINATE SYSTEM CENTER. LINES
MUST BE ENTERED IN CONSECUTIVE ORDER FROM LOWEST (NEG.) TO HIGHEST
(POS.) RADIUS. DATA MAY BE SIMULATED BY SPECIFYING NCODE=1,
FOLLOWED BY APERTURE POSITIONS FOR A FUNCTION NUMBER IN 'SUBFUNCT'.
SUB02170
SUB02180
SUB02190
SUB02200
SUB02210
SUB02220
SUB02230
SUB02240
SUB02250
SUB02260
SUB02270
SUB02280
SUB02290
SUB02300
SUB02310
SUB02320
SUB02330
SUB02340
SUB02350
SUB02360
SUB02370
SUB02380
SUB02390
SUB02400
SUB02410
SUB02420
SUB02430
SUB02440
SUB02450
SUB02460
SUB02470
SUB02480
SUB02490
SUB02500
SUB02510
SUB02520
SUB02530
SUB02540
SUB02550
SUB02560
SUB02570
SUB02580
SUB02590
SUB02600
SUB02610
SUB02620
SUB02630
SUB02640

COMMON IMAX,JMAX,IIMX,JJMX,IJMX,ALPHA,SIZE,EPS,MODE,BOX,SD,IX,Z
COMMON /SYM/ISYM,JSYM,MSYM,FCU,IMS,JMS,QSYM
COMMON /IO/ CMS,IN1,IN2,IN4
DIMENSION G(IMAX,JMAX),D(IMAX,JMAX),XI(303),RR(303)
DIMENSION XG(303),XD(303),YG(303),YD(303),XY(303)
NAR=303
PIE=3.141592653589793
MPIE=-PIE
MPIE=2.*PIE
MPIE=PIE/2.
PIET=PIE/2.
ZERO THE ARRAYS:
DO 1 J=1,JMAX
DO 1 I=1,IMAX
G(I,J)=0.
D(I,J)=0.
DO 2 I=1,NAR
XG(I)=0.
XD(I)=0.
YG(I)=0.
YD(I)=0.
XY(I)=0.
XI(I)=0.
RR(I)=0.
READ THE BASIC DATA:
IF (CMS.EQ.1.) REWIND 1
READ (IN1,59) NOF,NCODE
READ (IN1,58) Z,XO,YO,PHISYM,XXM,XMN,YMX,YMN
READ (IN1,59) JM
RIMX=IMAX
DR=SIZE/RIMX
R=(-DR-SIZE)/2.
RZO=SQRT(XO**2+YO**2)
CAM=ATANM(YO,XO)
TP=3-ISYM
BT=JSYM
DAN=PIE*TP/BT
HS=SIZE/2.

```

```

SUB02650
SUB02660
SUB02670
SUB02680
SUB02690
SUB02700
SUB02710
SUB02720
SUB02730
SUB02740
SUB02750
SUB02760
SUB02770
SUB02780
SUB02790
SUB02800
SUB02810
SUB02820
SUB02830
SUB02840
SUB02850
SUB02860
SUB02870
SUB02880
SUB02890
SUB02900
SUB02910
SUB02920
SUB02930
SUB02940
SUB02950
SUB02960
SUB02970
SUB02980
SUB02990
SUB03000
SUB03010
SUB03020
SUB03030
SUB03040
SUB03050
SUB03060
SUB03070
SUB03080
SUB03090
SUB03100
SUB03110
SUB03120

      MXY=1
      IF((XMX.NE.0.).OR.(XMN.NE.0.).OR.(YMX.NE.0.).OR.(YMN.NE.0.))MXY=0
      IF (MXY.EQ.1) GO TO 3
      XMX=XO+HS
      YMX=YO+HS
      XMN=XO-HS
      YMN=YO-HS
      YMN=YO-HS
      COMMENCE THE READ AND FILL LOOP:
      DO 12 J=1,JM
      READ (IN1,59)IM
      MN=0
      XH=0.
      YH=0.
      C READ THE LINES, DETERMINE CODE, CALCULATE RADIUS & ANGLE FOR CODE 1:
      DO 5 I=1,IM
      IF(NCODE.LE.0)READ(IN1,58) XD(I),YD(I),XG(I),YG(I),D(I,J),RR(I),
      1XI(I),XY(I)
      IF(NCODE.GE.1)CALL SIM(XD(I),YD(I),XG(I),YG(I),RR(I),XI(I),
      1XY(I),XO,YO,PHISYM,XMX,XMN,YMX,YMN,NOF,I,IM)
      IF (XY(I).EQ.3.) GO TO 5
      IF (XD(I).NE.0.).OR. (YD(I).NE.0.) XY(I)=1.
      IF (XG(I).NE.0.).OR. (YG(I).NE.0.) XY(I)=1.
      IF ((RR(I).NE.0.).OR. (XI(I).NE.0.)).AND. (XY(I).EQ.0.)) XY(I)=2.
      IF (XY(I).EQ.0.).AND. (D(I,J).NE.0.) XY(I)=2.
      IF (XY(I).NE.1.) GO TO 4
      DEN=SQRT((XG(I)-XD(I))**2+(YG(I)-YD(I))**2)
      IF (DEN.EQ.0.) XY(I)=4.
      IF (XY(I).EQ.4.) GO TO 4
      RR(I)=((XO-XD(I))*(YG(I)-YD(I))-(XG(I)-XD(I))*(YO-YD(I)))/DEN
      XI(I)=ATANM((YG(I)-YD(I)), (XG(I)-XD(I)))
      XIM=XI(I)
      IF (XY(I).EQ.2.) XIM=XI(I)
      XIN=XIM
      IF(XY(I).EQ.2.) RR(I)=RR(I)+RZO*SIN(GAM-XI(I))
      CONTINUE
      5 COMPUTE MAX AND MIN ANGLE INDEXES FOR APERTURE POSITION LOCATION:
      DO 6 I=1,IM
      IF ((XY(I).NE.1.).OR. (XY(I).NE.2.)) GO TO 6
      IF (XI(I).GT.XIM) XIM=XI(I)
      IF (XI(I).GT.XIM) IMT=I
      IF (XI(I).LT.XIN) XIN=XI(I)
      IF (XI(I).LE.XIN) INT=I
      CONTINUE
      6 DETERMINE APERTURE LOCATION:
      LPR=0
      XID=XI(IMT)-XI(INT)
      IF(ABS(XID).LT..00001) LPR=1
      XIH=(XI(IMT)+XI(INT))/2.

```


SUB03130
SUB03140
SUB03150
SUB03160
SUB03170
SUB03180
SUB03190
SUB03200
SUB03210
SUB03220
SUB03230
SUB03240
SUB03250
SUB03260
SUB03270
SUB03280
SUB03290
SUB03300
SUB03310
SUB03320
SUB03330
SUB03340
SUB03350
SUB03360
SUB03370
SUB03380
SUB03390
SUB03400
SUB03410
SUB03420
SUB03430
SUB03440
SUB03450
SUB03460
SUB03470
SUB03480
SUB03490
SUB03500
SUB03510
SUB03520
SUB03530
SUB03540
SUB03550
SUB03560
SUB03570
SUB03580
SUB03590
SUB03600

```

RRH=10000.
XH=RRH*COS(XIH)
YH=RRH*SIN(XIH)
IF (LPR.EQ.1) GO TO 7
YTX=-RR(IMT)*SIN(XI(IMT))-YO
YTN=-RR(INT)*SIN(XI(INT))-YO
XTX=RR(IMT)*COS(XI(IMT))-XO
XTN=RR(INT)*COS(XI(INT))-XO
UA=TAN(XI(IMT))
UC=TAN(XI(INT))
UB=YTX-UA*XTX
UD=YTN-UC*XTN
XH=(UD-UB)/(UA-UC)
YH=XH*UA+UB
RRH=SQRT((XH-XO)**2+(YH-YO)**2)
XIH=ATANM((YH-YO),(XH-XO))
CONTINUE
7 C  FILL THE ANGLE AND RADIUS FOR ANY CODE 3 OR 4 LINES:
DO 9 I=1,IM
IF(XY(I).NE.3.) GO TO 8
BAS=SQRT(RRH**2-RR(I)**2)
XI(I)=XIH-ATANM(RR(I),BAS)
GO TO 9
8 XI(I)= ATANM((YH-YD(I)),(XH-XD(I)))
RR(I)=RRH*SIN(XI(I)-XIH)
CONTINUE
9 C  ANGLES AND RADII ARE NOW FILLED FOR ALL POINTS IN THIS LINE.
C  VACATE THE SET OF VECTORS TO BE USED AS TEMPORARY STORAGE:
DO 10 I=1,IM
XD(I)=0.
YD(I)=0.
XG(I)=0.
YG(I)=RR(I)
XY(I)=D(I,J)
RR(I)=0.
D(I,J)=0.
XI(I)=0.
10 C  CONVERT THE LINE TO REGULAR RADII USING INTERPOLATION:
RR(1)=R+DR
CALL SPLINE(YG,XY,IM,RR(1),D(1,J))
DO 11 I=2,IMAX
RI=I
RR(I)=R+DR*RI
CALL SPLINN(YG,XY,IM,RR(I),D(I,J))
11 C  GENERATE THE VECTOR OF ANGLES FOR THIS COLUMN AND STORE IN G ARRAY:
DO 12 I=1,IMAX
BAS=SQRT(RRH**2-RR(I)**2)
G(I,J)=XIH-ATANM(RR(I),BAS)

```

```

12      YG(I)=0.
C      D(I,J)=XY(I)
C      XY(I)=0.
C      COLUMNS ARE NOW ALL REGULARLY FILLED.
C      NEXT, INTERPOLATE EACH ROW REGULARLY OVER THE ANGLES.
C      DO 23 I=1,IMAX
C      EXPAND THE DATA TO 2 SETS TO ESTABLISH SMOOTH INTERPOLATION.
      JM3=3*JM
      II=IMAX+1-I
      IF (JSYM.NE.0) GO TO 14
      DO 13 J=1,JMS
      J2=J+JMS
      J3=J2+JMS
      XD(J)=D(I,J)
      XD(J2)=D(I,J)
      XD(J3)=D(I,J)
      XG(J)=G(I,J)-TPIE-PHISYM
      XG(J2)=G(I,J)-PIE-PHISYM
      XG(J3)=G(I,J)-PHISYM
      GO TO 16
      DO 15 J=1,JMS
      J1=JMS+1-J
      J2=JMS+J
      J3=JM3+1-J
      XD(J1)=D(I,J)
      XD(J2)=D(I,J)
      XD(J3)=D(I,J)
      XG(J1)=G(I,J)-2.*(G(I,J)-PHISYM)-PIE-PHISYM
      XG(J2)=G(I,J)-PIE-PHISYM
      XG(J3)=G(I,J)+2.*(DAN+PHISYM-G(I,J))-PIE-PHISYM
      CONTINUE
      JM2=2*JMS
      JP=JMS/2
      DO 17 J=1,JM2
      XD(J)=XD(J+JP)
      XG(J)=XG(J+JP)
      JJS=JM2+1
      DO 18 J=JJS,JM3
      XD(J)=0.
      XG(J)=0.
      FIND THE SMALLEST ANGLE
      XY(1)=1.
      SA=XG(1)
      DO 19 J=1,JM2
      IF (XG(J).GE.SA) GO TO 19
      SA=XG(J)
      XY(1)=J
      CONTINUE
13
14
15
16
17
18
19

```

SUB03610
SUB03620
SUB03630
SUB03640
SUB03650
SUB03660
SUB03670
SUB03680
SUB03690
SUB03700
SUB03710
SUB03720
SUB03730
SUB03740
SUB03750
SUB03760
SUB03770
SUB03780
SUB03790
SUB03800
SUB03810
SUB03820
SUB03830
SUB03840
SUB03850
SUB03860
SUB03870
SUB03880
SUB03890
SUB03900
SUB03910
SUB03920
SUB03930
SUB03940
SUB03950
SUB03960
SUB03970
SUB03980
SUB03990
SUB04000
SUB04010
SUB04020
SUB04030
SUB04040
SUB04050
SUB04060
SUB04070
SUB04080


```

C      FIND THA MAX ANGLE IN THE ROW:
      XY(JM2)=JM2
      SB=XG(JM2)
      DO 20 J=1,JM2
      IF (XG(J).LE.SB) GO TO 20
      SB=XG(J)
      XY(JM2)=J
      CONTINUE
20 C      DETERMINE THE ORDER OF INCREASING ANGLE IN THE ROW
      SB=XG(JM2)
      JJ=2
      JSA=XY(JJ-1)
      SA=XG(JJ-1)
      JTS=0
      DO 22 J=1,JM2
      IF (XG(J).LE.SA) GO TO 22
      IF (XG(J).GT.SB) GO TO 22
      SB=XG(J)
      XY(JJ)=J
      JTS=1
      CONTINUE
22 IF (JTS.EQ.0) JM2=JJ
      JJ=JJ+1
      IF (JJ.LE.JM2) GO TO 21
      DO 23 J=1,JM2
      JX=XY(J)
      YD(J)=XD(JX)
      INTERPOLATE:
      DXI=2.*PIE/FCU
      XI(J)=DXI/2.-PIE-PHISYM
      CALL SPLINE (XG,YD,JM2,XI(J),G(I,J))
      DO 24 J=2,JMS
      XI(J)=XI(J-1)+DXI
      CALL SPLINN (XG,YD,JM2,XI(J),G(I,J))
      DO 25 J=1,JMS
      XIJ=XI(J)
      XU=XMX
      IF ((XIJ.GE.0.).AND.(XIJ.LT.PIE)) XU=XMN
      YU=YMN
      IF ((XIJ.GE.MPIT).AND.(XIJ.LT.PIT)) YU=YMX
      XL=XMN
      IF ((XIJ.GE.0.).AND.(XIJ.LT.PIE)) XL=XMX
      YL=YMX
      IF ((XIJ.GE.MPIT).AND.(XIJ.LT.PIT)) YL=YMN
      SXIJ=SIN(XIJ)
      CXIJ=COS(XIJ)
      RMN=(XO-XL)*SXIJ-(YO-YU)*CXIJ
      RMX=(XO-XU)*SXIJ-(YO-YU)*CXIJ

```

SUB04090
 SUB04100
 SUB04110
 SUB04120
 SUB04130
 SUB04140
 SUB04150
 SUB04160
 SUB04170
 SUB04180
 SUB04190
 SUB04200
 SUB04210
 SUB04220
 SUB04230
 SUB04240
 SUB04250
 SUB04260
 SUB04270
 SUB04280
 SUB04290
 SUB04300
 SUB04310
 SUB04320
 SUB04330
 SUB04340
 SUB04350
 SUB04360
 SUB04370
 SUB04380
 SUB04390
 SUB04400
 SUB04410
 SUB04420
 SUB04430
 SUB04440
 SUB04450
 SUB04460
 SUB04470
 SUB04480
 SUB04490
 SUB04500
 SUB04510
 SUB04520
 SUB04530
 SUB04540
 SUB04550
 SUB04560

```

25 C      DO 25 I=1,IMAX
      IF (RR(I).LT.RMN) G(I,J)=0.
      IF (RR(I).GT.RMX) G(I,J)=0.
      CONTINUE
      EXPAND SYMMETRY SECTOR INTO AN ORTHOGONAL INTERVAL.
      IF (ISYM.EQ.2) GO TO 27
      DO 26 J=1,JMS
      J2=JMAX/2+1-J
      J3=JMAX/2+J
      J4=JMAX+1-J
      DO 26 I=1,IMAX
      II=IMAX+1-I
      G(I,J2)=G(I,J)
      G(II,J3)=G(I,J)
      G(II,J4)=G(I,J)
      RETURN
26 C      FOR EVEN SYMMETRY, AVERAGE THE GARRY COLUMNS.
27 C      IMS=(2*IMAX+1)/2
      DO 28 J=1,JMAX
      DO 28 I=1,IMS
      II=IMAX+1-I
      GST=(G(I,J)+G(II,J))/2.
      G(I,J)=GST
      G(II,J)=GST
28 C      RETURN
59 C      FORMAT (5I5)
58 C      FORMAT (10F7.3)
      END
C000010
C
      FUNCTION ATANM(Y,X)
C      COMPUTES THE ARCTAN OF Y/X BETWEEN -PI AND +PI.
C
      PIE=3.141592653589793
      PI2=PI/2.
      ATANM=SIGN(PI2,Y)
      IF(X.NE.0.) ATANM=ATAN(Y/X)
      IF(X.GE.0.) RETURN
      IF(Y.GE.0.) ATANM=PI+ATANM
      IF(Y.LT.0.) ATANM=-PI+ATANM
      RETURN
      END
C000011
C
SUB04570
SUB04580
SUB04590
SUB04600
SUB04610
SUB04620
SUB04630
SUB04640
SUB04650
SUB04660
SUB04670
SUB04680
SUB04690
SUB04700
SUB04710
SUB04720
SUB04730
SUB04740
SUB04750
SUB04760
SUB04780
SUB04790
SUB04800
SUB04810
SUB04820
SUB04830
SUB04840
SUB04850
SUB04860
SUB04870
SUB04880
SUB04890
SUB04900
SUB04910
SUB04920
SUB04930
SUB04940
SUB04950
SUB04960
SUB04970
SUB04980
SUB04990
SUB05000
SUB05010

```

```

SUBROUTINE SIM (XD,YD,XG,YG,D,R,XI,XY,XO,YO,PS,XM,XN,YM,YN,I,IM,
1DG,NF)
C
C SIM SIMULATES THE FRINGE NUMBER DATA ONE WOULD OBTAIN FROM THE
C HOLOGRAPHIC INTERFEROGRAM PROCESS FOR A KNOWN FUNCTION AS
C CONTAINED IN SUBROUTINE FUNCT. THE GRID BOX DIMENSIONS MUST
C EXCEED THE INVERSION CIRCLE SIZE, AND APERTURE POINTS SPECIFIED
C MUST FALL BETWEEN XI=-40 DEGREES, AND XI=+130 DEGREES.
C
COMMON IMAX,JMAX,IIMX,JJMX,IJMX,ALF,SIZ,EPS,MOD,BOX,SD,IX,Z
COMMON /IO/ CMS,IN1,IN2,IN4
READ (IN1,29) XH,YH
ZER=0.
RIM=IM
RI=I
DX=(XM-XN)/(RIM-1.)
DY=(YM-YN)/(RIM-1.)
XI=XM-(RIM-1.)*DX
YI=YM-(RIM-1.)*DY
XI1=ATANM (YH-YI,XH-XI)-PS
RRH=SQRT((XH-XO)**2+(YH-YO)**2)
XIO=ATANM(YH-YO,XH-XO)-PS
RI=RRH*SIN(XI1-XIO)
IF ((I.GT.1).AND.(I.LT.IM)) GO TO 1
IF (ABS(RI).LT.SIZ/2.) RI=SIGN(SIZ/2.,RI)
XY=3.
GO TO 2
1 CALL GOLF (R,XI,D,NR,ZER,ZER)
XD=XN
YD=YN
IF (XH.NE.XI) YD=YI-(XI-XN)*(YH-YI)/(XH-XI)
IF (YS.GE.YN) GO TO 2
YD=YN
IF (YH.NE.YI) XD=XI-(YI-YN)*(XH-XI)/(YH-YI)
RETURN
FORMAT (10F7.3)
END
C000012
C
SUBROUTINE FREAD (NO,RO,NF,ZZ)
C
C FREAD READS THE NUMERIC ARRAY WHICH IS USED FOR EQUATION 8 OF
C SUBROUTINE FUNCT. FIRST CARD IS NUMBER OF POINTS (N.GE.1),
C FOLLOWED BY ONE POINT PER CARD.
C
C DIMENSION RO(101)
SUB05020
SUB05030
SUB05040
SUB05050
SUB05060
SUB05070
SUB05080
SUB05090
SUB05100
SUB05110
SUB05120
SUB05130
SUB05140
SUB05150
SUB05160
SUB05170
SUB05180
SUB05190
SUB05200
SUB05210
SUB05220
SUB05230
SUB05240
SUB05250
SUB05260
SUB05270
SUB05280
SUB05290
SUB05300
SUB05310
SUB05320
SUB05330
SUB05340
SUB05350
SUB05360
SUB05370
SUB05380
SUB00010
SUB00020
SUB00030
SUB00040
SUB00050
SUB00060
SUB00070
SUB00080
SUB00090

```

```

SUB000100
      READ (NF,89) NO,ZZ
      WRITE(6,90) NO,ZZ
      DO 10 I=1,NO
      READ(NF,88) RO(I)
      WRITE(6,88) RO(I)
      CONTINUE
      FORMAT (I5,F9.3)
      89  FORMAT(F8.5)
      90  FORMAT(1X,I5,F9.3)
      RETURN
      END
C0000013
C
      SUBROUTINE GPRINT (G,NUMB)
C
C  GPRINT PRINTS THE DATA ARRAY 'G' WHICH WAS INPUT TO
C  THE PROGRAM IN SUBROUTINE GARRAY.
C
      COMMON IMAX,JMAX,IIMX,JJMX,IJMX,ALPHA,SIZE,EPS,MODE,BOX,SD,IX,Z
      DIMENSION G(IJMX)
      DIMENSION X(15)
      DATA HYP,VERT/1H~,1H//
      IF (NUMB.EQ.1) WRITE (6,99) MODE,Z
      IF (NUMB.EQ.2) WRITE (6,92) Z
      JM2=JMAX/2
      RIMAX=IMAX
      RJMAX=JMAX
      DX=SIZE/RIMAX
      DXI=360./RJMAX
      INTRVL SETS THE NUMBER OF TERMS PRINTED PER LINE. IF IT IS ALTERED,
      ONE MUST ALSO REDIMENSION X AND ALTER FORMATS 98, 97, AND 95.
      INTRVL=15
      IB=1
      IT=IB+INTRVL-1
      IF (IT.GT.IMAX) IT=IMAX
      IBT=IT-IB+1
      WRITE (6,98) (II,II=IB,IT)
      DO 2 I=1,IBT
      RI=IB-1+I
      X(I)=--SIZE/2.+(RI-.5)*DX
      LM=7*IBT+1
      WRITE (6,97) (X(I),I=1,IBT)
      WRITE (6,96) (HYP,L=1,LM),VERT
      JMH=JM2+1
      DO 3 J=JMH,JMAX
      RJ=J

```

```

3      XI=-180.+DXI*(RJ-.5)
      IGB=(J-1)*IMAX+IB
      IGT=IGB-IB+IT
      WRITE (6,95) J,XI,(G(L),L=IGB,IGT)
      WRITE (6,94) (HYP,L=1,LM),VERT
      IB=IB+INTRVL
      ITOLD=IT
      IT=IT+INTRVL
      IF (ITOLD.LT.IMAX) GO TO 1
      WRITE (6,93)
      FORMAT (1H1//,
1      1MODE,1,11,1,
      98      THE ARRAY OF INPUT DATA (G), OBTAINED BY GARRAY,
      97      FOR Z=F7.3, CM: ')
      FORMAT (//11X,1=,15I7)
      96      FORMAT (11X,X=,15F7.3)
      95      FORMAT (1, J=,15F7.3)
      94      FORMAT (2X,I3,F9.2,1,1,15F7.3)
      93      FORMAT (14X,1,1,15F7.3)
      92      FORMAT (//5X)
      RETURN
      END
C000014
C

```

```

C      SUBROUTINE GPUNCH (Z,XO,YO,PHS,NOF,IMX,JMX,G)
C      GPUNCH PUNCHES OUT THE FIRST NON-SYMMETRIC PORTION OF GARRAY
C      (OR WRITES IT ON FILE 7 IN CMS VERSION)
C
C      COMMON /SYM/ ISM,JSM,MSM,FCU,IMS,JMS,QSM
C      DIMENSION G(IMX,JMX)
C      WRITE (7,39) NOF,IMX,JMX,ISM,JSM,IMS,JMS
C      WRITE (7,38) ((G(I,J),I=1,IMS),J=1,JMS)
39      FORMAT(10I5)
38      RETURN
      END
C000015
C

```

```

C      SUBROUTINE READ (Z,XO,YO,PHISYM,NOF,IMAX,JMAX,G)
C      READS THE NON-SYMMETRIC PORTION OF THE GARRAY AND EXPANDS IT TO AN
C      ORTHOGONAL SET. NOTE, INSURE SUFFICIENT DIMENSIONS IN MAIN PROGRAM.
C
C      COMMON /SYM/ ISYM,JSYM,MSYM,FCU,IMS,JMS,QSYM
C

```



```

COMMON /IO/ CMS, IN1, IN2, IN4
DIMENSION G(IMAX, JMAX)
READ (IN1, 39) NOF, IMAX, JMAX, ISYM, JSYM, IMS, JMS
READ (IN1, 38) Z, XC, YO, PHISYM
READ (IN1, 38) ((G(I, J), I=1, IMS), J=1, JMS)
WRITE(6, 37) NOF, Z, XC, YO, PHISYM, IMAX, JMAX, JSYM
RJMXX=JMAX
MSYM=JSYM
IF ((MSYM.EQ.0).OR.(MSYM.GT.JMAX)) MSYM=1
FCU=ISYM*JSYM*JMAX
IF (JSYM.GT.JMAX) FCU=JMAX
QSYM=FCU/RJMX
DO 4 J=1, JMS
IF (ISYM.EQ.1) GO TO 2
DO 1 I=1, IMS
II=IMAX+1-I
G(II, J)=G(I, J)
GO TO 4
J2=JMAX/2+1-J
J3=JMAX/2+J
J4=JMAX+1-J
DO 3 I=1, IMAX
II=IMAX+1-I
G(II, J2)=G(I, J)
G(II, J3)=G(I, J)
G(II, J4)=G(I, J)
CONTINUE
FORMAT(10I5)
FORMAT(10F7.3)
FORMAT(//, 'MODE 3 READS GARRAY DIRECTLY: NOF=', I4, '
1, , XC=', F7.3, ', YO=', F7.3, ', PHISYM=', F7.3, '
2, , JMAX=', I4, ', JSYM=', I4, '//)
RETURN
END
C000016
C

```

SUBROUTINE MAP (IM, JM, A, N, Z, BAND)

MAP CALLS SUBROUTINE MIMPII AND PLOTS A CONTOUR MAP OF THE ARRAY

DIMENSION A(IM, JM), T(24)

DATA BL/1H/

DO 1 I=1, 24

T(I)=BL

ICON=1

IF(BAND.LT.0.) ICON=0

SUB01310
SUB01320
SUB01330
SUB01340
SUB01350
SUB01360
SUB01370
SUB01380
SUB01390
SUB01400

SUB000950
SUB000960
SUB000970
SUB000980
SUB000990
SUB01000
SUB01010
SUB01020
SUB01030
SUB01040
SUB01050
SUB01060
SUB01070
SUB01080
SUB01090
SUB01100
SUB01110
SUB01120
SUB01130
SUB01140
SUB01150
SUB01160
SUB01170
SUB01180
SUB01190
SUB01200
SUB01210
SUB01220
SUB01230
SUB01240
SUB01250
SUB01260
SUB01270
SUB01280
SUB01290
SUB01300

SUB01410
SUB01420
SUB01430
SUB01440
SUB01450
SUB01460
SUB01470
SUB01480
SUB01490
SUB01500
SUB01510
SUB01520

```

IF(BAND.LT.0.) BAND=-BAND
AMIN=0.
IJT=0
AZ=1.
BZ=0.
WRITE(6,49) N,Z
CALL MTMPII (A,IM,JM,T,BAND,AZ,BZ,AMIN,IJT,ICON)
49  FORMAT (1H1//, ' THE FUNCTION SURFACE, TEST NO.,I3,' Z='F5.3//)
RETURN
END
C000017
C

```

SUB01530
SUB01540
SUB01550
SUB01560
SUB01570
SUB01580
SUB01590
SUB01600
SUB01610
SUB01620
SUB01630
SUB01640
SUB01650
SUB01660
SUB01670
SUB01680
SUB01690
SUB01700
SUB01710
SUB01720
SUB01730
SUB01740
SUB01750
SUB01760
SUB01770
SUB01780
SUB01790
SUB01800
SUB01810
SUB01820
SUB01830
SUB01840
SUB01850
SUB01860

```

SUBROUTINE GPLOT (G,GA,JMS)
C
C GPLOT PRINTS A ROUGH PLOT OF THE LINE INTEGRAL FUNCTIONS IN GARRAY.
C
COMMON IMAX,JMAX,IIMX,IJMX,ISYM,IJSYM
COMMON /TAB/ INDEX(7),JSYM,IJSYM
COMMON /TAB2/ IPT,KPT,LPT,MPT,REST(5)
DIMENSION G(IMAX,JMAX),GA(IMAX,JMAX),ROW(101)
JM=101
DATA BL,PL,ST,DH,EX/1H,1H+,1H*,1H-,1HX/
JMS2=JMAX/2+1
IF(ISYM.EQ.2) JMS2=1
JMS3=JMS2+JMS-1
DO 8 J=JMS2,JMS3
WRITE(6,67) (ST,I=1,120)
DO 1 I=1,IMAX
A(I)=G(I,J)
C(I)=GA(I,J)
AS=.5
BS=.0
CALL INTERP (A,IMAX,AS,B,JM,BS)
CALL INTERP (C,IMAX,AS,D,JM,BS)
WRITE (6,69) J
BIG=0.
SMALL=0.
DO 2 I=1,IMAX
IF(A(I).GT.BIG) BIG=A(I)
IF(C(I).GT.BIG) BIG=C(I)
IF(A(I).LT.SMALL) SMALL=A(I)
IF(C(I).LT.SMALL) SMALL=C(I)
RANGE=BIG-SMALL
RINK=RANGE/80.
TOP=BIG+RINK

```

SUB01870
SUB01880
SUB01890
SUB01900
SUB01910
SUB01920
SUB01930
SUB01940
SUB01950
SUB01960
SUB01970
SUB01980
SUB01990
SUB02000
SUB02010
SUB02020
SUB02030
SUB02040
SUB02050
SUB02060
SUB02070
SUB02080
SUB02090
SUB02100
SUB02110
SUB02120
SUB02130
SUB02140
SUB02150
SUB02160
SUB02170
SUB02180
SUB02190
SUB02200
SUB02210

```

CEN=BIG
BOT=BIG-RINK
KC=0
DO 7 K=1,41
IC=0
DO 6 I=1,101
ROW(I)=BL
IF((I.EQ.1).OR.(I.EQ.51).OR.(I.EQ.101))ROW(I)=PL
IF((K.EQ.1).OR.(K.EQ.41))ROW(I)=PL
IF((TOP.GE.0.).AND.(BOT.LE.0.))ROW(I)=DH
IF((IC.EQ.5)GO TO 3
GO TO 4
IC=0
IF(KC.EQ.10)ROW(I)=PL
IF(KPT.LE.2)GO TO 5
IF((D(I).LE.TOP).AND.(D(I).GE.BOT))ROW(I)=ST
IF((B(I).LE.TOP).AND.(B(I).GE.BOT))ROW(I)=EX
IC=IC+1
IF(KC.EQ.5)KC=0
IF(KC.NE.0)WRITE (6,65) (ROW(I),I=1,101)
IF(KC.EQ.0)WRITE (6,68)CEN,(ROW(I),I=1,101)
TOP=TOP-2.*RINK
CEN=CEN-2.*RINK
BOT=BOT-2.*RINK
KC=KC+1
WRITE (6,66) (ST,I=1,120)
FORMAT (//,J=,I3//)
FORMAT (1X,F8.3,1X,101A1)
FORMAT (1H,//121A1//)
FORMAT (//121A1//)
FORMAT (10X,101A1)
RETURN
END
C000018
C

```

SUB02220
SUB02230
SUB02240
SUB02250
SUB02260
SUB02270
SUB02280
SUB02290
SUB02300
SUB02310
SUB02320

```

SUBROUTINE INTERP (A,IM,AS,B,JM,BS)
C
C   INTERP CONVERTS A REGULAR VECTOR A OF IM POINTS TO A REGULAR VECTOR
C   B OF JM POINTS. OS=.5 FOR A VECTOR WITH POINTS DEFINED IN THE
C   CENTER OF THE INTERVAL, AS AND BS ARE THE % OF AN INTERVAL FROM THE
C   EDGE OF THE FIELD TO THE FIRST POINT (.0 OR .5 FOR EDGE OR CENTER
C   DEFINED POINTS)
C
C   DIMENSION A(IM),B(JM)
C   RIM=IM
C   RJM=JM

```

```

SUB02330
SUB02340
SUB02350
SUB02360
SUB02370
SUB02380
SUB02390
SUB02400
SUB02410
SUB02420
SUB02430
SUB02440
SUB02450
SUB02460
SUB02470

```

RAT=(RIM-1.+2.*AS)/(RJM-1.+2.*BS)
 DO 2 I=1,JM
 BI=I
 AI=RAT*(BI+BS)-AS
 IA=AI
 F=AI-FLOAT(IA)
 IF((IA.EQ.O).OR.(IA.EQ.JM)) GO TO 1
 B(I)=A(IA)+F*(A(IA+1)-A(IA))
 GO TO 2
 IF(IA.EQ.O) B(I)=A(1)*(F-AS)/(1.-AS)
 IF(IA.EQ.JM) B(I)=A(JM)*F/(1.-AS)
 CONTINUE
 RETURN
 END

```

C000019
SUBROUTINE SPLINE
  PROVIDES INTERPOLATED VALUE USING "CUBIC SPLINE FITTING"

  USAGE
    FIRST CALL TO SUBROUTINE:
      CALL SPLINE(X,Y,M,XINT,YINT)
    SUBSEQUENT CALLS:
      CALL SPLINN(X,Y,M,XINT,YINT)

  DESCRIPTION OF PARAMETERS
    X: MONOTONICALLY INCREASING ABSCISSA ARRAY
    Y: ONE-FOR-ONE CORRESPONDING ORDINATE ARRAY
    M: NUMBER OF X AND Y VALUES SUPPLIED < OR = 300
    XINT: VALUE OF ABSCISSA FOR WHICH CORRESPONDING ORDINATE
          IS TO BE INTERPOLATED (OR EXTRAPOLATED)
    YINT: INTERPOLATED (OR EXTRAPOLATED) ORDINATE VALUE

  REMARKS
    IF SPECIFIED X FALLS OUTSIDE OF RANGE, AN EXTRAPOLATED
    VALUE WILL BE SUPPLIED

  SUBROUTINES AND FUNCTION SUBPROGRAMS REQUIRED
    SUBROUTINE SPLICO IS INCLUDED IN SUBROUTINE SPLIN PACKAGE

  MATHEMATICAL METHOD
    UPON FIRST ENTRY TO SPLIN, A CALL TO SPLICO IS MADE TO

```

0000000000000000
4567890123
3333334444
000000000000
J J J J J J J J
P P P P P P P P
S S S S S S S S

DETERMINE THE COEFFICIENTS TO BE USED IN PERFORMING THE INTERPOLATIONS. SEARCH FOR BRACKETING ABSCISSA VALUES IS ALWAYS MADE FROM THE REFERENCE LAST USED IN INTERPOLATING.

REFERENCE
PENNINGTON, RALPH H., "INTRODUCTORY COMPUTER METHODS AND
NUMERICAL ANALYSIS", THE MACMILLAN COMPANY, NEW YORK, 1965

SP L0044
SP L00460
SP L00470
SP L00480
SP L00490
SP L0050
SP L00510
SP L00520
SP L00530
SP L00540
SP L00550
SP L00560
SP L00570
SP L00580
SP L00590
SP L00600
SP L00610
SP L00620
SP L00630
SP L00640
SP L00650
SP L00660
SP L00670
SP L00680
SP L00690
SP L00700
SP L00710
SP L00720

```

SUBROUTINE SPLINE(X,Y,M,XINT,YINT)
DIMENSION X(M),Y(M),C(4,300)
CALL SPLICO(X,Y,M,C)
K=1
ENTRY SPLINN(X,Y,M,XINT,YINT)
IF(XINT-X(1)) 70,1,2
3 70 K=1
GO TO 7
1 YINT=Y(1)
RETURN
2 IF(XINT-X(K+1)) 6,4,5
4 YINT=Y(K+1)
RETURN
5 K=K+1
IF(M-K) 71,71,3
71 K=M-1
GO TO 7
6 IF(XINT-X(K)) 13,12,11
12 YINT=Y(K)
RETURN
13 K=K-1
GO TO 6
7 PRINT 101,XINT
FORMAT(8H0XINT = E18.9,32H, OUT OF
01 YINT=(X(K+1)-XINT)*(C(1,K)*(X(K+1)
11 YINT=YINT+(XINT-X(K))*(C(2,K)*(XIN
RETURN
END

```

SPL00730
SPL00750
SPL00760
SPL00770
SPL00780
SPL00790

```

SUBROUTINE SPLICO(X,Y,M,C)
DIMENSION X(M),Y(M),C(4,300),E(300),P(300),A(300,3),B(300,
Z(300)
MM=M-1
DO 2 K=1,MM
D(K)=X(K+1)-X(K)

```

```

      P(K)=D(K)/6.
2  E(K)=(Y(K+1)-Y(K))/D(K)
      DO 3 K=2,MM
3  B(K)=E(K)-E(K-1)
      A(1,2)=-1.-D(1)/D(2)
      A(1,3)=D(1)/D(2)
      A(2,3)=P(2)-P(1)*A(1,3)
      A(2,2)=2.*(P(1)+P(2))-P(1)*A(1,2)
      A(2,3)=A(2,3)/A(2,2)
      B(2)=B(2)/A(2,2)
      DO 4 K=3,MM
      A(K,2)=2.*(P(K-1)+P(K))-P(K-1)*A(K-1,3)
      B(K)=B(K)-P(K-1)*B(K-1)
      A(K,3)=P(K)/A(K,2)
      B(K)=B(K)/A(K,2)
4  Q=D(M-2)/D(M-1)
      A(M,1)=1.+Q+A(M-2,3)
      A(M,2)=-Q-A(M,1)*A(M-1,3)
      B(M)=B(M-2)-A(M,1)*B(M-1)
      Z(M)=B(M)/A(M,2)
      MN=M-2
      DO 6 I=1,MN
      K=M-I
6  Z(K)=B(K)-A(K,3)*Z(K+1)
      Z(1)=-A(1,2)*Z(2)-A(1,3)*Z(3)
      DO 7 K=1,MM
      Q=1./(6.*D(K))
      C(1,K)=Z(K)*Q
      C(2,K)=Z(K+1)*Q
      C(3,K)=Y(K)/D(K)-Z(K)*P(K)
7  C(4,K)=Y(K+1)/D(K)-Z(K+1)*P(K)
      RETURN
      END

```

C000020

```

C *****
C SUBROUTINE MTMPII
C
C PURPOSE
C MTMPII WILL PRODUCE, ON THE PRINTER, A CONTOUR MAP
C OF ANY SINGLE PRECISION TWO DIMENSIONAL ARRAY.
C
C USAGE
C CALL MTMPII(Y,N,M,T,BND,AZ,BZ,AMIN,IJT,ICON)
C
C *****
C MET00010
C MET00020
C MET00030
C MET00040
C MET00050
C MET00060
C MET00070
C MET00080
C MET00090
C MET00100
C MET00110
C MET00120

```



```

C      OAKES CODE 5105    15 JAN 69
C
SUBROUTINE MTMPII(Y,N,M,T,BND,AZ,BZ,AMIN,IJT,ICON)
REAL*4 IH,KG,IJJZ
DIMENSION A(140),B(140),C(140),D(140),IH(20),Y(N,M),TPX(10)
Z ,TPM(10),XMT(10),BTM(10),BTX(10),BT(10),KG(10),T(24)
DIMENSION E(140),F(140),G(140),H(140)
DATA DUE/4H /,EPL/4H+ /,EMI/4H- /,IH/1H0,1H ,1H1,1H ,1H2,
11H ,1H3,1H ,1H4,1H ,1H5,1H ,1H6,1H ,1H7,1H ,1H8,1H /,KG/,
21H0,1H1,1H2,1H3,1H4,1H5,1H6,1H7,1H8,1H9/,BLK/4H
YMIN=Y(1,1)
YMAX=Y(1,1)
DO 20 I=1,M
DO 10 J=1,N
YMIN=AMIN1(YMIN,Y(J,I))
YMAX=AMAX1(YMAX,Y(J,I))
CONTINUE
10 CONTINUE
20 DELY=YMAX-YMIN
IF(BND) 25,25,30
30 BND=DELY/15.0
25 IF (IJJZ) 31,31,32
31 IF (IJT) 33,32,33
32 PD=YMIN/BND
PF=ABS(PD-INT(PD))
IF (YMIN) 2,1,1
1 AMIN=YMIN-PF*BND
GO TO 33
2 AMIN=YMIN-(1.0-PF)*BND
33 AHLD=AZ
IF(AZ) 55,35,55
35 SM=AMAX1(ABS(YMIN),ABS(YMAX))
NS=0
40 NS=NS+1
SM=10.0*SM
IF(SM-1.0)40,50,45
45 NS=NS-1
SM=SM/10.0
,F(SM-1.0)50,50,45
50 AHLD=10.0*NS
55 HBND=BND/2.0
PRINT 70.
PRINT 6,T
MET000610
MET000620
MET000630
MET000640
MET000650
MET000660
MET000670
MET000680
MET000690
MET000700
MET000710
MET000720
MET000730
MET000740
MET000750
MET000760
MET000770
MET000780
MET000790
MET000800
MET000810
MET000820
MET000830
MET000840
MET000850
MET000860
MET000870
MET000880
MET000890
MET000900
MET000910
MET000920
MET000930
MET000940
MET000950
MET000960
MET000970
MET000980
MET000990
MET010000
MET010010
MET010020
MET010030
MET010040
MET010050
MET010060

```

```

6  FORMAT(5X,24A4,/)
  PRINT 57,AHLD,BZ
57  FORMAT(1H0,65H THE FOLLOWING TRANSFORMATION WAS PERFORMED ON THE IN
  1PUT MATRIX /5X,1H(,E12.5,8H*Y(I,J)+,E12.5,1H) //2X,73HAND THREE
  2 DIGITS TO THE RIGHT OF THE DECIMAL POINT ARE PRINTED IN THE MAP )
C
  PRINT 54,YMAX,YMIN
54  FORMAT(/4X,5HYMAX=,E15.7,5X,5HYMIN=,E15.7)
  IF (ICON)5,58,5
5  PRINT 11,BND
11  FORMAT(2X,17H THE BAND WIDTH IS,E12.5,6H UNITS //4X,14H CONTOUR LEVE
  1LS
  I=0
  YTOP=AMIN
  IF (ABS(YMIN-YMAX)-100.0*BND)53,53,58
53  YB=YTOP
  YTOP=YTOP+BND
  I=I+1
  J=MOD(I,20)
  ITJZ=IH(J)
  IF (YB-YMAX)59,58,58
59  PRINT 61,YB,YTOP,ITJZ
61  FORMAT(/4X,E10.3,4H TO ,E10.3,2H =,1X,A1)
  GO TO 53
58  NCCP=0
  NCP=0
60  PRINT 70
70  FORMAT(1H1)
  PRINT 6,T
  NLINE=0
  NCCP=NCP+1
73  IF (NCP-M)80,80,75
75  NCP=M
80  CONTINUE
  J=-2
  NLINE=NLINE+1
  LLINE=N-NLINE+1
  UP HEADING
  IF (NCCP-1) 85,85,90
  J = -1
85  DO 100 I = 1,135
90  A(I)=BLK
  B(I)=BLK
  H(I)=BLK
100 CONTINUE
110 DO 160 L=NCCP,NCP
  J = J+8
MET01070
MET01080
MET01090
MET01100
MET01110
MET01120
MET01130
MET01140
MET01150
MET01160
MET01170
MET01180
MET01190
MET01200
MET01210
MET01220
MET01230
MET01240
MET01250
MET01260
MET01270
MET01280
MET01290
MET01300
MET01310
MET01320
MET01330
MET01340
MET01350
MET01360
MET01370
MET01380
MET01390
MET01400
MET01410
MET01420
MET01430
MET01440
MET01450
MET01460
MET01470
MET01480
MET01490
MET01500
MET01510
MET01520
MET01530
MET01540

```

MET01550
 MET01560
 MET01570
 MET01580
 MET01590
 MET01600
 MET01610
 MET01620
 MET01630
 MET01640
 MET01650
 MET01660
 MET01670
 MET01680
 MET01690
 MET01700
 MET01710
 MET01720
 MET01730
 MET01740
 MET01750
 MET01760
 MET01770
 MET01780
 MET01790
 MET01800
 MET01810
 MET01820
 MET01830
 MET01840
 MET01850
 MET01860
 MET01870
 MET01880
 MET01890
 MET01900
 MET01910
 MET01920
 MET01930
 MET01940
 MET01950
 MET01960
 MET01970
 MET01980
 MET01990
 MET02000
 MET02010
 MET02020

```

    KI=L
    IF(KI-100) 130,120,120
    LL=KI/100
    A(J)=KG(LL+1)
    KI=KI-100*LL
    GO TO 135
    130 A(J)=KG(1)
    135 J=J+1
    IF(KI-10) 150,140,140
    140 LL=KI/10
    A(J)=KG(LL+1)
    KI=KI-10*LL
    GO TO 155
    150 A(J)=KG(1)
    155 J=J+1
    A(J)=KG(KI+1)
    160 CONTINUE
    C SETUP FIRST ROW OF ARRAY
    170 GO TO 260
    NLINE=NLINE+1
    LLINE=N-NLINE+1
    IF(NLINE-N) 180,180,380
    180 DO 190 I=1,135
    A(I)=BLK
    B(I)=BLK
    C(I)=BLK
    D(I)=BLK
    E(I)=BLK
    F(I)=BLK
    G(I)=BLK
    H(I)=BLK
    190 CONTINUE
    IF (ICON)195,260,195
    195 NCV=NCCP-I
    J=4
    IF(NCY)200,200,210
    200 J=5
    210 NCV=NCY+1
    IF(NCY-NCP) 220,220,260
    220 IF(NCY-M) 230,260,260
    230 NLINE = NLINE - 1
    YD1 = Y(NLINE,NCY) - Y(NLINE+1,NCY)
    YD2=Y(NLINE,NCY+1)-Y(NLINE+1,NCY+1)
    TP(1) = Y(NLINE,NCY)-0.125*YD1
    TPX(1)=Y(NLINE,NCY)-0.250*YD1
    TPM(1)=Y(NLINE,NCY)-0.375*YD1
    XMT(1)=Y(NLINE,NCY)-0.500*YD1
    BTM(1)=Y(NLINE,NCY)-0.625*YD1
  
```

```

BTX(1)=Y(NLINE,NCY)-0.750*YD1
BT(1)=Y(NLINE,NCY)-0.875*YD1
TP(10)=Y(NLINE,NCY+1)-0.125*YD2
TPX(10)=Y(NLINE,NCY+1)-0.250*YD2
TPM(10)=Y(NLINE,NCY+1)-0.375*YD2
XMT(10)=Y(NLINE,NCY+1)-0.500*YD2
BTM(10)=Y(NLINE,NCY+1)-0.625*YD2
BTX(10)=Y(NLINE,NCY+1)-0.750*YD2
BT(10)=Y(NLINE,NCY+1)-0.875*YD2
NLINE = NLINE + 1
D1=0.1 * (TP(10)-TP(1))
D2=0.1 * (TPX(10)-TPX(1))
D3=0.1 * (TPM(10)-TPM(1))
D4=0.1 * (XMT(10)-XMT(1))
D5=0.1 * (BTM(10)-BTM(1))
D6=0.1 * (BTX(10)-BTX(1))
D7=0.1 * (BT(10)-BT(1))
DO 240 I = 2,9
TP(I)=TP(I-1)+D1
TPX(I)=TPX(I-1)+D2
TPM(I)=TPM(I-1)+D3
XMT(I)=XMT(I-1)+D4
BTM(I)=BTM(I-1)+D5
BTX(I)=BTX(I-1)+D6
BT(I)=BT(I-1)+D7
240 CONTINUE
DO 250 I=1,10
J=J+1
I1=MOD(IFIX((TP(I)-AMIN)/BND),20)+1
I2=MOD(IFIX((TPX(I)-AMIN)/BND),20)+1
I3=MOD(IFIX((TPM(I)-AMIN)/BND),20)+1
I4=MOD(IFIX((XMT(I)-AMIN)/BND),20)+1
I5=MOD(IFIX((BTM(I)-AMIN)/BND),20)+1
I6=MOD(IFIX((BTX(I)-AMIN)/BND),20)+1
I7=MOD(IFIX((BT(I)-AMIN)/BND),20)+1
A(J)=IH(I1)
B(J)=IH(I2)
C(J)=IH(I3)
D(J)=IH(I4)
E(J)=IH(I5)
F(J)=IH(I6)
G(J)=IH(I7)
250 CONTINUE
GO TO 210
260 NCY=NCCP-1
J=-2
IF(NCY) 265,265,270
265 J=-1

```

```

MET02030
MET02040
MET02050
MET02060
MET02070
MET02080
MET02090
MET02100
MET02110
MET02120
MET02130
MET02140
MET02150
MET02160
MET02170
MET02180
MET02190
MET02200
MET02210
MET02220
MET02230
MET02240
MET02250
MET02260
MET02270
MET02280
MET02290
MET02300
MET02310
MET02320
MET02330
MET02340
MET02350
MET02360
MET02370
MET02380
MET02390
MET02400
MET02410
MET02420
MET02430
MET02440
MET02450
MET02460
MET02470
MET02480
MET02490
MET02500

```

```

270 GO TO 330
    NCY=NCY+1
280 IF(NCY-NCP) 280,280,310
    J=J+7
    THLD=AHLD*Y(NLINE,NCY)+BZ
285 IF(THLD) 285,290,290
    H(J)=EMI
    GO TO 295
290 H(J)=EPL
295 NUM=INT((ABS(THLD-INT(THLD)))*1000.0+0.5)
    NDS=100
    DO 300 KK=1,3
        J=J+1
        KI=NUM/NDS
        H(J)=KG(KI+1)
        NUM=NUM-KI*NDS
        NDS=NDS/10
    CONTINUE
300 GO TO 270
310 IF(NCP-M) 360,320,320
320 IF(J-127) 330,330,360
330 J=J+3
    KI=NLINE
    IF(KI-100) 340,335,335
    LL=KI/100
    H(J)=KG(LL+1)
    KI=KI-100*LL
    GO TO 343
340 H(J)=KG(1)
343 J=J+1
    IF(KI-10) 350,345,345
    LL=KI/10
    H(J)=KG(LL+1)
    KI=KI-10*LL
    GO TO 355
350 H(J)=KG(1)
355 J=J+1
    H(J)=KG(KI+1)
    J=J-5
    IF(NCY-1) 270,270,360
360 IF(NLINE-1) 362,362,368
362 PRINT 370,(A(I),I=1,132),(B(IP1),IP1=1,132),(H(IP2),IP2=1,132)
368 GO TO 170
    PRINT 370,(A(I),I=1,132),(B(IP1),IP1=1,132),(C(IP2),IP2=1,132),
1(D(IP3),IP3=1,132),(E(IP4),IP4=1,132),(F(IP5),IP5=1,132),
2(G(IP6),IP6=1,132),(H(IP7),IP7=1,132)
370 FORMAT(132A1)
    GO TO 170

```

```

MET02510
MET02520
MET02530
MET02540
MET02550
MET02560
MET02570
MET02580
MET02590
MET02600
MET02610
MET02620
MET02630
MET02640
MET02650
MET02660
MET02670
MET02680
MET02690
MET02700
MET02710
MET02720
MET02730
MET02740
MET02750
MET02760
MET02770
MET02780
MET02790
MET02800
MET02810
MET02820
MET02830
MET02840
MET02850
MET02860
MET02870
MET02880
MET02890
MET02900
MET02910
MET02920
MET02930
MET02940
MET02950
MET02960
MET02970
MET02980
MET02990

```



```

380 DO 390 I=1,135
    A(I)=BLK
    B(I)=BLK
    C(I)=BLK
    D(I)=BLK
390 CONTINUE
    J=-2
    IF(NCCP-1) 395,395,400
    J=-1
    DO 430 L=NCCP,NCP
        J=J+8
        KI=L
        IF(KI-100) 410,405,405
        LL=KI/100
        C(J)=KG(LL+1)
        KI=KI-100*LL
        GO TO 412
        C(J)=KG(1)
410 J=J+1
412 IF(KI-10) 420,415,415
415 LL=KI/10
        C(J)=KG(LL+1)
        KI=KI-10*LL
        GO TO 422
        C(J)=KG(1)
420 J=J+1
422 IF(KI-10) 430,425,425
430 CONTINUE
        PRINT 370, (B(IP1), IP1=1,132), (C(IP2), IP2=1,132)
        IF(NCP-M)60,500,500
500 RETURN
    END

```

```

MET02990
MET03000
MET03010
MET03020
MET03030
MET03040
MET03050
MET03060
MET03070
MET03080
MET03090
MET03100
MET03110
MET03120
MET03130
MET03140
MET03150
MET03160
MET03170
MET03180

```

```

MET03200
MET03210
MET03220
MET03230
MET03240
MET03250
MET03260
MET03270
MET03280
MET03290
MET03300

```

```

C000021
C.....
C      SUBROUTINE GAUSS
C
C      PURPOSE
C      COMPUTES A NORMALLY DISTRIBUTED RANDOM NUMBER WITH A GIVEN
C      MEAN AND STANDARD DEVIATION
C
C      USAGE
C      CALL GAUSS(IX,S,AM,V)
C
C      DESCRIPTION OF PARAMETERS
C
C      GAUS 10
C      GAUS 20
C      GAUS 30
C      GAUS 40
C      GAUS 50
C      GAUS 60
C      GAUS 70
C      GAUS 80
C      GAUS 90
C      GAUS 100
C      GAUS 110
C      GAUS 120
C      GAUS 130

```



```

AND PRODUCES A NEW INTEGER AND REAL RANDOM NUMBER.
USAGE
CALL RANDU(IX,IY,YFL)
DESCRIPTION OF PARAMETERS
IX - FOR THE FIRST ENTRY THIS MUST CONTAIN ANY ODD INTEGER
    NUMBER WITH NINE OR LESS DIGITS. AFTER THE FIRST ENTRY,
    IX SHOULD BE THE PREVIOUS VALUE OF IY COMPUTED BY THIS
    SUBROUTINE.
IY - A RESULTANT INTEGER RANDOM NUMBER REQUIRED FOR THE NEXT
    ENTRY TO THIS SUBROUTINE. THE RANGE OF THIS NUMBER IS
    BETWEEN ZERO AND 2**31
YFL- THE RESULTANT UNIFORMLY DISTRIBUTED, FLOATING POINT,
    RANDOM NUMBER IN THE RANGE 0 TO 1.0

REMARKS
THIS SUBROUTINE IS SPECIFIC TO SYSTEM/360 AND WILL PRODUCE
2**29 TERMS BEFORE REPEATING. THE REFERENCE BELOW DISCUSSES
SEEDS (65539 HERE), RUN PROBLEMS, AND PROBLEMS CONCERNING
RANDOM DIGITS USING THIS GENERATION SCHEME. MACLAREN AND
MARSAGLIA, JACM 12, P. 83-89, DISCUSS CONGRUENTIAL
GENERATION METHODS AND TESTS. THE USE OF TWO GENERATORS OF
THE RANDU TYPE, ONE FILLING A TABLE AND ONE PICKING FROM THE
TABLE, IS OF BENEFIT IN SOME CASES. 65549 HAS BEEN
SUGGESTED AS A SEED WHICH HAS BETTER STATISTICAL PROPERTIES
FOR HIGH ORDER BITS OF THE GENERATED DEVIATE.
SEEDS SHOULD BE CHOSEN IN ACCORDANCE WITH THE DISCUSSION THAT
GIVEN IN THE REFERENCE BELOW. ALSO, IT SHOULD BE NOTED THAT
IF FLOATING POINT RANDOM NUMBERS ARE DESIRED, AS ARE
AVAILABLE FROM RANDU, THE RANDOM CHARACTERISTICS OF THE
FLOATING POINT DEVIATES ARE MODIFIED AND IN FACT THESE
DEVIATES HAVE HIGH PROBABILITY OF HAVING A TRAILING LOW
ORDER ZERO BIT IN THEIR FRACTIONAL PART.

SUBROUTINES AND FUNCTION SUBPROGRAMS REQUIRED
NONE

METHOD
POWER RESIDUE METHOD DISCUSSED IN IBM MANUAL C20-8011,
RANDOM NUMBER GENERATION AND TESTING
.....

```

```

RAND 100
RAND 110
RAND 120
RAND 130
RAND 140
RAND 150
RAND 160
RAND 170
RAND 180
RAND 190
RAND 200
RAND 210
RAND 220
RAND 230
RAND 240
RAND 250
RAND 260
RAND 270
RAND 280
RAND 290
RAND 300
RAND 310
RAND 320
RAND 330
RAND 340
RAND 350
RAND 360
RAND 370
RAND 380
RAND 390
RAND 400
RAND 410
RAND 420
RAND 430
RAND 440
RAND 450
RAND 460
RAND 470
RAND 480
RAND 490
RAND 500
RAND 510
RAND 520
RAND 530

```

```

CCCCCCCCCCCCCCCCCCCCCCCCCCCCCCCCCCCCCCCCCCCCCCCCCCCCCCCC

```

```

SUBROUTINE RANDU(IX,IY,YFL)
IY=IX*65539
IF(IY)5,6,6
5 IY=IY+2147483647+1
6 YFL=IY
YFL=YFL*.4656613E-9
RETURN
END

```

```

RAND 540
RAND 550
RAND 560
RAND 570
RAND 580
RAND 590
RAND 600

```

APPENDIX C

```
// EXEC FORTCLGP, TIME.GC=3, REGION.GC=100K
```

```
// FORT.SYSIN DD
```

```
CCOMPUTER PROGRAM 1
```

THIS COMPUTER PROGRAM IS DESIGNED TO INTERPOLATE THE DENSITY VALUES AS OBTAINED FROM THE AGARD 167 TABLES AND INPUT ALONG A LINE OF SIGHT THAT PASSES THROUGH THE CONE AXIS. SUBROUTINE LSQPL2 FROM THE IBM SUBROUTINE PACKAGE IS USED TO PASS A TENTH DEGREE POLYNOMIAL THROUGH THE INPUT VALUES AND THIS IS THEN USED TO OBTAIN THE DENSITY AT 201 EQUIDISTANT POINTS ALONG THE LINE OF SIGHT. THESE VALUES ARE PUNCHED OUT ACCORDING TO THE FORMAT REQUESTED FOR INPUT INTO SUBROUTINE FREAD OF COMPUTER PROGRAM HOLOVERT. ANY NUMBER OF LINES OF SIGHT MAY BE READ IN AT A TIME BY SPECIFYING THE VALUE OF 'W' AS 1.0 ACCORDING TO FORMAT 60 IN THE DATA CARDS READ IN. THE DATA CARDS TO BE READ IN ARE AS FOLLOWS

CARD 1... UPPER AND LOWER SHOCK WAVE ANGLES IN THE ORDER IN WHICH THE DENSITY IS READ IN ... FORMAT 10

CARDS 2 TO 5 DENSITY VALUES ALONG A LINE OF SIGHT AS OBTAINED FROM AGARD 167 ... FORMAT 30

CARD 6 THE VALUE OF 'W' IF MORE THAN ONE LINE OF SIGHT IS BEING INPUT, SET 'W' EQUAL TO 1.0. IF NO DATA SET FOLLOWS, SET 'W' EQUAL TO ANY OTHER VALUE... FORMAT 60

NOTE... THE CARDS PUNCHED OUT FOR THE VARIOUS LINES OF SIGHT ARE SEPARATED BY A CARD HAVING FORMAT 43. THIS CARD MUST BE REMOVED BEFORE THE DATA IS FED IN INTO SUBROUTINE FREAD.

```
//GO.FTC6F001 DD DCB=BLKSIZE=133
```

```
//GC.SYSIN DD
```

```
DIMENSION AX(100), X(28), RHC(28), WI(28), RHOP(28), DELY(28), B(30),
```

```
1 SB(30), XP(201), ARHO(201)
```

```
1 REAL*8 TITLE(10)/10/
```

```
REAL*8 B,X,RHO,WI,RHOP,DELY,SB,ARHO,Y,XP,T
```

```
REAL*8 A1,A2,A3,A4,A5,A6,A7,A8,A9,A10,A11
```

```
Y(A1,A2,A3,A4,A5,A6,A7,A8,A9,A10,A11,T)=A1+A2*T+A3*T**2+A4*T**3+
```

```
1 A5*T**4+A6*T**5+A7*T**6+A8*T**7+A9*T**8+A10*T**9+A11*T**10
```

```
PIE=3.14159265
```

```
R=1.0
```

```

1  READ(5,10) U,V
   SU=(U*PIE)/180.
   Z=.95/TAN(SU)
   SL=(V*PIE)/180.
   THETA=(29.677*PIE)/180.
   R2=Z*TAN(10.*PIE)/180.)
   R3=Z*TAN(SL)
   R1=Z*TAN(SU)
   R4=(1.-R3)
   R5=(1.-R2)
   R6=(1.-R2)
   R7=(1.-R1)
   DELR1=(R1-R2)/10.
   DELR2=(R3-R2)/10.
   DELR3=(1.-R1)/25.
   DELR4=(1.-R3)/25.
   DELR5=R2/12.5
   RHO(1)=0.
   READ(5,30) (RHO(I),I=2,14)
   READ(5,30) (RHO(I),I=15,27)
   RHO(28)=0.
   AX(1)=0.
   DO 2 I=2,26
2  AX(I)=AX(I-1)+DEL R4
   X(1)=0.
   X(2)=AX(26)
   DO 3 I=27,35
3  AX(I)=AX(I-1)+DEL R2
   J=I-24
   X(J)=AX(I)
   AX(36)=AX(35)+DEL R2/2.
   X(12)=AX(36)
   DO 31 I=37,38
31 X(I)=AX(I-1)+DEL R2/4.
   J=I-24
   X(J)=AX(I)
   DO 4 I=39,63
4  AX(I)=AX(I-1)+DEL R5
   X(15)=AX(63)
   DO 5 I=64,65
5  AX(I)=AX(I-1)+DEL R1/4.
   J=I-48
   X(J)=AX(I)
   AX(66)=AX(65)+DEL R1/2.
   X(18)=AX(66)
   DO 32 I=67,75
32 AX(I)=AX(I-1)+DEL R1
   J=I-48

```



```

32 X(J)=AX(I)
X(28)=2.0
DO 6 I=1,28
6  WI(I)=1.0
CALL LSQPL2(28,-10,X,RHO,WI,RHOP,DELY,B,SB,TITLE)
WRITE(6,50)
50  FORMAT(//,' LSQPL2 RETURNS')
10  FORMAT(2F10.7)
30  FORMAT(10F8.5/,3F8.5)
A1=B(1)
A2=B(2)
A3=B(3)
A4=B(4)
A5=B(5)
A6=B(6)
A7=B(7)
A8=B(8)
A9=B(9)
A10=B(10)
A11=B(11)
ARHO(1)=0.
DELX=2./200.
XP(1)=0.
DO 7 I=2,201
51  XP(I)=XP(I-1)+DELX
IF(XP(I).LT.R4) GO TO 9
IF(XP(I).GT.R7) GO TO 9
FORMAT(//,' COMPUTING ARHO(I)')
ARHO(I)=Y(A1,A2,A3,A4,A5,A6,A7,A8,A9,A10,A11,XP(I))
GO TO 7
ARHO(1)=0.
CONTINUE
WRITE(6,41)
43  WRITE(6,40) (I,X(I),RHO(I),I=1,28)
60  WRITE(6,40) (I,XP(I),ARHO(I),I=1,201)
39  WRITE(6,40) (ARHO(I),I=1,201)
42  WRITE(7,42)
49  WRITE(7,43)
40  READ(5,60) W
41  IF(W.EQ.1.) GO TO 1
FORMAT(//,'XXXXXXXXXXXXXXXXXXXXXXXXXXXXXXXXXXXXXXXXXXXXX')
60  FORMAT(F5.0)
39  FORMAT(//'/')
42  FORMAT(F8.5)
49  FORMAT(//'/',5X,'I',10X,XP(I),'10X,ARHO(I)',//')
40  FORMAT(5X,I3,10X,F10.5,10X,F10.5)
41  FORMAT(//'/',5X,'I',10X,X(I),'10X,RHO(I)',//')
STOP

```


END

A SAMPLE DATA DECK

2	22.696	22.696	2383	2574	2749	2908	3053	3178	3271
1	1555	1913	2168	2574	2749	2908	3053	3178	3271
3	3300	3308	3310	3178	3053	2908	2749	2574	2383
3	3310	3308	3300	3178	3053	2908	2749	2574	2383
3	2168	1913	1555	3178	3053	2908	2749	2574	2383
1	22.99	22.99	2300	2489	2661	2802	2964	3088	3181
2	1482	1837	2089	2489	2661	2802	2964	3088	3181
3	3210	3219	3221	3088	2964	2802	2661	2489	2300
3	3221	3219	3210	3088	2964	2802	2661	2489	2300
3	2089	1837	1482	3088	2964	2802	2661	2489	2300
5	5.	5.	5.	5.	5.	5.	5.	5.	5.

COMPUTER PROGRAM 2

THIS COMPUTER PROGRAM IS DESIGNED TO INTERPOLATE THE DENSITY VALUES GIVEN IN AGARD 167 FOR MACH NUMBERS BETWEEN 2.5 AND 3.0. INTERPOLATION IS DONE BY CALLING ON SUBROUTINE LSQPL2 OF THE IBM SUBROUTINE PACKAGE TO PASS A CUBIC CURVE THROUGH THE FOUR INPUT VALUES OF DENSITY AT MACH NUMBERS 1.5, 2.0, 3.0 AND 4.0. THE VALUES OF THE DENSITY FOR MACH NUMBERS FROM 2.5 TO 3.0 IN INCREMENTS OF M=0.01 ARE THEN EVALUATED AND PRINTED FOR EACH SET OF INPUT DATA VALUES.

INPUT DATA...

EACH CARD HAS 4 DENSITY VALUES CORRESPONDING TO THE VALUES AT M=1.5, 2.0, 3.0 AND 4.0 IN THAT ORDER. ACCORDING TO FORMAT 10. FOR EACH VALUE OF PHI, THERE ARE 14 SUCH CARDS, THE LAST ONE BEING THAT OF THE SHOCK ANGLE. CARDS ARE INPUT IN THE ORDER OF INCREASING XI, FOR EACH PHI, AND IN THE ORDER OF INCREASING PHI.

```
// EXEC FORTCLGP, TIME.GO=5, REGION.GO=100K
//FCRT. SYSIN DD *
DIMENSION AM(4), RO(4), WI(10), AROP(10), DELY(10), B(10), SR(10),
1AAM(50), ROP(50), PHI(10)
REAL*8 TITLE(10)/1000, /
```

```
REAL*8 B, AM, RO, WI, AROP, DELY, SB, AAM, ROP, T, A1, A2, A3, A4
FUN(A1, A2, A3, A4, T)=A1+A2-T+A3-T**2+A4-T**3
CALL ERRSET(209, 256, -1, 1, 0, 203)
PHI(1)=0.
DELPHI=22.5
```

```
DO 2 K=1, 10 PHI(K)
WRITE(6, 30) PHI(K)
FORMAT(///, 1X, PHI=, F10.5, ///)
PHI(K+1)=PHI(K)+DELPHI
```

```
AXI=0.
DELXI=0.1
AM(1)=1.5
AM(2)=2.0
AM(3)=3.0
AM(4)=4.0
DO 2 I=1, 14
READ(5, 10) (RO(M), M=1, 4)
FORMAT(4F10.5)
```

```

40  WRITE(6,40) AXI
    FORMAT(///,1X,'XI=',F10.5,///)
    AXI=AXI+DELXI
    DO 3 L=1,10
    WI(L)=1.000 (RO(II),II=1,4)
    WRITE(6,10) (AM(II),II=1,4)
    WRITE(6,10) (WI(II),II=1,10)
    CALL LSQPL2(4,-3,AM,RO,WI,AROP,DELY,R,SB,TITLE)
    A1=B(1)
    A2=B(2)
    A3=B(3)
    A4=B(4)
    WRITE(6,50)
    FORMAT(///,3X,'MACH NO.',5X,'DENSITY',///)
    AAM(1)=2.5
    DLM=.01
    DO 2 J=1,50
    ROP(J)=FUN(A1,A2,A3,A4,AAM(J))
    WRITE(6,20) AAM(J),ROP(J)
    FORMAT(1X,F15.7,10X,F15.7)
    20  AAM(J+1)=AAM(J)+DLM
    2   CONTINUE
      STOP
      END

```

```

C C A TYPICAL DATA DECK .....
C C //GO.FT06F001 DD SPACE=(CYL,(10,2))
//GO.SYSIN DD *
1.6252 1.9494 2.6869 3.3792
1.6244 1.9490 2.6866 3.3790
1.6223 1.9478 2.6859 3.3784
1.6154 1.9437 2.6830 3.3760
1.5954 1.9296 2.6726 3.3669
1.5717 1.9102 2.6567 3.3524
1.5468 1.8873 2.6363 3.3332
1.5215 1.8618 2.6118 3.3094
1.4961 1.8342 2.5836 3.2813
1.4705 1.8047 2.5519 3.2491
1.4444 1.7730 2.5166 3.2126
1.4172 1.7387 2.4774 3.1715
1.3877 1.7008 2.4338 3.1256
1.2407 1.7343 2.4003 3.1289
1.6006 1.9109 2.6169 3.2783
1.5993 1.9115 2.6197 3.2857
1.5538 1.9111 2.6203 3.2870
1.5538 1.9082 2.6195 3.2887

```

25521	43	26521	43	27521	43	28521	43	29521	43	30521	43	31521	43	32521	43	33521	43	34521	43	35521	43	36521	43	37521	43	38521	43	39521	43	40521	43	41521	43	42521	43	43521	43	44521	43	45521	43	46521	43	47521	43	48521	43	49521	43	50521	43	51521	43	52521	43	53521	43	54521	43	55521	43	56521	43	57521	43	58521	43	59521	43	60521	43	61521	43	62521	43	63521	43	64521	43	65521	43	66521	43	67521	43	68521	43	69521	43	70521	43	71521	43	72521	43	73521	43	74521	43	75521	43	76521	43	77521	43	78521	43	79521	43	80521	43	81521	43	82521	43	83521	43	84521	43	85521	43	86521	43	87521	43	88521	43	89521	43	90521	43	91521	43	92521	43	93521	43	94521	43	95521	43	96521	43	97521	43	98521	43	99521	43	100521	43	101521	43	102521	43	103521	43	104521	43	105521	43	106521	43	107521	43	108521	43	109521	43	110521	43	111521	43	112521	43	113521	43	114521	43	115521	43	116521	43	117521	43	118521	43	119521	43	120521	43	121521	43	122521	43	123521	43	124521	43	125521	43	126521	43	127521	43	128521	43	129521	43	130521	43	131521	43	132521	43	133521	43	134521	43	135521	43	136521	43	137521	43	138521	43	139521	43	140521	43	141521	43	142521	43	143521	43	144521	43	145521	43	146521	43	147521	43	148521	43	149521	43	150521	43	151521	43	152521	43	153521	43	154521	43	155521	43	156521	43	157521	43	158521	43	159521	43	160521	43	161521	43	162521	43	163521	43	164521	43	165521	43	166521	43	167521	43	168521	43	169521	43	170521	43	171521	43	172521	43	173521	43	174521	43	175521	43	176521	43	177521	43	178521	43	179521	43	180521	43	181521	43	182521	43	183521	43	184521	43	185521	43	186521	43	187521	43	188521	43	189521	43	190521	43	191521	43	192521	43	193521	43	194521	43	195521	43	196521	43	197521	43	198521	43	199521	43	200521	43	201521	43	202521	43	203521	43	204521	43	205521	43	206521	43	207521	43	208521	43	209521	43	210521	43	211521	43	212521	43	213521	43	214521	43	215521	43	216521	43	217521	43	218521	43	219521	43	220521	43	221521	43	222521	43	223521	43	224521	43	225521	43	226521	43	227521	43	228521	43	229521	43	230521	43	231521	43	232521	43	233521	43	234521	43	235521	43	236521	43	237521	43	238521	43	239521	43	240521	43	241521	43	242521	43	243521	43	244521	43	245521	43	246521	43	247521	43	248521	43	249521	43	250521	43	251521	43	252521	43	253521	43	254521	43	255521	43	25
-------	----	-------	----	-------	----	-------	----	-------	----	-------	----	-------	----	-------	----	-------	----	-------	----	-------	----	-------	----	-------	----	-------	----	-------	----	-------	----	-------	----	-------	----	-------	----	-------	----	-------	----	-------	----	-------	----	-------	----	-------	----	-------	----	-------	----	-------	----	-------	----	-------	----	-------	----	-------	----	-------	----	-------	----	-------	----	-------	----	-------	----	-------	----	-------	----	-------	----	-------	----	-------	----	-------	----	-------	----	-------	----	-------	----	-------	----	-------	----	-------	----	-------	----	-------	----	-------	----	-------	----	-------	----	-------	----	-------	----	-------	----	-------	----	-------	----	-------	----	-------	----	-------	----	-------	----	-------	----	-------	----	-------	----	-------	----	-------	----	-------	----	-------	----	-------	----	-------	----	-------	----	-------	----	-------	----	--------	----	--------	----	--------	----	--------	----	--------	----	--------	----	--------	----	--------	----	--------	----	--------	----	--------	----	--------	----	--------	----	--------	----	--------	----	--------	----	--------	----	--------	----	--------	----	--------	----	--------	----	--------	----	--------	----	--------	----	--------	----	--------	----	--------	----	--------	----	--------	----	--------	----	--------	----	--------	----	--------	----	--------	----	--------	----	--------	----	--------	----	--------	----	--------	----	--------	----	--------	----	--------	----	--------	----	--------	----	--------	----	--------	----	--------	----	--------	----	--------	----	--------	----	--------	----	--------	----	--------	----	--------	----	--------	----	--------	----	--------	----	--------	----	--------	----	--------	----	--------	----	--------	----	--------	----	--------	----	--------	----	--------	----	--------	----	--------	----	--------	----	--------	----	--------	----	--------	----	--------	----	--------	----	--------	----	--------	----	--------	----	--------	----	--------	----	--------	----	--------	----	--------	----	--------	----	--------	----	--------	----	--------	----	--------	----	--------	----	--------	----	--------	----	--------	----	--------	----	--------	----	--------	----	--------	----	--------	----	--------	----	--------	----	--------	----	--------	----	--------	----	--------	----	--------	----	--------	----	--------	----	--------	----	--------	----	--------	----	--------	----	--------	----	--------	----	--------	----	--------	----	--------	----	--------	----	--------	----	--------	----	--------	----	--------	----	--------	----	--------	----	--------	----	--------	----	--------	----	--------	----	--------	----	--------	----	--------	----	--------	----	--------	----	--------	----	--------	----	--------	----	--------	----	--------	----	--------	----	--------	----	--------	----	--------	----	--------	----	--------	----	--------	----	--------	----	--------	----	--------	----	--------	----	--------	----	--------	----	--------	----	--------	----	--------	----	--------	----	--------	----	--------	----	--------	----	--------	----	----

BIBLIOGRAPHY

1. Heflinger, L. O., Wuerker, R. F., and Brooks, R. F., "Holographic Interferometry," Journal of Applied Physics, Vol. 37, No. 2, pp. 642-649, February 1966.
2. Brooks, R. E., Heflinger, L. O., and Wuerker, R. F., "9A9-Pulsed Laser Holograms," IEEE Journal of Quantum Electronics, Vol. EQ-2, No. 8, pp. 275-299, August 1966.
3. Matulka, R. D., "The Application of Holographic Interferometry to the Determination of Asymmetric Three-dimensional Density Fields in Free Jet Flow," PhD Thesis, Naval Postgraduate School, June 1970.
4. Maldonado, C. D., Caron, A. P., and Olsen, H. N., "New Method for Obtaining Emission Coefficients from Emitted Spectral Intensities. Part I - Circularly Symmetric Light Sources," Journal of the Optical Society of America, Vol. 55, No. 10, pp. 1247-1254, October 1965.
5. Maldonado, C. D., and Olsen, H. N., "New Method for Obtaining Emission Coefficients from Emitted Spectral Intensities. Part II - Asymmetric Sources," Journal of the Optical Society of America, Vol. 56, No. 10, pp. 1305-1312, October 1966.
6. Jones, D. J., "Tables of Inviscid Supersonic Flow About Circular Cones at Incidence, Part I and II," Advisory Group for AeroSpace Research and Development, November 1969.
7. Liepmann, H. W., and Roshko, A., "Elements of Gas Dynamics," pp. 165, John Wiley and Sons, Inc., 1957.
8. Olsen, H. N., Maldonado, C. D., and Duckworth, G. D., "A Numerical Method for Obtaining Internal Emission Coefficients from Externally Measured Spectral Intensities of Asymmetric Plasmas," Journal of Quantum Spectroscopy and Radiation Transfer, Vol. 8, pp. 1419-1439, 1968.
9. Olsen, H. N., Maldonado, C. D., Duckworth, G. D., and Caron, A. P., "Investigation of the Interaction of an External Magnetic Field with an Electric Arc," Aero-Space Research Laboratories Report ARL66-0016, January, 1966.

10. Sullivan, J. B., "An Investigation of Three-Dimensionality in Holographic Interferometry," Masters Thesis, Naval Postgraduate School, 1968.
11. Matulka, R. D., and Collins, D. J., "The Application of Holographic Interferometry to the Determination of Asymmetric Three-Dimensional Density Field in Free Jet Flow."
12. Taylor, G. I., and Maccoll, J. W., "The Air Pressure on a Cone Moving at High Speed," Proceedings of the Royal Society, London, Series A, Vol. 139, 1933.
13. Stone, A. H., "On Supersonic Flow Past a Slightly Yawing Cone," Journal of Mathematics and Physics, Vol. 27, 1948.
14. Staff of the Computing Section of Analysis (under the direction of Zdenek Kopal), "Tables of Supersonic Flow Around Cones," Technical Report No. 1, NOrd Contract No. 9169, M.I.T., 1947.
15. Staff of the Computing Section, Centre of Analysis (under the direction of Zdenek Kopal), "Tables of Supersonic Flow Around Yawing Cones," Technical Report No. 3, NOrd Contract No. 9169, M.I.T., 1949.
16. Staff of the Computing Section (under the direction of Zdenek Kopal), "Tables of Supersonic Flow Around Cones of Large Yaw," NOrd Contract No. 8555 and 9169, M.I.T., 1949.
17. Jones, D. J., "Numerical Solutions of the Supersonic Flow Field for Conical Bodies in a Supersonic Stream," National Research Council of Canada National Aeronautical Establishment, Aeronautical Report LR-507, 1968.
18. Ladenburg, R., Van Voorhis, C. C., and Winckler, J., "Interferometric Study of Supersonic Phenomena - Part II," NAVORD Report 93-46, September, 1946.

INITIAL DISTRIBUTION LIST

	No. Copies
1. Defense Documentation Center Cameron Station Alexandria, Virginia 22314	2
2. Library, Code 0212 Naval Postgraduate School Monterey, California 93940	2
3. Professor D. J. Collins Department of Aeronautics Naval Postgraduate School Monterey, California 93940	1
4. LCDR R. C. Jagota, I.N. Engineer Officer I.N.S. "Trishul" c/o Fleet Mail Office Bombay, India	1

DOCUMENT CONTROL DATA - R & D

(Security classification of title, body of abstract and indexing annotation must be entered when the overall report is classified)

1. ORIGINATING ACTIVITY (Corporate author) Naval Postgraduate School Monterey, California 93940		2a. REPORT SECURITY CLASSIFICATION Unclassified	
		2b. GROUP	
3. REPORT TITLE THE APPLICATION OF HOLOGRAPHIC INTERFEROMETRY TO THE DETERMINATION OF THE FLOW FIELD AROUND A RIGHT CIRCULAR CONE AT ANGLE OF ATTACK			
4. DESCRIPTIVE NOTES (Type of report and inclusive dates) Aeronautical Engineer's Thesis			
5. AUTHOR(S) (First name, middle initial, last name) Ravi Chandar Jagota, Lieutenant Commander, Indian Navy			
6. REPORT DATE December 1970		7a. TOTAL NO. OF PAGES 150	7b. NO. OF REFS 18
8a. CONTRACT OR GRANT NO.		9a. ORIGINATOR'S REPORT NUMBER(S)	
b. PROJECT NO.			
c.		9b. OTHER REPORT NO(S) (Any other numbers that may be assigned this report)	
d.			
10. DISTRIBUTION STATEMENT This document has been approved for public release and sale; its distribution is unlimited.			
11. SUPPLEMENTARY NOTES		12. SPONSORING MILITARY ACTIVITY Naval Postgraduate School Monterey, California 93940	
13. ABSTRACT <p>The successful application of holography to the study of three dimensional flow fields due to phase objects has been reported in the literature. The present report extends this technique to the study of density fields around opaque bodies as would normally be encountered in wind tunnel experiments. The density field around a 10 degree half-angle cone at zero and ten degree angle of attack has been investigated in the Naval Postgraduate School supersonic wind tunnel. In these experiments, the finite fringe method for the production of interferograms has, for the first time, been applied to holographic interferometry. The density field obtained from the reduction of the interferograms was found to agree with that obtained from an analytical solution of the governing equations as reported by D. J. Jones in Reference 1. The computer program used for the reduction of the interferograms has been evaluated for the effect of the presence of the cone and the shock wave and has been found to yield stable and accurate results.</p>			

14 KEY WORDS	LINK A		LINK B		LINK C	
	ROLE	WT	ROLE	WT	ROLE	WT
HOLOGRAPHY						
FLOW VISUALIZATION						
CONICAL FLOW						

DISTRIBUTION

1.	Defense Documentation Center Cameron Station Alexandria, Virginia 22314	20
2.	Library (Code 0212) Naval Postgraduate School Monterey, California 93940	
3.	Commander Naval Air Systems Command Department of the Navy Washington, D. C. 20360	2
	Attn: AIR 310	2
	AIR 604	2
4.	Chairman Department of Aeronautics Naval Postgraduate School Monterey, California 93940	1
5.	Professor D. J. Collins Department of Aeronautics Code 57C0 Naval Postgraduate School Monterey, California 93940	2
6.	Mr. L. S. McDonald Naval Air Systems Command Code AIR 3033 Department of the Navy Washington, D. C. 20360	1
7.	Dean of Research Administration Naval Postgraduate School Monterey, California 93940	2

DOCUMENT CONTROL DATA - R & D

(Security classification of title, body of abstract and indexing annotation must be entered when the overall report is classified)

1. ORIGINATING ACTIVITY (Corporate author) Naval Postgraduate School Monterey, California 93940		2a. REPORT SECURITY CLASSIFICATION Unclassified	
		2b. GROUP	
3. REPORT TITLE The Application of Holographic Interferometry to the Determination of the Flow Field Around a Right Circular Cone at Angle of Attack			
4. DESCRIPTIVE NOTES (Type of report and, inclusive dates) Technical Report, NPS-57C071111A			
5. AUTHOR(S) (First name, middle initial, last name) Daniel J. Collins and Ravi C. Jagota			
6. REPORT DATE November 1971		7a. TOTAL NO. OF PAGES 153	7b. NO. OF REFS 18
8a. CONTRACT OR GRANT NO.		9a. ORIGINATOR'S REPORT NUMBER(S)	
b. PROJECT NO.			
c. Airtask No. A310310A/551A/1 R010-03-01		9b. OTHER REPORT NO(S) (Any other numbers that may be assigned this report)	
d.			
10. DISTRIBUTION STATEMENT Approved for public release; distribution unlimited			
11. SUPPLEMENTARY NOTES		12. SPONSORING MILITARY ACTIVITY Naval Air Systems Command Washington, D. C 20360	
13. ABSTRACT The successful application of holography to the study of three dimensional flow fields due to phase objects has been reported in the literature. The present report extends this technique to the study of density fields around opaque bodies as would normally be encountered in wind tunnel experiments. The density field around a 10 degree half-angle cone at zero and ten degree angle of attack has been investigated by means of the finite fringe holographic interferometry. The three dimensional density field obtained from the reduction of the interferograms was found to agree with that obtained from an analytical solution of the governing equations.			

14 KEY WORDS	LINK A		LINK B		LINK C	
	ROLE	WT	ROLE	WT	ROLE	WT
Holography Flow Visualization Conical Flow						

U144819

DUDLEY KNOX LIBRARY - RESEARCH REPORTS



5 6853 01058135 8

U 14481